

**ADDITIVES DERIVED FROM LOCAL SOURCES FOR ENHANCED OIL  
RECOVERY (EOR) PROCESSES**

**(BAHAN PENGKALAK DARIPADA SUMBER TEMPATAN UNTUK PROSES  
PENGELUARAN MINYAK)**

**ASSOC. PROF. DR. ANI IDRIS  
ASSOC. PROF. DR. MARIYAMNI AWANG**

**FAKULTI KEJURUTERAAN KIMIA DAN KEJURUTERAAN SUMBER ASLI  
UNIVERSITI TEKNOLOGI MALAYSIA**

## **ABSTRACT**

The cost of chemicals prohibits many technically feasible enhanced oil recovery methods to be applied in the oilfields. This research produced surfactants from phenols that were extracted from the pyrolysis oil of oil palm shells which are a byproduct of the palm oil industry. Xanthans which are imported can be produced from many available local sources such as starches and fruits. All of the additives produced were tested for enhanced oil recovery use and were found to have suitable properties. The recoveries for surfactant polymer flooding measured in the laboratory were comparable with the values reported in literature i.e. between 7 to 15 %. This work has proved that expensive chemicals can be produced locally using local sources and byproducts, consequently posing a potential savings in EOR processes.

## ABSTRAK

Kos bahan kimia telah menghalang banyak proses pengeluaran minyak tertingkat yang baik secara teknikal untuk digunakan di lapangan minyak. Kajian ini telah menghasilkan surfaktan daripada fenol yang dikeluarkan dari minyak pirolisis tempurung minyak sawit yang merupakan bahan buangan industri sawit. Xanthans yang diimpot boleh dibuat daripada bahan tempatan yang sediada seperti kanji dan buah buahan. Kesemua bahan tambahan yang dihasilkan telah diuji untuk kegunaan pengeluaran minyak tertingkat dan didapati mempunyai ciri-ciri yang sesuai. Perolehan banjir surfaktan/polimer yang diukur dalam makmal adalah baik jika dibandingkan dengan nilai yang dilaporkan dalam literatur iaitu antara 7 hingga 15 %. Usaha ini telah membuktikan bahan kimia boleh dikeluarkan dengan menggunakan bahan tempatan dan bahan sampingan, sekaligus mempunyai potensi untuk mengurangkan perbelanjaan dalam proses PMT.

## **ACKNOWLEDGEMENTS**

First and foremost, I would like to express my gratitude and appreciation to IRPA for the grant (Vot 74277). My deep gratefulness also goes to all the researchers and all the supporting staff in the Petroleum Laboratory, FKKS SA for their invaluable assistance during the course of the project completion. Last but not least to all the Research Management Centre staff who has laid their helping hands throughout the project.

## **CHAPTER 1**

### **INTRODUCTION**

#### **1.1 Overview**

##### **1.1.1 Introduction on enhanced oil recovery (EOR)**

Enhanced oil recovery (EOR) refers to reservoir processes that recover oil not produced from secondary processes. Primary recovery uses the natural energy of the reservoir to produce oil and gas. Secondary recovery uses injectants to re-pressurize the reservoir and to displace oil to producers. Enhanced oil recovery processes target what is left. The processes focus on the rock/oil/injectant system on the interplay of capillary and viscous forces (Stosur, 2003).

There are many types of EOR processes. Thermal processes are the most common type of EOR, wherein a hot invading face, such as steam, hot water or a combustible gas, is injected in order to increase the temperature of oil and gas in the reservoir and facilitate their flow to the production wells. Another type of EOR process consists of injecting miscible phase with the oil and gas into the reservoir in order to eliminate the interfacial tension effects. The miscible phase can be miscible hydrocarbon, CO<sub>2</sub> or an inert gas. Another lesser used EOR technique is called chemical flooding, where chemicals are

injected into the reservoir. The polymer is used to improve the sweep efficiency by changing the mobility ratio. The surfactant is used to reduce the interfacial tension between the oil and the displacing fluid.

According to Austad and Milter (2000), chemical flooding of oil reservoirs is one of the most successful methods to enhance oil recovery from depleted reservoirs at low pressure. However, it is well documented in their publishing that chemical flooding is only marginally economical, or in most cases very costly. It was concluded by most oil companies at the end of 1980s that the method was not economical, or the financial and technical risk was too high presenting compare to the oil price at the time. Researches declined drastically during the 1990s. However, there are still some researchers who are trying to improve the technique by simplifying the flooding process, improving the efficiency of the surfactants or developing new surfactants.

Many EOR methods have been devised to squeeze the extra oil out of the rocks. Beginning from injection of water to various types of gases and liquids, singly or in combination, many studies have been reported to be a success technically, however the additional cost of injection in relation to the cost of oil often kept the study at the laboratory level. Polymer-surfactant flooding is a process of displacing oil that combined reduction of surface tension that helped to release oil from pore spaces due to the surfactant and an improvement in the sweep efficiency due to the high viscosity of the polymer that provides the drive in pushing the oil towards the well. Since the 70s hydrolysed polyacrylamide (HPAM) or xanthan are the main additives. The number of field applications of xanthan, however, is much less than HPAM due to the higher xanthan cost. Injection of surfactant is relatively new and much of it now is in generating foam to augment CO<sub>2</sub> injection. Similarly, additional cost is incurred with use of surfactant.

### **1.1.2 Introduction of surfactant**

In 2002, Berger and Lee developed a new type of surfactant that could be used at very low concentrations to produce ultra low interfacial tensions (IFT) for sandstone and limestone formations. These surfactants could be used for Alkaline Surfactant Polymer

(ASP) floods, surfactant floods and also as an additive for water floods. These new surfactants had their advantages, particularly their effectiveness at low concentration levels, and their high salt tolerance and did not require alkali to produce ultra low interfacial tensions. The authors used the olefin sulfonic acid to simultaneously alkylate and sulfonate the aromatic compound and synthesize a new family of anionic surfactants. The aromatic compounds that could be used include benzene, toluene, xylene, naphthalene, phenol, diphenylether and substituted derivatives of these compounds. The authors reduced the cost of the alkylation and sulfonation process.

Zaitoun *et al.* (2003) conducted a series of experiments on surfactant screening and evaluation for surfactant flood in the Chihuido de la Sierra Negra field in Argentina. They developed a new anionic surfactant that provides solubility in high salinities and low interfacial tension at low concentration. They used a sulfoalkylated nonylphenol/formaldehyde oligomer to reduce adsorption of the primary surfactant. The synthesis of this material had been described by Berger (2002).

Purwono and Murachman (2001) described that Sodium Lignosulphonate (SLS), which is produced as a result of sulfonation of lignin formed from the waste pulp industries and hydrolysis of oil palm husks, had potential to be used in EOR. Surfactant or co-surfactant from the pyrolysis of oil palm husks could also be used as EOR chemicals. Mainly alcohols like methanol, ethanol and propanol were produced from the pyrolysis of oil palm fibres. They used the surfactant in the form of microemulsions during the chemical process experiment. The methane produced from the pyrolysis of palm oil fibres and fruit stems could be used as tertiary oil recovery flood material since hydrocarbons gases were dissolved in the oil to reduce the oil viscosity. The process is known as miscible process. However, in their works, they did not describe the method to produce the surfactant.

Surfactant use for EOR is not a recent development in petroleum field. However, the cost of the surfactants has been the main reason for the limited use in the EOR processes. One problem with many surfactants is their high cost of manufacture and the raw material. The above mentioned studies show that the research groups have paid much attention to the alkylated and sulfonated aromatic compounds which included phenol and its derivatives to synthesize new surfactants for EOR uses (Berger and Lee, 2002). They produced a new series of alkylaryl sulfonic acids that did not require costly alkylation units and hazardous

catalyst and employed relatively inexpensive equipment. Besides, Purwono and Murachman (2001) used the palm oil husks from industrial waste as raw materials to develop the chemicals for EOR.

Since Malaysia is world's largest palm oil producer, it generates significant amount of oil palm wastes. The wastes include large amount of solid wastes and a wastewater called palm oil mill effluent (POME). Thirty one million tons of fresh fruit bunch is locally produced annually and processed in 265 mills, from which 14.8 million tons of oil palm empty bunch, 9.1 million tons of fibre and 3.7 million tons of fruit shell are generated as solid wastes, and more than 10 million tons of palm oil mill effluent (POME) are generated as wastewater (Wong, 2002). Currently, a part of fibre and fruit shell wastes are utilized as boiler fuels for steam generation in some palm oil mills. Unfortunately, no experiment has been done using the oil palm wastes as the raw materials to develop the chemicals for EOR in Malaysia.

In 1999, Islam *et al.* reported the pyrolysis oil from fluidized bed pyrolysis of oil palm shell contained a high fraction of phenol based compounds. Jamil and co-worker (2000) had described another successful fluidized bed pyrolysis technique that produced pyrolysis oil with high contains of phenol and its derivatives from oil palm shell. Wong *et al.* (2003) also concluded that there was 25.6 wt % of phenol and phenolic compounds from oil palm shell. Extraction of the pyrolysis oil from oil palm shell yielded valuable phenolic compounds. It was believed that the phenolic compounds can be further processed to produce useful chemical products.

### **1.1.3 Introduction on xanthan gum**

Malaysia has a great variety of refreshing tropical fruits. Some are seasonal while others are available throughout the year. Conversely tropical Malaysian fruits are plentiful all year round in Malaysia. Local fruits which are especially popular include papaya, passion fruit, watermelon and pineapple. The possibility of using local tropical fruits and starches as an alternative substrate for xanthan production is reported in this thesis.



Thirty percent of the cost of producing xanthan is estimated to be due to the carbon source. Since Malaysia has an abundance of cheap starches and local fruits, xanthan produced using cheap local sources poses a promising substitute to imported xanthan. For enhanced oil recovery, the cost is expected to be further reduced since little processing of the xanthan is needed as compared with food grade xanthan. Although the properties of xanthan gum have been extensively studied on the variations in xanthan properties when different operating conditions, nutrients and carbon sources were used (J. A. Casas, V.E. Santos and F. Garcia Ochoa, 2000). A starch consists of two major components. Chemically, it contains amylose, a linear polymer with a molecular weight in the range of 100,000 - 500,000 and amylopectin, a highly branched polymer with a molecular weight in the range of 1-2 million (L.S. Guinesi *et al.*, 2006). If xanthans produced using various starches were to result in similar xanthans, seasonal fluctuations in starch supply may be overcome and the cheapest source may be used at any time.

In this study, we aim to produce surfactant and xanthan gum from waste and local sources for additives in enhanced oil recovery. The surfactant was produced from pyrolysis oil of oil palm shells. The surfactant produced from oil palm shells industries by simultaneously alkylating and sulfonating the phenolic compounds extracted from the pyrolysis oil of oil palm shell. There are several advantages for selecting oil palm shell as a starting raw material to produce surfactant for EOR processes. First and foremost, it is an inexpensive industrial waste and always readily available. Secondly, it is not a petroleum derivative. Therefore, pyrolysis oil derived from oil palm shell has been selected as the starting raw material. There are very few previous works on the production of surfactant from oil palm shell by alkylating and sulfonating the phenolic compounds in pyrolysis oil. The research on the recycling of oil palm shell to surfactant is a relatively new area. Thus, in this work, the production of the surfactant from pyrolysis oil of oil palm shell is presented.

We also report a laboratory study on the medium formulation and culture conditions for the growth of *X. campestris* and for the production of the extracellular polysaccharide from local fruit and starches as sole feedstock source. In this sense the objective of this work was to determine the feasibility of producing a lower cost xanthan gum alternative from local fruits and starches. This study also focused on the ten types of local fruits and four starches as local carbon sources to produce economically of xanthan gum. In order to

make a comparative analysis of xanthan gum produced, four starches which are tapioca, rice, sweet potato and sago as carbon sources were used to the same conditions. The local fruits and starches were selected as a carbon sources because it was readily available and inexpensive. In the present work also study is the determination of the amylose and amylopectin content based on thermal degradation of starches by thermogravimetric analysis (TGA). The flow properties of the xanthan gum and surfactant produced were compared with a commercial xanthan used in oilfields. The additives were characterised and applied in laboratory displacement experiments.

## **1.2 Statement of Problems**

In this study, the new surfactant and xanthan gum as additives was developed from the oil palm shell, local starches and fruits. The oil palm shell, local starches and fruits were selected as a starting material because it was readily available and inexpensive. Since the research on the production of surfactant from pyrolysis oil of oil palm shell and xanthan gum from local starches and fruits have not been explored and developed to any significant extent, thus, this study would solve the following problems:

1. How to extract the phenolic compounds from the pyrolysis oil?
2. How to synthesize the surfactant from the extracted phenolic compounds of the pyrolysis oil?
3. How to produced xanthan gum from local fruits and starches as carbon sources via shaker fermentantion and fermentation.
4. How is the oil recovery performance if the locally produced surfactant and xanthan gum are applied in the EOR processes, such as surfactant polymer flooding?

### 1.3 Objectives

The objectives of this study are:

1. To extract the phenol and phenolic compounds from produced pyrolysis oil
2. To synthesize a surfactant from pyrolysis oil of oil palm shell and xanthan gum from local starches and fruits via shaker fermentantion and fermentation for enhanced oil recovery applications.
3. To characterize the locally produced surfactant and xanthan gum properties.
4. To investigate the additional incremental oil recovery by the locally produced surfactant and xanthan gum after waterflooding through surfactant-polymer flooding experiment.

### 1.5 Scopes

1. Pyrolysis oil from oil palm shell will be produced using fluidized bed pyrolysis technique at 450 °C, particle size of 212 – 252 µm and feed rate of 0.6 kg/hr.
2. Phenol and its derivatives from the pyrolysis oil will be extracted using liquid-liquid extraction.
3. Surfactants from the extracted phenol of pyrolysis oil from oil palm shell will be synthesized by simultaneously alkylating and sulfonating the extracted phenol with C14 and C16 alpha olefin sulfonic acid. The weight ratio of extracted phenol to olefin sulfonic acid will be set to 100:30, 100:60 and 100:90. Six types of surfactant will be produced.
4. Xanthans from local starches and fruits juice will be produced via fermentation and shaker fermentantion. Ten types of xanthans from local fruits juice and four types from starches will be produced.

5. Locally produced surfactants will be classified using Fourier Transform Infra-Red (FTIR) analysis and the anionic active matter will be determined. Surface tension of the surfactant at ambient temperature, 26° C, will be measured at various concentrations. The surfactant concentration will be set to vary from 0.05 wt. % to 5.0 wt. %.
6. Oil displacement experiment in sand pack model will be conducted using the locally produced surfactant and xanthans to test their flooding efficiency at 26 °C. Six types of surfactant, 14 of xanthan gum will be used. The injected surfactant slug size will be set to 2 PV and the surfactant concentration will be set to 0.5 wt%.

## **CHAPTER 2**

### **LITERATURE REVIEW**

#### **2.1 Surfactant-polymer flooding**

Enhanced oil recovery (EOR) consists of injecting a displacing fluid into injection wells in order to displace the oil and gas in a reservoir towards producing wells. The major EOR processes include thermal, miscible, and chemical methods. Thermal recovery methods add heat to the reservoir by the use of steam or in-situ combustion to reduce oil viscosity. Miscible recovery methods are based on injecting solvents that will mix with the oil under reservoir conditions to dissolve and displace more oil, such as carbon dioxide, CO<sub>2</sub>, light hydrocarbon gases and nitrogen. Chemical EOR methods are designed to improve the sweep efficiency by adding chemicals, such as polymer or surfactant to the injected water in order to reduce interfacial tensions or create a favourable mobility ratio, and thus enhance oil production.

In enhanced oil recovery, surfactants can be used in micellar polymer flooding, surfactant flooding, alkaline surfactant polymer (ASP) flooding or in foams for mobility control of blocking and diverting. Surfactants can be used in several ways to enhance oil production: by reducing the interfacial tension (IFT) between oil

trapped in small capillary pores and the water surrounding those pores, thus allowing the oil to be mobilized; by solubilizing oil in micellar systems; by forming emulsions of oil and water; by changing the wettability of the oil reservoir in alkaline methods or by simply enhancing the mobility of the oil (Taber *et al.*, 1997).

In selecting a suitable surfactant for EOR application, one of the criteria for economic success is minimizing surfactant loss to adsorption. Factors affecting surfactant adsorption include temperature, pH, salinity, type of surfactants and type of solids found in the reservoir. Usually the only factor which can be manipulated for EOR is the type of surfactant to be used; the other factors being determined by reservoir conditions (Laura *et al.*, 2000).

From a technical point of view, chemical flooding of oil reservoirs is one of the most successful methods to enhance oil recovery from depleted reservoirs at low pressure. Surfactants and polymers are the principal components used in chemical flooding. The surfactants lower the IFT between the reservoir oil and injected water, while the polymer as agent to lower water mobility or water–oil mobility ratio to create good mobility control for the surfactant slug. The oil is then displaced by the viscous forces acting on the oil by the flowing water. The surfactant chemical floods that involve combination of other chemical methods including:

- Micellar polymer flooding
- Surfactant polymer flooding
- Microemulsion flooding
- Alkaline surfactant polymer flooding

Surfactant polymer flooding is shown in Figure 2.1. The various regions of immiscible flow during a typical displacement of oil by a surfactant solution are illustrated. The various zones are described as:

- Region 1: Water flooded residual oil saturation; only water is flowing.
- Region 2: An oil bank is formed; both oil and water are flowing.
- Region 3: Surfactant slug forming the low IFT region, two or three phase flow of oil, brine, and microemulsion depending on the actual phase behaviour.
- Region 4: Polymer solution for mobility control, single phase flow of water.

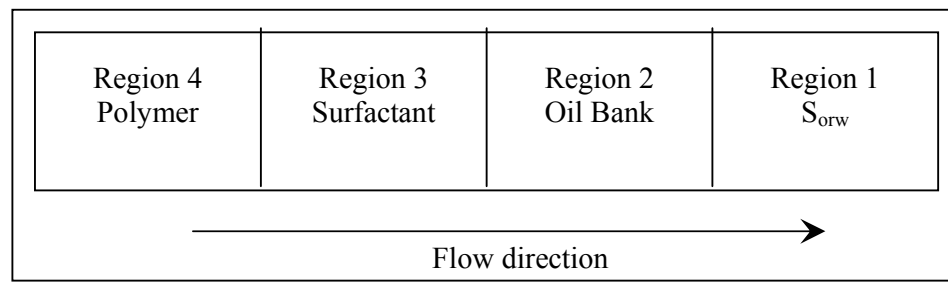


**Figure 2.1** Schematic illustration of a surfactant polymer flooding

The capillary number,  $N_c$ , is related to the residual oil saturation through the desaturation curve illustrated by Figure 2.2.  $N_c$  is defined as the ratio between the viscous and local capillary forces and can be calculated from (Gogarty, 1976):

$$N_c = \frac{v \mu_w}{\sigma}$$

where  $v$  is the effective flow rate,  $\mu_w$  is the viscosity of displacing fluid, and  $\sigma$  is the IFT. If the wettability preference of the rock is taken into account, the formula for  $N_c$  becomes (Thomas *et al.*, 1987):

$$N_c = \frac{v \mu_w}{\sigma \cos \theta}$$

where  $\theta$  is the contact angle measured through the fluid with the highest density. The capillary number, corresponding to the break in the desaturation curve, is designated as the critical capillary number,  $N_{cri}$ . Thus, to improve the oil recovery relative to a

waterflood by using chemicals,  $N_c$  must be significantly higher than the critical capillary number,  $N_c \gg N_{cri}$ .

For an ordinary waterflood under water-wet conditions,  $N_c$  is usually in the range of  $10^{-7}$  to  $10^{-5}$ . The critical capillary number may be in the range of  $10^{-5}$  to  $10^{-4}$ , whereas complete desaturation of the nonwetting phase (oil) may occur at a capillary number in the range of  $10^{-2}$  to  $10^{-1}$  (Lake, 1989). The waterflooded residual oil saturation may be in the range of 30 to 40%. These data are mainly based on model cores, such as Berea cores and other outcrop sandstone cores which have never been in contact with reservoir crude oil. Much lower values are, however, observed under mixed-wet conditions. This implies that 10 times more difficult to remobilize capillary trapped discontinuous oil, compared to continuous oil.

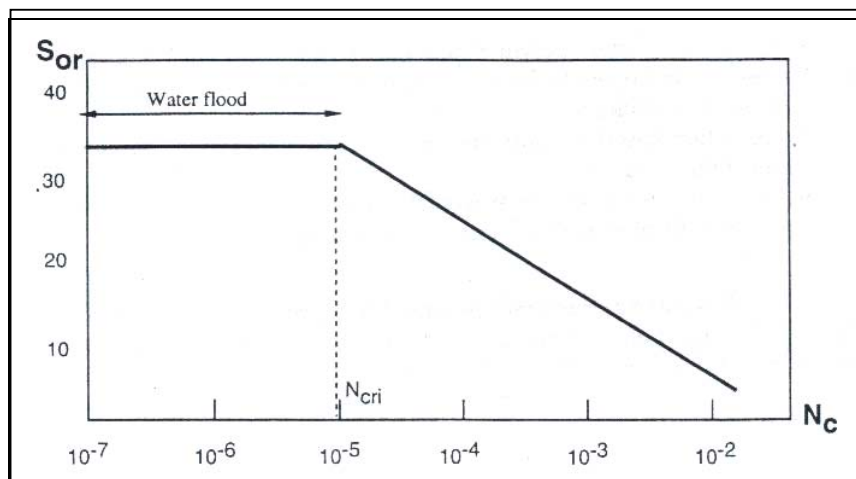


**Figure 2.2** Schematic capillary desaturation curve for a nonwetting phase (Lake, 1989)

In order to be able to mobilize a significant amount of the waterflooded residual oil, it is expected that the capillary number must be increased by a factor of  $10^3$  to  $10^4$ . The only practical way to do this is to reduce the IFT between the reservoir oil and the injected water by the same factor using surfactants, which normally means that the IFT should be between about 0.01 and 0.001 mN/m.



The goal of research on surfactant flooding during the 1990s was to develop surfactants that can recover additional oil in a cost-effective manner during a normal waterflood using produced brine or seawater as injection fluid. In order to avoid many of the problems associated with complicated chemical slugs with high concentration of surfactants and cosurfactants/ alcohols, the following criteria should apply (Austad *et al.*, 2000):

- The only chemicals used are surfactant and polymer
- Low chemical concentration (surfactant 0.1 – 0.5 wt%; polymer < 500ppm)
- No imposed salinity gradient or other phase gradients
- The chemicals should be insensitive to multivalent cations
- The flooding conditions should be a two-phase flood with the surfactant and polymer present in the aqueous phase, forming an oil-in-water microemulsion, termed Type II(-)

The flooding performance is termed Low Tension Polymer Flood, LTPF, or low surfactant concentration enhanced waterflood. Low Tension Polymer Flood (LTPF) or low surfactant concentration enhanced waterflood has been suggested as one of the way to improve the chemical flooding. Coinjection of low concentration surfactant and a biopolymer, followed by a further mobility control buffer, leads to much reduced overall chemical consumption. This method approach addresses a cost effective chemical flooding (Kalpakci *et al.*, 1990). Figure 2.3 shows a LTPF flooding sequence.

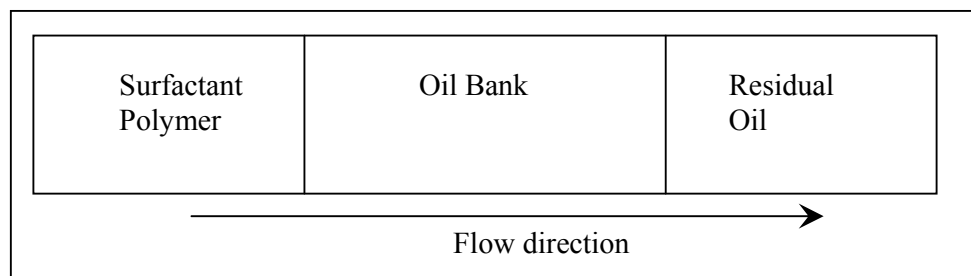


**Figure 2.3** Schematic illustration of a LTPF

### 2.1.1 Field Tests

Surfactant use for oil recovery is not a recent development in petroleum field. Surfactant polymer flooding was tested in several pilots in 1960s. In 1967, Gogarty of Marathon described the Maraflood Oil Recovery Process. A small pore volume injection (5 to 15 PV) of high concentration (5 to 12 %) surfactant was injected to displace oil and water.

Large-scale field tests of surfactant polymer flooding were carried out in the late 1970. A large-scale application of the Maraflood oil recovery process was applied on the (113 acres) Henry Unit in Crawford County, Illinois (Robinson 219-R Project). The oil recovery was around 25 % ROIP.

Vargo (1978) and Holm (1982) presented the micellar/polymer project in Bell Creek field (40 acres) in Montana. This project was a technical success, but an economic failure. 10 % OOIP was produced and the chemical cost was estimated to be \$12/bbl.

Gilliland and Conley (1976) reported surfactant flooding in Big Muddy (1.25 acres). The oil recovery was 36 % of ROIP. The injected chemical slug was 0.25 PV surfactants containing 2.5 % petroleum sulfonate, 3 % isobutyl alcohol, 0–2 wt% sodium hydroxide and 200 ppm xanthan. The chemical slug was then followed by 0.5 PV polymer drive.

Whiteley and Wave (1977) and Widmyer *et al.* (1979) reported on the Salem unit LTPF project. This project used a surfactant slug containing 2 % petroleum sulfonate in softened water (6,000 ppm each of  $\text{Na}_2\text{CO}_3$  and  $\text{NaCl}$ , 1,000 ppm sodium triphosphate). The chemical slug then followed by xanthan polymer slug. The oil recovery was in between 37 % and 43 % ROIP. Tracers were used in attempt to determine sweep efficiency, changes in flow path distribution and chemical utilization.

Maerker and Gale (1992) and Reppert *et al.* (1990) reported pilot test for the Loudon field. Approximately 68 % of waterflooded residual oil was recovered by injecting a 0.3 PV chemical slug contained 2.3 wt% of surfactant with coinjection xanthan biopolymer without cosolvent, followed by 1.0 PV or higher polymer viscosity polymer drive. The chemical formulation containing a blend of two PO-EO sulfates,  $R-O-(PO)_m-E(O)_n SO_3Na$ . The retention of surfactant was low (less than 0.08 mg/g of rock).

Michels *et al.* (1996) represented enhanced waterflooding design with dilute surfactant concentrations for North Sea conditions. It was concluded that alkyl – PO – EO glyceryl sulfonate surfactants could be used in a dilute (0.1 wt %) surfactant flood at North Sea reservoir temperature (<120 °C) without polymer drive but with a sacrificial agent.

Most pilot reported in 1990s were seen to have higher oil recovery than those in 1970s and 1980s. The improvements in chemicals and understanding of process mechanisms were the causes for these successes. These field tests indicated that surfactant polymer flooding can be technically successful. However, the success of surfactant flooding in EOR depends on many factors, including formulations of the chemical used, the cost of the surfactants, the availability of chemicals, environmental impact and oil prices in the market.

Recently, there are surfactants in particular have emerged from the literature search as being newer, intriguing ideas for EOR applications. For example, sulfonated alkyl aromatics have been reported as a new series of surfactants for EOR applications (Berger and Lee, 2002). The new surfactants are different structures where the sulfonated group is attached to the alkyl chain as opposed to the benzene ring. One advantage claimed for this new type of surfactant is that it can be produced in one step process.

Alkyl polyglycosides (APG) are suggested as being candidates for EOR applications (Balzer, 1991). Iglaue *et al.* (2004) concluded that APG surfactants may be formulated in brine solutions that can create IFT approaching 0.01 dyne/cm, or less, versus simple alkane hydrocarbons.

The recent literatures have paid more attention to the new candidates for EOR and to create low IFT conditions.

## **2.2 EOR Chemicals**

EOR chemicals have to be formulated into stable products that meet the requirements for it to be usable in the oil field. First, it has to be stable in a wide range of temperatures, depending on storage conditions. In the oil field, it should be easy and safe to handle with normal precautions. Viscosity is also one of the requirements for extreme weather conditions (-10 °C to 45 °C), not exceeding 800 cP at the lowest temperature. Other considerations, such as flash point, toxicity and biodegradability may also be on the checklist.

Surfactant–brine–oil phase behaviour is the most important feature of a surfactant polymer flooding. Possible combinations of oil, brine, and surfactant will give different phase behaviour. The terminology of surfactant-system phase behaviour has developed through Wilson (1960), Nelson and Pope (1977) and Healy and Reed (1976). The phase behaviour of the chemical formulation has to be evaluated to define which formulation has the best potential to recover additional oil. The formulations are first blended with alkali and polymer. Then an equal amount of crude oil and polymer blend are further mixed together in test tubes by a shaking machine. The mixture of crude oil and chemicals is set for about one week of equilibration at 60 °C. The appearance and numbers of phases are observed and recorded. The best case is considered when only two distinct phases are observed: one water phase and one oil phase, and no third mixed phase are seen.

Adsorption of surfactant on reservoir rock is another important consideration in surfactant flooding formulations. It is well known that high equivalent molecular weight surfactants are adsorbed preferentially on the rock surface while the lower equivalent molecular weight surfactants show a very little adsorption. Since the high equivalent weight surfactants are responsible for most interfacial tension reduction, their losses decrease the surfactant slug ability to displace the residual oil in the reservoir. The solution to reduce the adsorption is either add sacrificial agents into the formulation or pre-flood the reservoir with sacrificial agents. It is also possible to adjust the molecular spectrum (equivalent molecular weight distribution) of the formulation to minimize the adsorption.

In the typical adsorption test, a field core is initially flooded with 3 pore volume (PV) of formation water to satisfy any ion exchange. Then the core is cut into pieces and dried at 80 °C. The crushed core rocks are then mixed mildly with the surfactant solution for 1 day and set for 7 days before the test. The adsorption is determined using a heterogeneous titration method. The surfactant adsorption values range normally between 100 to 450 mg of surfactant/100 g of rock. Tolerable ranges are less than 200 mg of surfactant /100 g of rock.

Other important criteria in EOR surfactant flooding is to determine if the IFT can be reduced enough to produce incremental oil. A spinning drop interfacial tensiometer is usually used to measure IFT. Since the spinning drop test is a dynamic test, IFT is a function of contact time. Until recently, no single surfactant or mixture of surfactants was able to decrease the IFT between water and oil to about 0.01 and 0.001 mN/m by adding a small concentration of surfactant (about 0.1 to 0.5 wt %) to the water injected in an ongoing water flood.

### 2.2.1 Surfactants

A typical surfactant monomer is composed of a non polar (lypophile) portion, or moiety, and a polar (hydrophile) moiety; the entire monomer is sometimes an amphiphile because of this dual nature. Figure 2.4 shows the molecular structure of two common surfactants and illustrates a shorthand notation for surfactant monomers. The monomer is represented by a “tadpole” symbol, with the non polar moiety being the tail and the polar being the head.

Surfactants are classified into four groups depending on their polar moieties. *Anionic surfactants* are dissociated in water in an amphiphilic anion, and a cation, which is in general an alkaline metal ( $\text{Na}^+$ ,  $\text{K}^+$ ). They are the most commonly used surfactants. They include alkylbenzene sulfonates, lauryl sulfate, di-alkyl sulfosuccinate, lignosulfonates etc. They are relatively resistant to retention, stable, and can be made relatively cheaply.

*Cationic surfactants* are dissociated in water into an amphiphilic cation and an anion, most often of the halogen type. A very large proportion of this class corresponds to nitrogen compounds such as fatty amine salts and quaternary ammoniums, with one or several long chains of the alkyl type, often coming from fatty acids. These surfactants are in general more expensive than anionic, because of a high pressure hydrogenation reaction to be carried out during their synthesis. They are highly adsorbed by the anionic surfaces of interstitial clays.

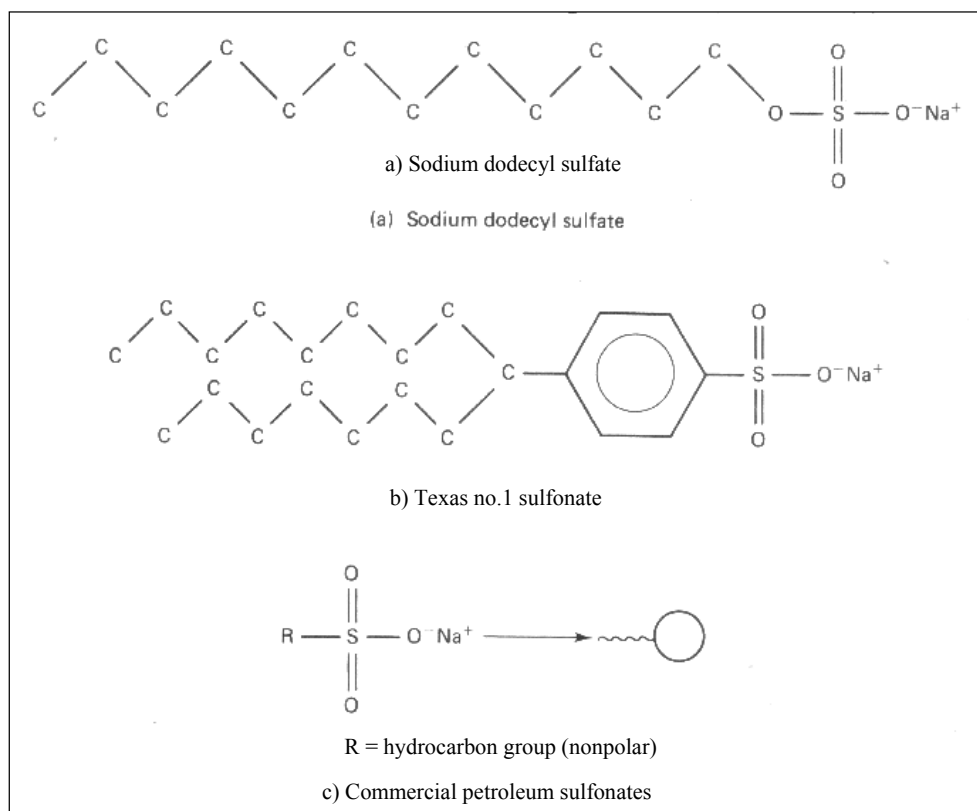


**Figure 2.4** Representative surfactant molecular structures (Larry, 2000)

*Nonionic surfactants* do not ionize in aqueous solution, because their hydrophilic group is a non-dissociate type, such as alcohol, phenol, ether, ester, or amide. These surfactants do not form ionic bonds but, when dissolved in aqueous solutions, exhibit surfactant properties by electronegativity contrasts between their constituents. Nonionics are much more tolerant of high salinities than anionics and historically have been poorer surfactants.

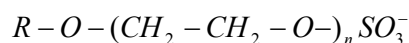
When a single surfactant molecule exhibit both anionic and cationic dissociations it is called *amphoteric* or *zwitterionic*. This is the case of synthetic products like betaines or sulfobetaines and natural substances such as amino acids and phospholipids. These surfactants have not been used in oil recovery.

The unique amphiphilic property of surfactants has made them useful in oil field applications. Their abilities to solubilize, emulsify/demulsify, foam, alter interfacial tension, viscosity and friction have made them ingredients in a variety of fluids. However, on a volume basis, the greatest potential usage would be surfactant flooding for enhanced oil recovery (Larry, 2000). The 1970s and 1980s were active periods for research on surfactants for EOR, and a large number of patents were issued. The following surfactants classes are representative of the large number of surfactant candidates for EOR:

- Alcohol ether sulfates
- Alcohol ethoxylates (alkoxylates)
- Alkyl aryl sulfonates and petroleum sulfonates
- Alkyl phenol ethoxylates
- Dialkyl sulfosuccinates
- Quaternary ammonium (cationic) surfactants

#### **2.2.1.1 Alcohol Ether Sulfates (AES)**

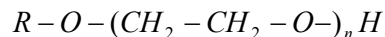
AES can be represented by the following structure:



where R represents a linear or branched alkyl moiety of primary and secondary alcohols or the alkylbenzene part of alkylphenol. Although not shown above, AES may contain repeating units of butylene oxide, propylene oxide (PO) or mixtures of PO and ethylene oxide (EO).



### 2.2.1.2 Alcohol Ethoxylates (Alkoxylates)



where R represents a linear or branched alkyl moiety of a primary or secondary alcohol. Although the ethoxylate structure is shown, alcohol alkoxylates can contain units of ethylene oxide, propylene oxide, butylene oxide or mixtures. Alkyl phenol ethoxylates technically are alcohol ethoxylates; however, they are discussed separately below.

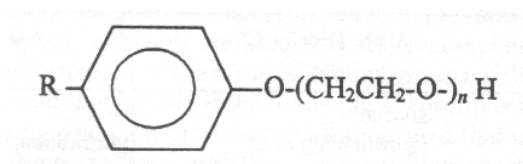
### 2.2.1.3 Alkyl Aryl Sulfonates and Petroleum Sulfonates

Alkyl aryl sulfonates, by definition, have a branched or linear alkyl group attached to a sulfonated aromatic structure (benzene, substituted benzene, naphthalene, etc.). This definition could also be applied to petroleum sulfonates. Alkyl aryl sulfonates history probably begins in the 1930s with kerylbenzene sulfonates, which were synthesized by alkylating benzene with chlorinated kerosene, and the generic name “alkylarylsulfonate” was applied (Feighner, 1976). An improved detergent alkylarylsulfonate was introduced after World War II. The alkyl group was tetrapropylene, and the surfactant was known as dodecylbenzene sulfonate or DBS, TPBS or ABS, also known as “hard” alkylate because of its poor biodegradability. In 1965 the linear alkyl version was introduced to give good biodegradability, and this started a worldwide conversion to “soft” alkylate which is almost complete.

Petroleum sulfonates are distinguished somewhat from alkyl aryl sulfonates by often containing more than one alkyl group (e.g., dialkyl benzene sulfonates), by higher molecular weight and oil solubility thereby making them useful in motor oils, and by the feedstock. Petroleum sulfonates are commonly associated with white oil manufacturing, and are formed by the oleum (SO<sub>3</sub> plus sulfuric acid) sulfonation of streams such as raffinate from lubricating oil streams or bottoms from other operations. Thus, they are a by-product of petroleum refining and are often called

natural sulfonates. These petroleum sulfonates such as alkyl orthoxylene sulfonates are produced to replace the natural products, usually when a more defined chemical structure is needed. The concept of producing petroleum sulfonates from crude oil, specifically for EOR, has been investigated.

#### 2.2.1.4 Alkyl Phenol Ethoxylates (APE)

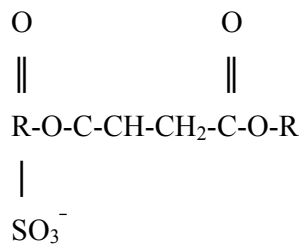


where  $R = C_8 - C_{16}$  linear or branched alkyl chain, and  $n = 1 - 30$ . The structure above shows the para positional isomer which accounts for 90% or more of the ring substitution positions; however, meta and ortho isomers also occur at lesser frequency. Phenol (or hydroxylbenzene) is mostly prepared as a subproduct of acetone manufacturing via the peroxidation of cumene (isopropyl benzene).

APE is produced by two ways, depending on the available raw material. The first method consists in alkylating the phenol according to a classical Friedel-Crafts reaction. The second method consists in adding an alpha-olefin such as propylene trimer or tetramer, or isobutylene dimer, on an aromatic ring.

The most common APE is nonylphenol ethoxylate (NPE) containing around 9 EO and is prepared from the propylene trimer which produces a multitude of highly branched alkyl chains. A  $C_8$  APE, called octylphenol ethoxylate (OPE) is prepared from the dimer of isobutylene to produce the 1, 1, 3, 3-tetramethylbutyl chain.

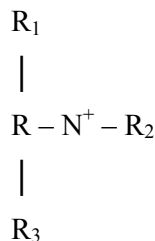
### 2.2.1.5 Dialkyl Sulfosuccinates



where R = linear or branched alkyl groups, usually C<sub>6</sub>, C<sub>8</sub>, C<sub>9</sub>.

The dialkyl sulfosuccinates are more of an industrial-use surfactant class rather than for use in detergents. These surfactants are the best wetting agent; they are also foaming agents, dispersants and emulsifiers. However, their usage is limited by their price which is high in the anionic category.

### 2.2.1.6 Quaternary Ammonium Surfactant



where the R groups may be methyl groups, linear or branched aliphatics, or aromatics.

Quaternary ammonium compounds or “quat” that are monoalkyl structures typically have a C<sub>12-16</sub> alkyl chain and three methyl groups bonded to the quaternary nitrogen atom. Dialkyl quats have two alkyl groups and two methyl groups. Quats can also have aromatic structures such as benzyl group as one of the R groups. Also, the quaternary nitrogen can be in pyridine or an imidazole structure. Quats are included in the list of surfactants for EOR, but technically they are used in other oil field operations, particularly on drilling mud.

It has been known that surfactants lower oil/water interfacial tensions, thus reducing capillary forces such as those trapping the remaining oil. This raises the possibility of releasing trapped oil droplets by injecting surfactants into the reservoir, early demonstrations of the technical feasibility of enhanced oil recovery by surfactant flooding (sometimes referred to micellar or chemical flooding) were done in the laboratory by Novosad *et al.* in 1982 and in field tests by Lake and Pope in 1979 and by Holm in 1982. In addition to the technical feasibility, economic feasibility must also be determined; however, the economic feasibility depends on the complex factors such as oil prices, international economies, and the cost of surfactants. Generally the cost of the surfactant is the single most expensive item in the cost of a chemical flood. These costs include both the initial investment in purchasing the surfactant, as well as the cost of replacing surfactant which has been lost to adsorption. Since these surfactants are synthesized from petroleum, their costs will rise at least as fast as that of the oil they are used to produce. So simply waiting for oil prices to increase will not necessarily make EOR economically feasible (Laura *et al.*, 2000).

#### **2.2.1.7 Fast Pyrolysis Principles**

Pyrolysis is being considered to be an emerging, new and potential technology to produce value-added products, fuels and chemicals from oil palm waste. Chemicals have been produced from biomass in the past, are being produced at present, and will be produced in the future due to the demand for the organic chemicals have increased on a worldwide basis. For example, isolation of chemicals at the industrial scale has been performed to recover commodity compounds such as methanol, acetone, acetic acid and mixture of phenols (Solter and Elder, 1983). Chum and Black (1990) fractionated phenolic/neutral fraction from pine sawdust derived pyrolysis oil using liquid-liquid extraction. Isolation of phenols from *Eucalyptus* wood pyrolysis tar was carried out with the objective of recovering valuable pure phenols, such as phenol, cresols, guaiacol, 4-methylguaiacol, catechol and syringol by Carlos *et al.* (1997).

Pyrolysis may be described as the thermal degradation of materials in the complete absence of inadequate presence of oxygen (Bridgewater and Bridge, 1991). Three products are usually obtained from pyrolysis process: gas, liquid and char. Both the product yield and chemical composition of pyrolysis oil can be varied according to the pyrolysis methods and process conditions (Soltes, 1988).

Fast pyrolysis is a high temperature process in which biomass is rapidly heated in the absence of oxygen. As a result it decomposes to generate mostly vapours and aerosols and some charcoal. Liquid production requires very low vapour residence time to minimize secondary reactions of typically 1 second, although acceptable yields can be obtained at residence times of up to 5 seconds if the vapour temperature is kept below 400 °C. After cooling and condensation, a dark brown mobile liquid is formed which has a heating value about half that of conventional fuel oil. While it is related to the traditional pyrolysis processes for making charcoal, fast pyrolysis is an advanced process which is carefully controlled to give high yields of liquid (Bridgewater *et al.*, 1999).

Research has shown that maximum liquid yields are obtained with high heating rates, at reaction temperatures around 500°C and with short vapour residence times to minimize secondary reactions. A compilation of published data is shown in Figure 2.5 for typical products from fast pyrolysis of wood (Toft and Bridgewater, 1996).

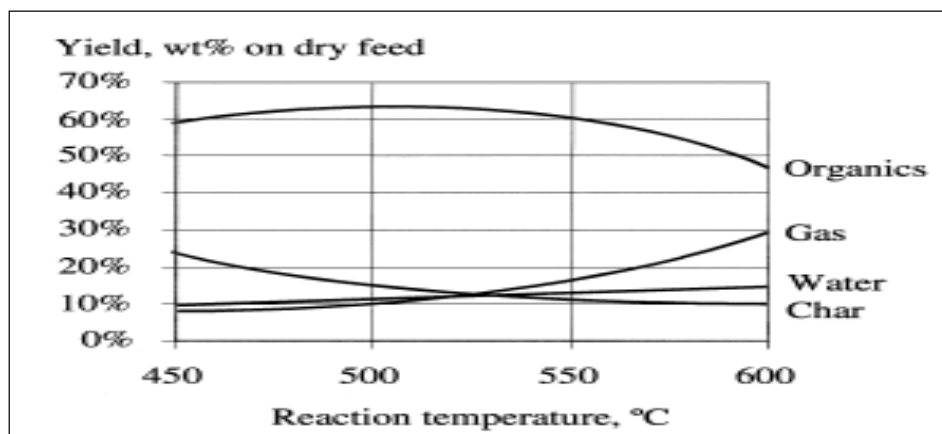


**Figure 2.5** Typical yields of organic liquid, reaction water, gas and char from fast pyrolysis of wood, wt % on dry feed basis (Toft and Bridgewater, 1996).

A variety of reactor configurations have been investigated. Pyrolysis, perhaps more than any other conversion technology, has received considerable creativity and innovation in devising reactor systems that provide the essential ingredients of high heating rates, moderate temperatures and short vapour product residence times for liquids. A thorough review of the technologies has recently been completed (Bridgwater and Peacocke, 1999). There are three main methods of achieving fast pyrolysis.

1. *Ablative pyrolysis* in which wood is pressed against a heated surface and rapidly moved during which the wood melts at the heated surface and leaves an oil film behind which evaporates. This process uses larger particles of wood and is typically limited by the rate of heat supply to the reactor. It leads to compact and intensive reactors that do not need a carrier gas, but with the penalty of a surface area controlled system and moving parts at high temperature.
2. *Fluid bed and circulating fluid bed pyrolysis* which transfers heat from a heat source to the biomass by a mixture of convection and conduction. The heat transfer limitation is within the particle, thus, requiring very small particles of typically not more than 3 mm to obtain good liquid yields. Substantial carrier gas is needed for fluidization or transport.
3. *Vacuum pyrolysis* which has slow heating rates but removes pyrolysis products as rapidly as in the previous methods which thus simulates fast pyrolysis. Larger particles are needed and the vacuum leads to larger equipment and higher costs. Total liquid yields are typically lower at up to  $60\pm 65\%$  compared to  $75\pm 80\text{ wt}\%$  from the previous two methods.

While a wide range of reactor configurations have been operated (Bridgwater, 1999), fluid beds are the most popular configurations due to their ease of operation and ready scale-up. A typical bubbling fluid bed configuration is depicted in Figure 2.6 with utilization of the by-product gas and char to provide the process heat. The figure includes the necessary steps of drying the feed to less than 10% water to minimize the water in the product liquid oil, and grinding the feed to around 2 mm to give sufficiently small particles to ensure rapid reaction. This configuration is used below for processing waste wood.

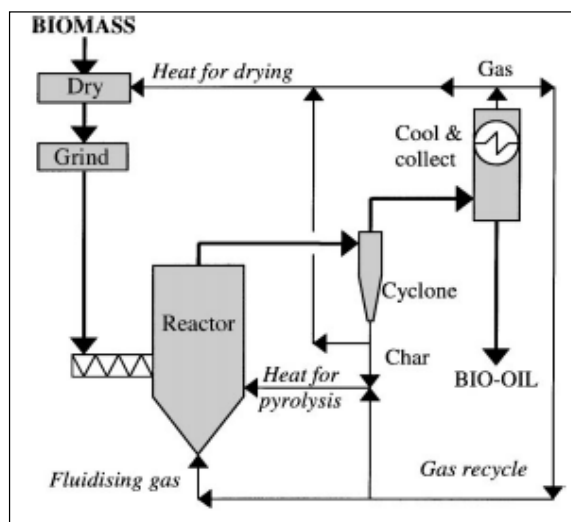


**Figure 2.6** Conceptual fluid bed fast pyrolysis process (Bridgwater and Peacocke, 1999).

### 2.2.1.8 Pyrolysis Oil

Biomass pyrolysis oil differs a great deal from petroleum-based fuels in both physical properties and chemical composition. There are many applications of pyrolysis oil, such as liquid fuel, transport fuel, and as a source of chemicals (Spitzer and Tustin, 2001). Pyrolysis oil can be upgraded to high quality hydrocarbon fuels and recoverable for production of valuable chemicals as well.

According to Diebold and Bridgwater (1997), the commercial uses of the fast pyrolysis oil are as a source of high valued specialty chemicals in the short term and as petroleum fuel substitute in long term. The high valued specialty chemicals include hydroxyacetaldehyde, food flavours for meat preservation, the recovery of levoglucosan sugars to ethanol, organic acid for road de-icing and phenolics for phenol formaldehyde resins (Ani and Zailani, 1996).

Wong (2002) reported that as comparing phenol price at RM 3270/ton with the production cost of palm shell based phenol at RM 923.60/ton, the price was less 71.76 %. Thus, the usage of palm shell based phenol to replace the petroleum based phenol is very promising.

The physical properties of pyrolysis oil from different raw materials are given in Table 2.1. Islam *et al.* (1999) described the chemical composition of oil palm based pyrolysis oil (Table 2.2). It was found that the pyrolysis oil contained a very low concentration of paraffin and no polycyclic aromatic hydrocarbons. The oil palm shell based pyrolysis oil contained a high concentration of phenolics and acetic acid.

**Table 2.1:** Physical properties of different pyrolysis oils

Physical properties	Kai Spila <i>et al.</i> (1997)	Kai Spila <i>et al.</i> (1997)	Islam <i>et al.</i> (1999)
	Pine Oil	Hardwood oil	Palm Shell Oil
Ash (wt%) (ASTM D482)	0.07	0.09	0.1
Moisture content (wt%) (ASTM 4928-89)	11.1	23.3	10
Calorific value (MJ/kg) (ASTM D240)	19.2	18.1	22.1
Density (g/cm <sup>3</sup> ) (ASTM D 5004)	1.266	1.23	1.2



Viscosity ( at 50°C)			
(cSt)	46	50	14.63
(ASTM D 445)			
pH	2.6	2.8	2.7
Flash Point (°C)	18	>106	54
(ASTM D 93)			
Pour point (°C)	76	-9	-10
(ASTM D 97)			
Distillation (°C)			
(ASTM D 86)			
IBP(initial boiling point)	ND	ND	94
10%			100
30%			120
50%			155
70%			182
75%			190
80%			
90%			
Decomposed at			190

\*ND = Not determined

**Table 2.2:** Identification and quantification of chemical compounds in pyrolysis oil from oil palm shell (Islam *et al.*, 1999)

Chemical compounds	Quantification (wt% of pyrolysis oil from oil palm shell)
Phenol	28.3
Acetic acid	16.9
3-hydroxy 2-propanone	7.78
2 methoxy phenol	4.82
Ally acetate-2 ene	4.73
2-Furaldehyde	4.41
2,6-dimethoxy phenol	2.75
Methyl crotonate	2.69
Ortho-hydroxy phenol	2.16
Butandial	2.13
2-methoxy -4 methyl phenol	2.02
3-methyl cyclopentanedione	1.38
4-propene 2-methoxy phenol	1.36
Cyclopentanone	1.34
4-ethyl -2 methoxy phenol	1.09
2-methyl pentyl ether	0.838
2-Butanone	0.837
2-methyl phenol (o-cresol)	0.79
2-methyl propane	0.524

### 2.2.2 Extraction of Phenol from Pyrolysis Oil

In 1980, Gallivian and Matschei obtained a phenolic fraction from wood pyrolysis oil by aqueous alkaline extraction, followed by acidification of the aqueous phase. The phenols were recovered by organic solvent extraction. The biomass-derived phenols could replace 25 – 75 % of commercial phenol used in the production of adhesives.

In accordance with this invention the oil derived from pyrolysis of lignocelluloses waste materials was first mixed with a strong basic solution such as a sodium hydroxide solution. The resulting black colour mixture with a pH range of from about 11 to about 13 was then contacted with an appropriate solvent such as methylene chloride in a suitable extraction unit. A first extract was removed from this unit comprising the neutral fraction of the oil which was subjected to distillate operation to remove the solvent and recover the neutral fraction.

The raffinate from this unit was mixed with mineral acid, such as sulfuric acid, or with carbon dioxide to lower its pH to the range of from about 7.5 to about 9.0, before it was introduced into a second extraction unit wherein it was contacted with a solvent such as methylene chloride. By this extraction step the phenolic fraction was removed with the solvent as the second extract which was distilled to recover the solvent and the phenolic product. The second raffinate from the second extraction unit was mixed with a mineral acid such as sulfuric acid to reduce its pH to the range of from about 1.0 to about 4.0, the tarry residues separated and the mixture was then introduced into a third extraction unit wherein it was contacted with methylene chloride. The third extract from this unit, after the removal of the tarry product was distilled to separate the solvent and recover the organic acids fraction. The third raffinate from the third extraction unit was neutralized and transported to a waste disposal system.

The phenolic fraction obtained by this extraction method was used as total or partial replacement for petroleum-derived phenol in making phenol-formaldehyde resins. Generally, the extraction method is summarized by the flow sheet in Figure 2.7.

The previous extraction method by Gallivian *et al.* (1980) used pyrolysis oils which were usually formed at ill-defined temperatures and which had undergone phase separation cracking and some condensation, and suffered from very low yields. Chum and Black (1990) published an improved and simplified process of fractionating fast-pyrolysis oils derived from lignocellulosic materials.

The process included mixing the oils with an organic solvent having at least a moderate solubility parameter and good hydrogen bonding capability, the solvent extracted the phenol and neutral fractions from the oils. The organic solvent-soluble fraction contained the phenol and neutral fractions was separated from the mixture and admixed with water to extract water-soluble materials.

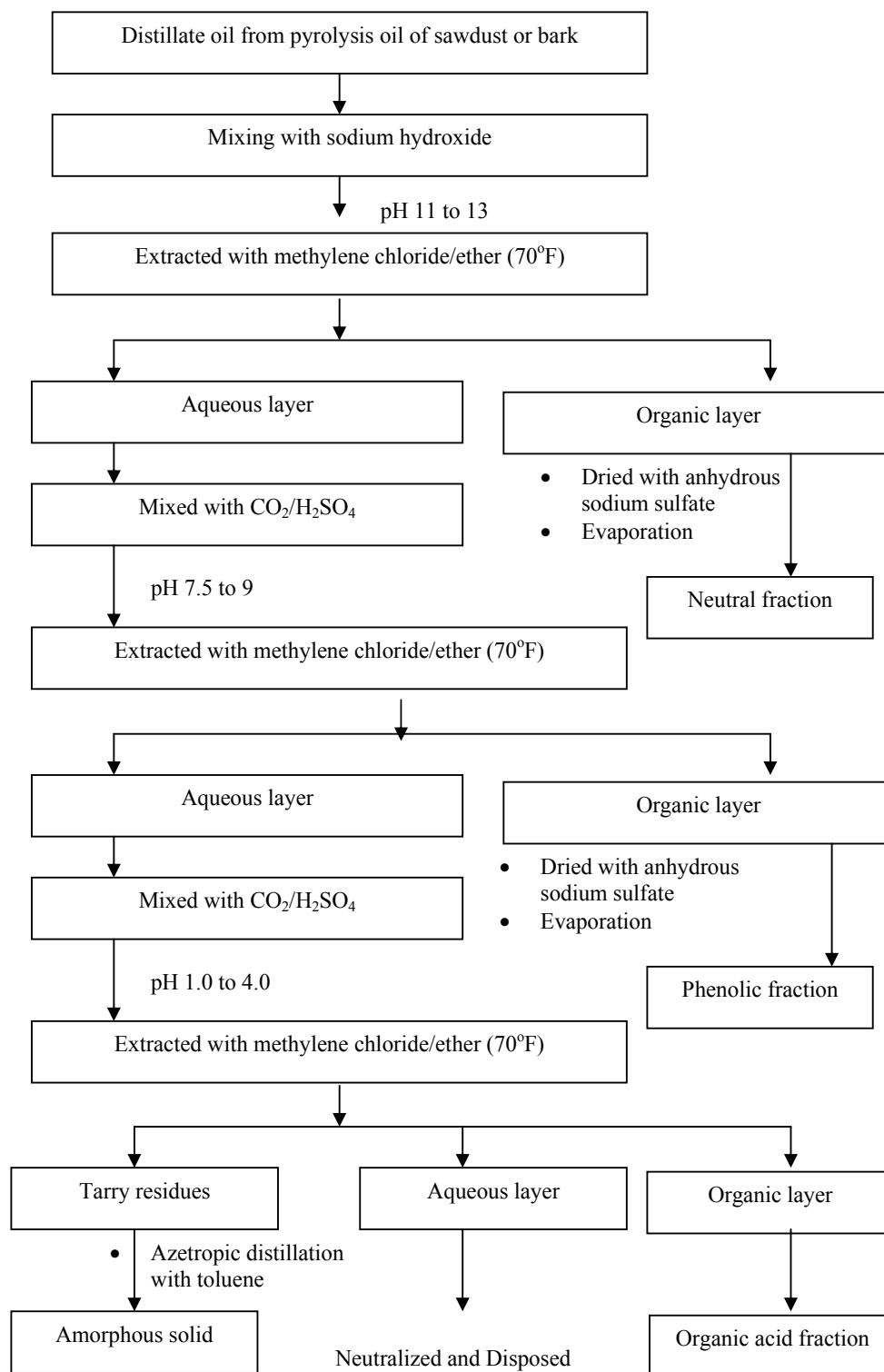


**Figure 2.7** Flow sheet of extraction of phenol from pyrolysis oil  
(Gallivan *et al.*, 1980)

The organic solvent soluble fraction was then separated from the water fraction and admixed with an aqueous alkali metals bicarbonate solution to extract strong organic acids and highly polar compounds from the solvent fraction. Finally, the residual organic solvent-soluble fraction was separated, and the organic solvent was removed to produce phenol-containing compositions.

In general, the whole oil was first dissolved in the organic solvent preferably in oil: solvent ratio of 0.5:1 to 1:3 by weight. The preferred solvent was ethyl acetate. The oil was initially filtered to separate char which was carried over from the pyrolysis reactor operations. Upon standing, the solvent/oil mixture then separated into two phases, the solvent-soluble phase and the solvent-insoluble phase. Chemical spectroscopic analysis revealed that the ethyl acetate-insoluble fraction contained carbohydrate and carbohydrate-derived products.

The ethyl acetate-soluble fraction, containing the phenol/neutral fractions, was then separated and washed with water to remove the remaining water-soluble carbohydrate and carbohydrate-derived materials, preferably in a 1:6 to 1:1, water: oil weight ratio. The ethyl acetate-soluble fraction was then further extracted with an aqueous metal bicarbonate solution, preferably an aqueous sodium bicarbonate solution, 5% by weight. The pH of the bicarbonate extraction solution was preferably maintained at approximately 8-9.5, and a 6:1 to 0.5:1 bicarbonate solution: oil weight ratio was preferably utilized. The aqueous bicarbonate layer extracted the strong organic acids and highly polar compounds, and the remaining ethyl acetate-soluble layer contained the phenols and neutral fractions.

This ethyl acetate-soluble layer was then separated, and the ethyl acetate solvent was evaporated using any known evaporation technique, including vacuum evaporation techniques. The dried phenol/neutral fraction typically contains 0.5-1% of water with traces of ethyl acetate.

The phenols/neutrals fraction could be further fractionated into isolated phenolics and neutrals if desired. This could be accomplished by utilizing a 5% by weight solution of sodium hydroxide in a volume ratio of 5:1 of solution: extract. The aqueous layer was then acidified to a pH of about 2 utilizing a 50% solution of phosphoric acid although other acids could be used. It was then saturated with sodium chloride and extracted with ethyl acetate. Evaporation of the solvent led to the isolation of the phenolics fraction; evaporation of the initial ethyl acetate solution free from phenolics led to the neutrals fraction.

In 1997, Carlos *et al.* investigated the possibility of isolating valuable phenols from raw wood tar at laboratory scales with a potential application at a higher scale. Isolation of phenols from Eucalyptus wood pyrolysis tar was carried out with the objective of recovering valuable pure phenols, such as phenol, cresols, guaiacol, 4-methyl guaiacol, catechol and syringol.

The procedure consisted of four main steps:

- (1) The wood tar-derived oil containing the desired phenols was dissolved in ethyl acetate;
- (2) An aqueous alkaline solution was added to extract phenols by converting them into water-soluble phenolate ions;
- (3) Phenols were regenerated by acidification of the aqueous layer with sulfuric acid; and
- (4) A phenolic-rich fraction was recovered by ethyl acetate extraction of the acidic aqueous layer. The procedure was performed at room temperature.

The detailed procedure was as follows:

- a) An accurate amount of primary oil weighing between 2 and 6 g was dissolved in ethyl acetate at a 1: 1 weight ratio to improve the flow ability and to decrease the density of the original oil.
- b) The solution was mixed with an aqueous sodium hydroxide solution in a 1: 1 ratio by weight in a 125 ml separatory funnel. The phases could be clearly

distinguished at this ratio. The funnel was shaken and phases were separated on standing and pH was measured.

- c) The alkaline extraction of the solvent phase was repeated five times with fresh alkali solution.
- d) The combined aqueous phases were collected in a 125 ml separatory funnel and the phenols were regenerated by acidifying the solution with a solution of sulfuric acid 50% by weight to a pH near 6. It had been observed that phenols were better extracted from the aqueous phase at a pH below 7.

Ethyl acetate was used as the organic solvent to recover the phenols from the aqueous phase. An earlier study has shown that ketones and esters were good solvents for the removal of phenols from water (Won and Prausnitz, 1975). Ethyl acetate in particular, had been used for the extraction of wood tar phenols with optimum results. The extraction was repeated four times with a 0.5:1 solvent/aqueous phase weight ratio.

The extraction procedure was carried out using NaOH solutions of 2, 0.3 and 0.05 M to determine the effect of pH on the recovery of phenols. Complete recovery of phenols was achieved at a pH of 12-13 by using a concentrated alkaline solution. A scheme of the liquid-liquid extraction procedure is shown in Figure 2.8.

In 2000, Jamil *et al.* extracted the phenolic compounds from the pyrolysis of oil palm shell. A standard solvent was selected for the purpose of extraction of phenols from the pyrolysis oil. The requirements for the organic solvent were low boiling point, relatively low solubility in water, high solubility in oil.

The preferred solvent was ethyl acetate. The whole oil was dissolved in the ethyl acetate to oil: solvent ratio of 1:3 at pH of 3.1 and then filtered with Whatman filter paper of specification 12.5 cm 100 circles. The oil solvent mixture was collected in a separating funnel and the thick residual tarry portion was removed. A 5% sodium bicarbonate solution was mixed with the oil solvent mixture at a proportion of 1:2 bicarbonate solution: oil weight ratio, the pH value of this standard solution was maintained at 8.9. As a result of mixing, the mixture separated into two



phases. The aqueous bicarbonate layer extracted the strong organic acids and highly polar compounds, and the remaining ethyl acetate-soluble layer contained the phenols and neutral fractions. This ethyl acetate-soluble layer was then separated, and the ethyl acetate solvent was evaporated using an E-01611-00 Economy Rotary evaporator.

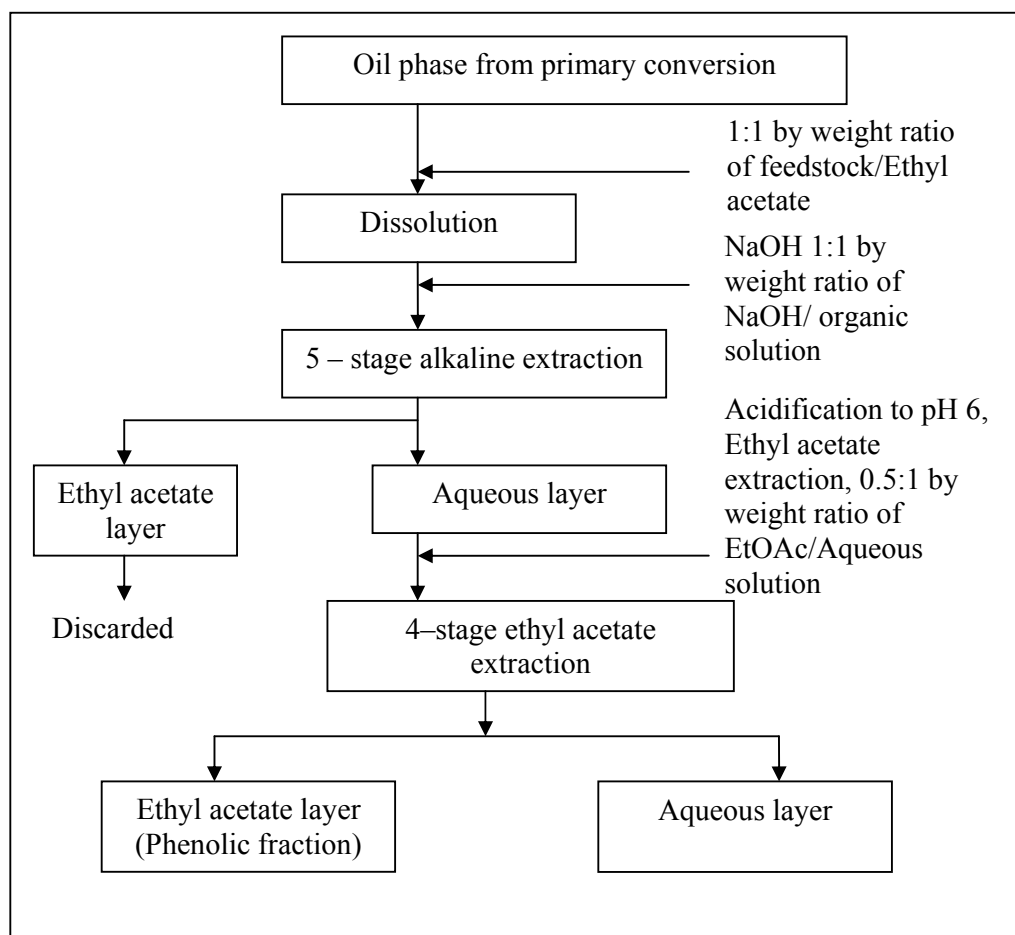


**Figure 2.8** Liquid-liquid extraction of phenols from primary oil (Carlos *et al.*, 1997)

After evaporating, the liquid product was collected and stored in refrigerator at 5 -10 °C. This was then subjected to Gas Chromatograph – Flame Ionization Detector (GC–FID) analysis using DB -1701 160 mm x 0.25 mm x 0.25µm capillary column in order to identify the quantify the phenols content in the liquid product. The carrier gas used is helium.

A simple flow sheet of extraction of phenol from oil palm shell pyrolysis oil is shown as below. This extraction method is similar to the Chum *et al.* (1980) s' work.

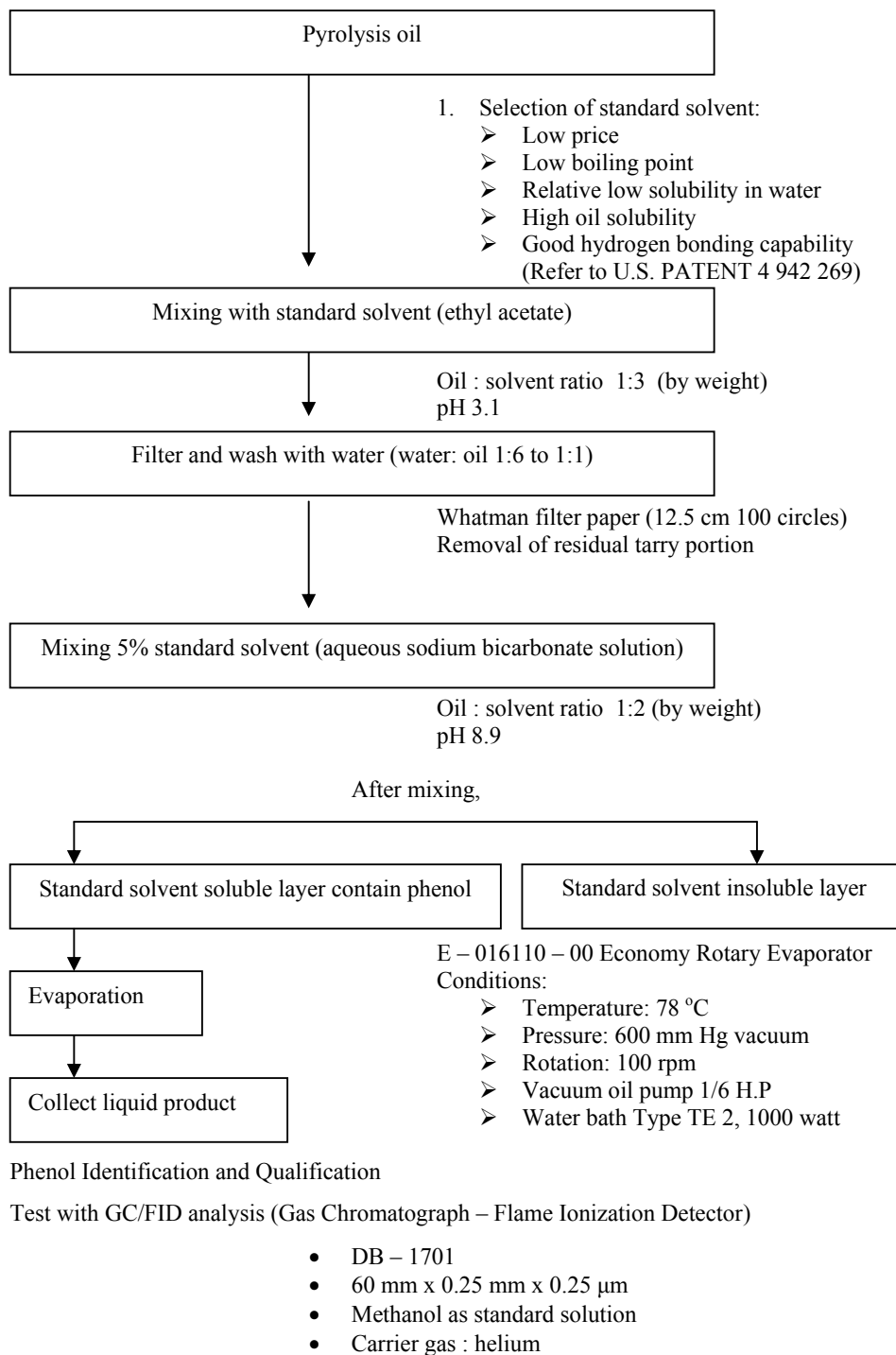
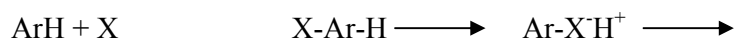


**Figure 2.9** Flow sheet of extraction of phenol from oil palm shell pyrolysis oil  
(Jamil *et al.* 2000)

### 2.2.3 Basic Chemistry of Sulfonation and Sulfatation

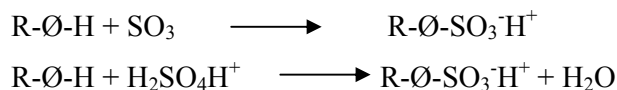
Sulfonation and sulfation are major industrial chemical processes used to make a diverse range of products, including dyes and color intensifiers, pigments, medicinals, pesticides and organic intermediates. Additionally, almost 500,000 metric tons per year of lignin sulfonates are produced as a by-product from paper pulping. Petroleum sulfonates are widely used as chemicals in chemical flooding in EOR.

Sulfonation of an aromatic ring takes place according to an electrophilic substitution, to produce an intermediate sigma complex that rearranges as an alkylbenzene sulfonic acid:



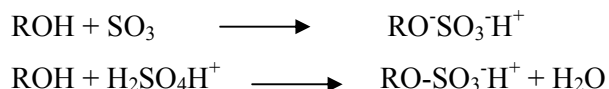
where Ar-H represents the aromatic ring and X an electrophilic group:  $\text{SO}_3$ ,  $\text{H}_2\text{SO}_4$ , etc.

Symbol  $\text{Ar-X}^-\text{H}^+$  is used because the sulfonic acid is a strong acid, i.e., completely dissociated, even at low pH. With an alkylbenzene  $\text{R-O-H}$  the reaction will be:



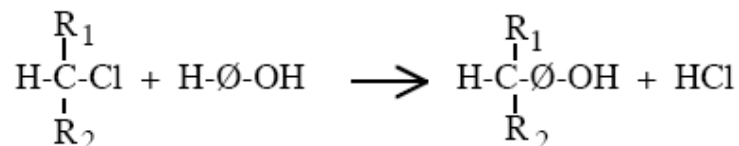
There exist other mechanisms, such as addition on the double bond of an olefin or an unsaturated acid, or the nucleophilic substitution ( $\text{S}_\text{N}2$ ) in alpha position of a carboxylic acid.

Sulfatation is the esterification of an alcohol by one of the two acidities of sulfuric acid or anhydride. It results in an alkyl ester monosulfuric acid.

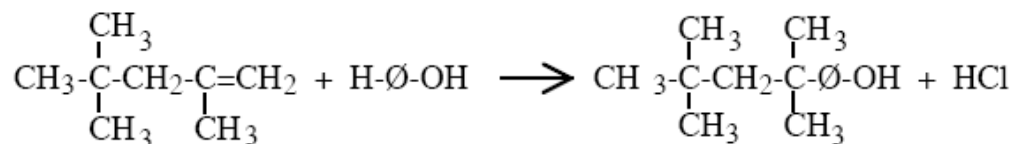


## 2.2.4 Ethoxylated Alkyl-Phenols

Phenol (or hydroxybenzene) is mostly prepared as a sub product of acetone manufacturing via the peroxidation of cumene (isopropyl benzene). Ethoxylated alkyl-phenols are produced by two ways, depending on the available raw material. The first method consists in alkylating the phenol according to classical Friedel-Crafts reaction:



The second method consists in adding an alpha-olefin such as propylene trimer or tetramer, or isobutylene dimer, on an aromatic ring. This technique results in nonyl, dodecyl and octyl phenols, with branched, thus non biodegradable alkylates. One of the most common alkylphenol has been for many years the ter-octyl-phenol produced by the Friedel-Crafts alkylation of phenol by isobutylene dimer. As seen in the following formula this substance exhibits two tertiary carbon atoms which are a challenge to biodegradation.



Common commercial products are the octyl, nonyl and dodecyl-phenol with a degree of ethoxylation ranging from 4 to 40. Octyl and nonyl-phenols with EON = 8-12 are used in detergents. With EON < 5 the attained products are antifoaming agents or detergent in non aqueous media. With EON ranging from 12 to 20, they are wetting agents and O/W emulsifiers. Beyond EON = 20 they exhibit detergent properties at high temperature and high salinity.

The main use of alkyl phenols is as ingredients for domestic and industrial detergents, particularly for high electrolyte level: acid solution for metal cleaning, detergents for dairy plants, agrochemical emulsions and styrene polymerization.

Since branched alkylates are not readily biodegradable, the trend has been in the past decades to go into more linear products. However the additional cost has restrained that trend, which has been substituted in the past decade by another way to cut price and toxicity alike, i.e. the elimination of the benzene ring altogether, e.g. the substitution by ethoxylated linear alcohols. The dilemma is that alcohol ethoxylates are not as good detergents as their counterpart phenol compounds, just as it is the case with alkylbenzene sulfonates versus alkane or olefin sulfonates.

#### **2.2.5 Synthesis of New Alkylaryl Sulfonic Acids as Potential Surfactant for EOR Application**

The most commonly used anionic surfactants in oil recovery are synthetic and “natural” alkylbenzene sulfonates, alkyl toluene sulfonates, alkyl xylene sulfonates, alkyl diphenylether sulfonates, alpha-olefin sulfonates, sulfonated or sulfated alkoxyated alkylphenols or mixtures of two or more of these surfactants. Many of the above surfactants can be easily synthesized by simultaneously alkylating and sulfonating the aromatics as described in Berger *et al.* (2002).

Berger *et al.* (2000) developed a new process for producing novel sulfonated alkylaromatic compounds in which the aromatic group is sulfonated and alkylated in one step. The new process uses an alpha-olefin sulfonic acid to alkylate and sulfonate an aromatic compound, such as benzene or naphthalene; or a substituted aromatic compound, or any other polycyclic aromatic compounds, such as alkylbenzene, alkylnaphthalene, phenol, alkoxyated phenol, or alkoxyated alkylphenol.

The resulting alkylaryl sulfonic acids differ from existing products by having the sulfonate group attached to the alkyl chain rather than the ring. This allows for better solubility in water and more thermal stability than conventional alkyl or alkylaryl sulfonates.

Figure 2.10 compares the new process with the conventional process for making alkylaryl sulfonic acids and also shows the structural differences between the two products.

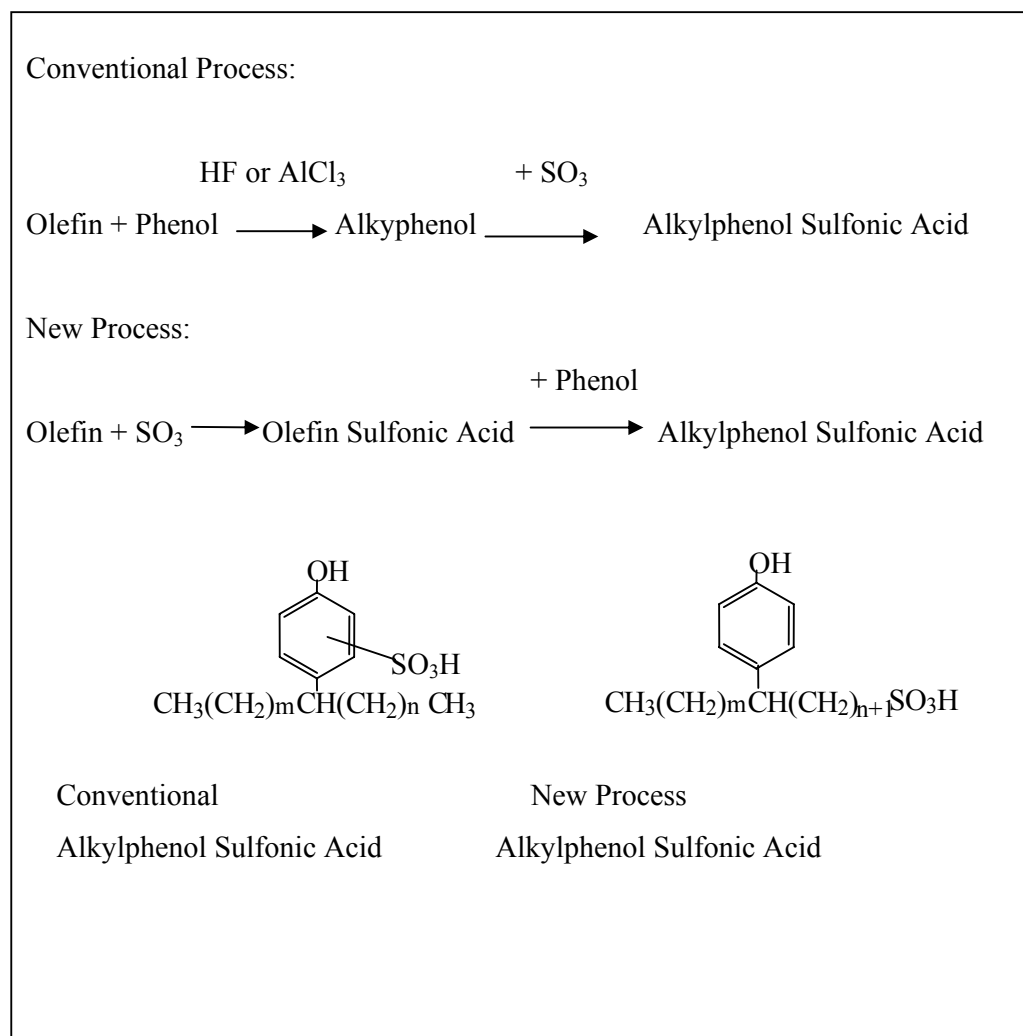


**Figure 2.10** Comparison of conventional and new process alkylphenol sulfonic acid

The alpha-olefin sulfonic acid used is a mixture of alkene sulfonic acid and sultone. It is made by the thin-film sulfonation of an alpha-olefin using SO<sub>3</sub>. During the reaction, in the presence of water and heat, sultone is converted into hydroxyalkane sulfonic acid. Subsequent removal of the water at elevated temperatures dehydrates the hydroxyalkane sulfonic acid, converting it back into sultone and additional alkene sulfonic acid. This procedure is used in the synthesis process to convert the sultone to alkene sulfonic acid and allow it to react with aromatic compounds. The ratio of alkene sulfonic acid to sultone is from about 1:1 to about 1:4 in alpha-olefin sulfonic acid, depending on manufacturing temperature, pressure, flow rates and other parameters known to those skilled in the art. The position of the double bond of the alkene sulfonic acid, and the number of carbons in the sultone ring can also vary depending on these same parameters (Berger et al., 2000). Figure 2.11 shows the reactions to produce the new family of surfactants.

Where,

R' = H, alkyl (branched or linear) or alkoxyate (EO, PO BO or mixtures) or OH

R'' = H, alkyl (branched or linear)

R''' = H, alkyl (branched or linear)

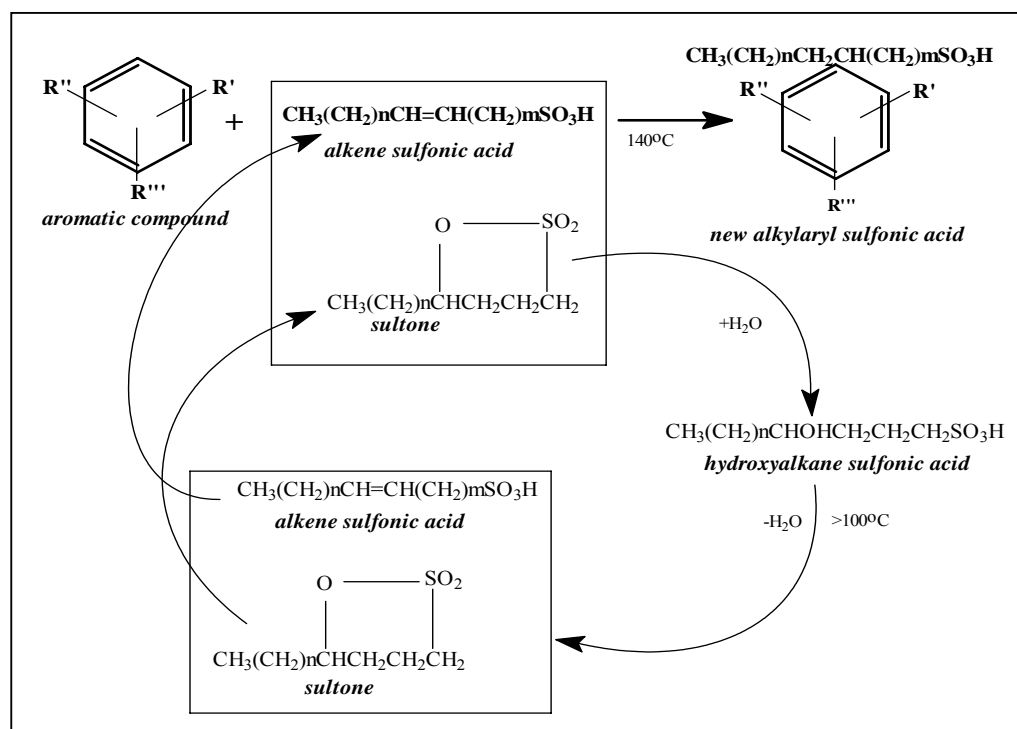
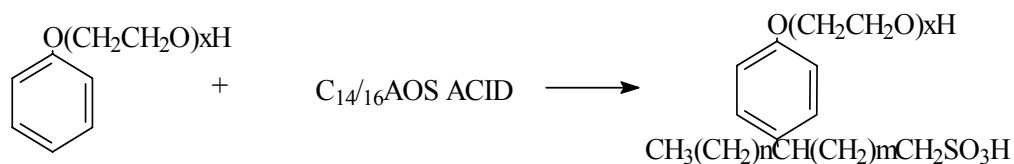


**Figure 2.11** Reaction of alpha-olefin sulfonic acid with alkylaryl compounds

A catalyst may be useful to reduce the reaction temperature, the reaction time and improve yields. Useful catalysts include sulfuric acid, methane sulfonic acid, methane di-sulfonic acid, sulfosuccinic acid, sulfomalonic acid, and other strong acid catalysts. Pressure may be necessary in order to reach the desired higher temperatures when using low boiling starting materials such as benzene and to prevent water from escaping during the early stages of the reaction. The free acid may be further reacted with any of a number of cations such as Na, K, NH<sub>4</sub>, Ca, Mg, Ba, Amines, etc. to form anionic surface active salts.

#### 2.2.5.1 Example of Preparation of Alkoxyated Alkylphenol Sulfonic Acid



58 grams (0.2 Moles) of C14/16 AOS acid along with 71.6 grams (0.2 Moles) phenol + 6 EO (Crisanol™ 0606) were added to a 250 ml glass round-bottomed flask equipped with a stirrer, thermocouple temperature controller and reflux condenser. The charge was gradually heated to 130 °C and held at temperature. A sample was taken periodically and analyzed for sulfonic acid concentration until the sulfonic content remained constant.



### 2.3 Xanthan gum

Xanthan gum is a polysaccharide with a  $\beta$ -D-glucose backbone like cellulose, but every second glucose unit is attached to a trisaccharide consisting of mannose, glucuronic acid, and mannose. The mannose closest to the backbone has an acetic acid ester on carbon 6, and the mannose at the end of the trisaccharide is linked through carbons 6 and 4 to the second carbon of pyruvic acid (Figure 2.12). The presence of anionic side chains on the xanthan gum molecules enhances hydration and makes xanthan gum soluble in cold water. Xanthan gum is produced by the bacterium *Xanthomonas campestris*, which is found on cruciferous vegetables such as cabbage and cauliflower. The negatively charged carboxyl groups on the side chains cause the molecules to form very viscous fluids when mixed with water. Xanthan gum is used as a thickener for sauces, to prevent ice crystal formation in ice cream, and as a low-calorie substitute for fat. Xanthan gum is frequently mixed with guar gum because the viscosity of the combination is greater than when either one is used alone. The acetylation and pyruvylation levels vary depending on fermentation conditions but typical values. Typically pyruvate residues can be found on 30-40% of the terminal mannose residues whereas 60-70% of the internal mannose residues may contain acetate groups. Recent work has looked at the properties of GM modified strains of xanthan gum that are either deficient in acetate groups, pyruvate groups or both (R.Rosalam and R.England, 2005).

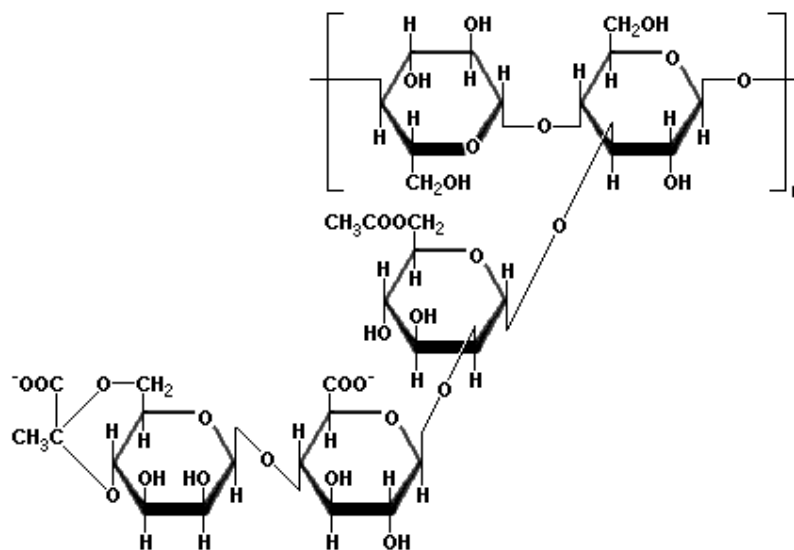


**Figure 2.12** The repeating unit of xanthan gum (R.Rosalam and R.England, 2005).

Xanthan gum solutions have ability to form highly viscous solutions at low concentrations and stable viscosity over a wide range of environmental conditions namely ionic strengths, heat and pH as well as enzymes. The effect of salt on viscosity depends on the concentration of the xanthan gum in solution. At low gum concentrations (below 0.3 % w/w), mono-valent salts such as NaCl, it can cause a slight decrease in viscosity. Conversely, NaCl addition at higher gum concentrations increases solution viscosity, the same effects occur with most divalent metals salts. Xanthan has several advantages as a mobility control agent in enhanced oil recovery. It is high pseudoplasticity (shear thinning properties), flocculent, stable to pH and temperature changes and to high salt concentrations, effective lubricant, thermal stability, salt compatibility and allows easy injectability. The special rheological properties of xanthan are technologically suitable for the 'Enhanced Oil Recovery' (EOR) applications. At low concentration, the gum forms high viscosity solution that exhibit pseudoplasticity. For the efficient displacement of oil the pumping of xanthan gum solution in the rocks is necessary. As a result oil held in the pores of the sand stone rocks is displaced. Currently, the world wide consumption of xanthan gum is approximately 23 million kg/y, approximately 5 million kg/y are used as a drilling fluid viscosifier in the oil industry. The petrochemical industry uses other plant-derived polysaccharide and synthetic polymers instead of xanthan gum based

on the relative costs of xanthan gum to the other polymers (F.kamal et. al. 2003 and P.adhikary et.al. 2004).

Several researchers have investigated using less expensive carbon sources to produce xanthan gum. S.D. Yoo, *et. al.* 1999 used waste sugar beet pulp to produce xanthan gum. O.S.Azeez, 2005 demonstrated that cashew tree latex could be used to produce xanthan gum. Lopez and Cormenzana, 1996 investigated the use of olive-mill wastewaters as low cost substrate for xanthan gum production. Variation in the amount of amylose and amylopectin in a starch changes the behaviour of the starch. The amylose component of starch controls the gelling behaviour since gelling is the result of re-association of the linear chain molecules. Amylopectin is usually larger in size. The large size and the branched nature of amylopectin reduce the mobility of the polymer and their orientation in an aqueous environment. Figure 2.13 (a) and (b) shows the structures of the amylose and amylopectin components of a starch molecule. The abundance in hydroxyl groups in the starch molecules impart hydrophilic properties to the polymer and thus its potential to disperse in water. Starch is the second most abundant biomass found in nature, next to cellulose.

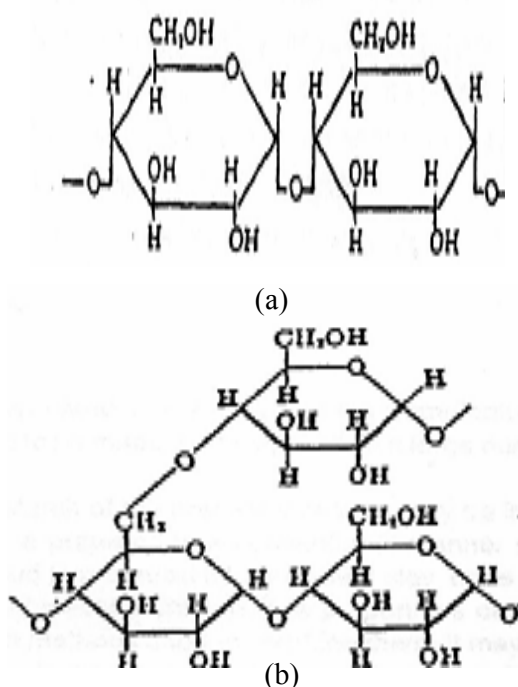


**Figure 2.13** Building Units of Starch (a) Amylose and (b) Amylopectin

Xanthan gum is a polysaccharide with a  $\beta$ -D-glucose backbone like cellulose, but every second glucose unit is attached to a trisaccharide consisting of mannose, glucuronic acid, and mannose. The mannose closest to the backbone has an acetic acid ester on carbon 6, and the mannose at the end of the trisaccharide is linked through carbons 6 and 4 to the second carbon of pyruvic acid (Figure 2.14) The presence of anionic side chains on the xanthan gum molecules enhances hydration and makes xanthan gum soluble in cold water.

Xanthan gum is produced by the bacterium *Xanthomonas campestris*, which is found on cruciferous vegetables such as cabbage and cauliflower. The negatively charged carboxyl groups on the side chains because the molecules to form very viscous fluids when mixed with water. Xanthan gum is used as a thickener for sauces, to prevent ice crystal formation in ice cream, and as a low-calorie substitute for fat. Xanthan gum is frequently mixed with guar gum because the viscosity of the combination is greater than when either one is used alone. The acetylation and pyruvylation levels vary depending on fermentation conditions but typical values. Typically pyruvate residues can be found on 30-40% of the terminal mannose residues whereas 60-70% of the internal mannose residues may contain acetate groups. Recent work has looked at the properties of GM modified strains of xanthan gum that are either deficient in acetate groups, pyruvate groups or both.

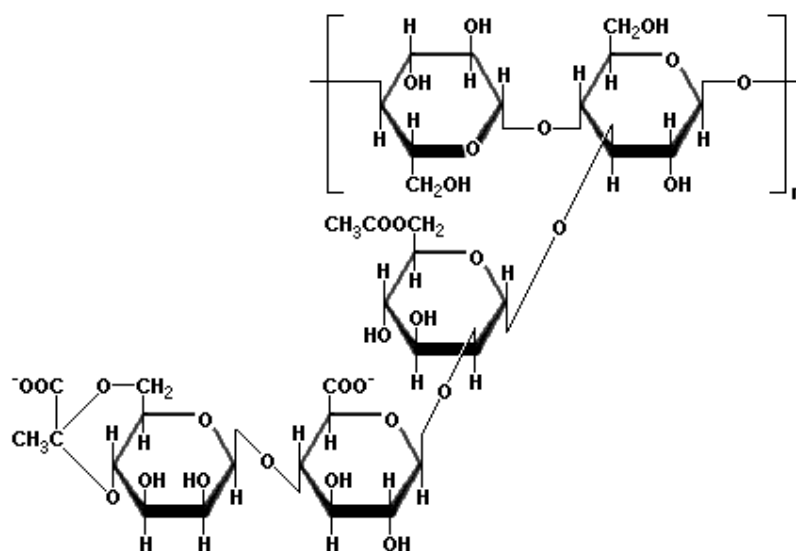


**Figure 2.14** The repeating unit of xanthan gum

Xanthan is produced in its native state as a twin stranded, right handed five fold helix. The stability of the helix is strongly affected by the ionic environment. Upon heating the xanthan helix goes through a transition to a disordered state and upon cooling it reverts to a helical structure. However it is believed that native xanthan exists in a form where chains are paired and once that has been lost and the xanthan molecules allowed to reorder the exact pairing cannot be retained and a partially crosslinked structure is formed as helices twist around various neighbors.

Xanthan gum solutions have ability to form highly viscous solutions at low concentrations and stable viscosity over a wide range of environmental conditions namely ionic strengths, heat and pH as well as enzymes. The effect of salt on viscosity depends on the concentration of the xanthan gum in solution. At low gum concentrations (below 0.3 % w/w), mono-valent salts such as NaCl, it can cause a slight decrease in viscosity. Conversely, NaCl addition at higher gum concentrations increases solution viscosity, the same effects occur with most divalent metals salts.

Xanthan has several advantages as a mobility control agent in enhanced oil recovery. It is high pseudoplasticity (shear thinning properties), flocculent, stable to pH and temperature changes and to high salt concentrations, effective lubricant, thermal stability, salt compatibility and allows easy injectability.

The special rheological properties of xanthan are technologically suitable for the 'Enhanced Oil Recovery' (EOR) applications. At low concentration, the gum forms high viscosity solution that exhibit pseudoplasticity. For the efficient displacement of oil the pumping of xanthan gum solution in the rocks is necessary. As a result oil held in the pores of the sand stone rocks is displaced.

The biosynthesis of microbial heteropolysaccharides such as xanthan is a complicated process involving a multi enzyme system. The initial step in the biosynthesis of xanthan is the uptake of carbohydrate, which may occur by active transport or facilitated diffusion. This is followed by phosphorylation of the substrate with a hexokinase enzyme that utilizes adenosine 5'-triphosphate. The biosynthesis

involves conversion of the phosphorylated substrate to the various sugar nucleotides required for assembly of the polysaccharide-repeating unit via enzyme such as UDP-Glc pyrophosphorylase. UDP-glucose, GDP-mannose and UDP-glucuronic acid are necessary for the synthesis of xanthan with the appropriate repeating unit (P.adhikary et.al 2004).

## **CHAPTER 3**

### **MATERIALS AND METHODOLOGY**

Production of chemicals from biomass always has been a goal of many researchers. This chapter describes the research methodology and procedures on the synthesis of surfactant and xanthan gum as additives from waste and local sources that potentially used in EOR applications. The chemicals and apparatus used in the experimental study are also presented in this chapter.

#### **3.1 Preparation of surfactants**

##### **3.1.1 Procedures**

The procedures started from the production of pyrolysis oil, physical characterization of pyrolysis oil, extraction of phenol from pyrolysis oil, sulfonation of the extracted phenol, and analysis of produced surfactant until surfactant polymer flooding experiments are discussed in this chapter. Figure 3.2 shows the production process of surfactant.

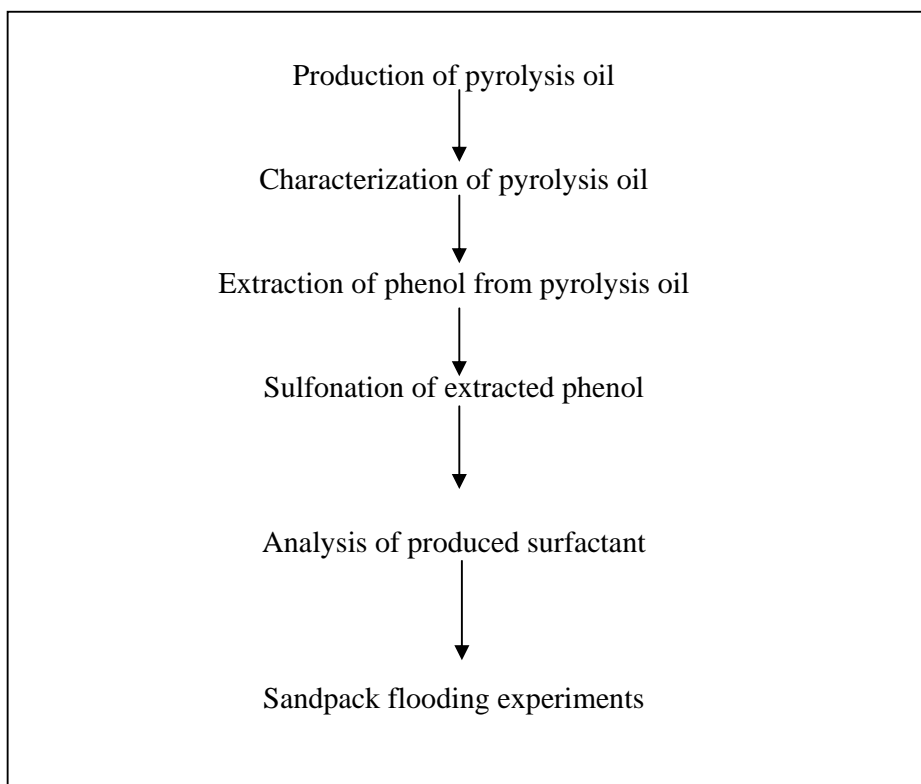


**Figure 3.1** Flow chart of surfactant production process

### 3.1.2 Production of Pyrolysis Oil

The first step in this study involves the application of a raw oil palm shell conversion to pyrolysis oil by a fluidized bed pyrolysis technology. The fluidized bed pyrolysis unit was set up by Dr. Farid's biomass research group from Faculty of Mechanical Engineering, UTM, Skudai, Johor.



### 3.1.3 Material

Oil palm shell waste was obtained from Kulai Palm Oil Mills of Federal Land Development Authority (FELDA), Johor. The oil palm shell waste was ground and sieved to a particle size of 212 – 425  $\mu\text{m}$ . It was then dried in an oven for 24 hours at 100 °C prior to pyrolysis process.

### 3.1.4 Experiments

The procedures start from grinding, sieving and oven – drying of the oil palm shells. Figure 3.3 shows the production process of pyrolysis oil.

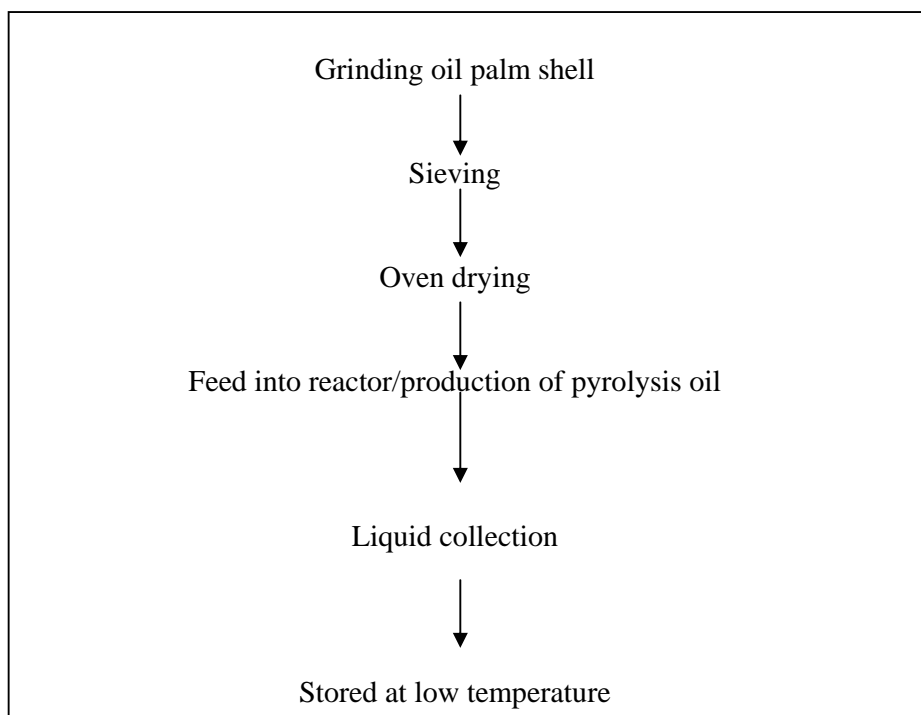


**Figure 3.2** Flow chart of pyrolysis oil production process

The equipment used to produce pyrolysis oil was a fluidized bed pyrolysis unit with silica sand as the bed material (Figure 3.4). The reactor was 5 cm diameter x 30 cm high, constructed of stainless steel with full gas flow and temperature control. The volume of the reactor was 520 cm<sup>3</sup>. The reactor was heated externally. The incoming fluidizing gas was nitrogen and was preheated before entering the reactor.

The silica sand in the fluidized bed was of mean size 256 µm diameter with a static bed depth of 6 cm. The fluidizing velocity was 1.7-3 units of the minimum fluidizing velocity. The biomass waste fed via a screw feeder and nitrogen gas stream to the fluidized bed at a feed rate of 0.6 kg/hr. The motor driven screw feeder was installed in order to feed the particles into the reactor. Two electric tube heaters, each 1kW power, supplied the heat to the pyrolysis reactor and the gas preheat chamber. The fluidization gas flow rate was measured and controlled by gas flow meters.

The outlet from the fluidized bed was to a cyclone where the char was separated by a method known as “blown-through” mode. In this method, the char was entrained and blown from the fluidized bed while retaining the sand in the bed. The vapours and the gases were passed through a water-cooler condenser to ice-cooled collectors to trap the derived liquid oil. The fluidized bed oil consisted of a single liquid phase.

The preparatory stages included grinding, sieving and oven drying of the oil palm shells. It was employed the particle size of 212 – 425 µm. In this study, the operating temperature was 450 °C. The running time of the pyrolysis process was set to 30 min in each run at feed rate of 0.6 kg/hr. The nitrogen gas flow rate was 1.26 m<sup>3</sup>/hr. 6 kg of pyrolysis oil was prepared as a starting raw material. Each time of the pyrolysis experiment produced around 250 g of pyrolysis oil. Total of 24 runs were done to collect the needed oil.

The general layout of the pyrolysis process is shown in the Figure 3.3. The real picture of fluidized bed pyrolysis unit is shown in the Figure 3.4.

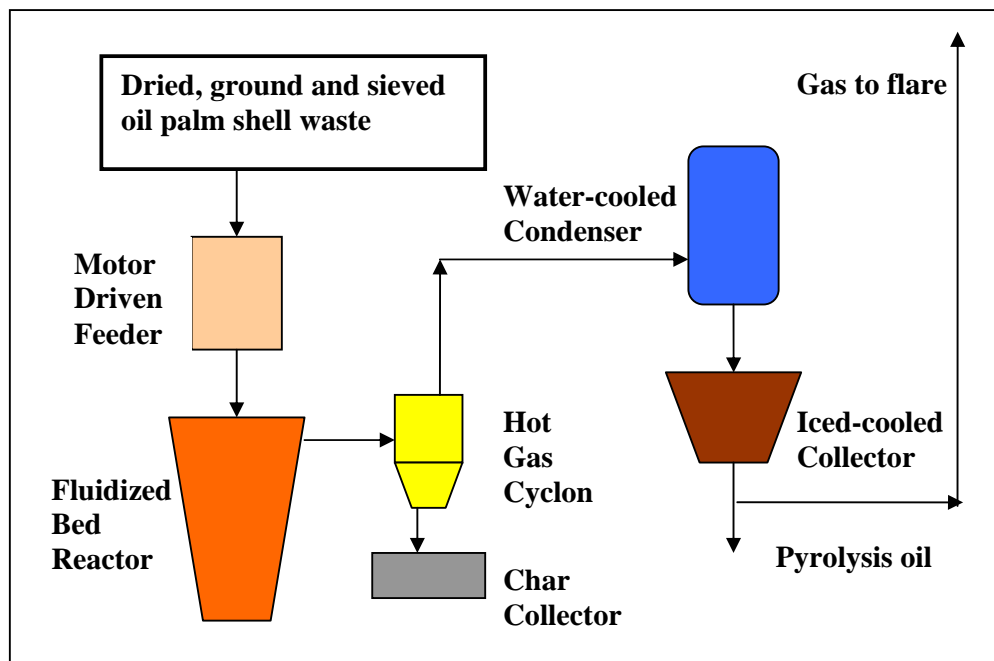


**Figure 3.3** Pyrolysis process–general layout

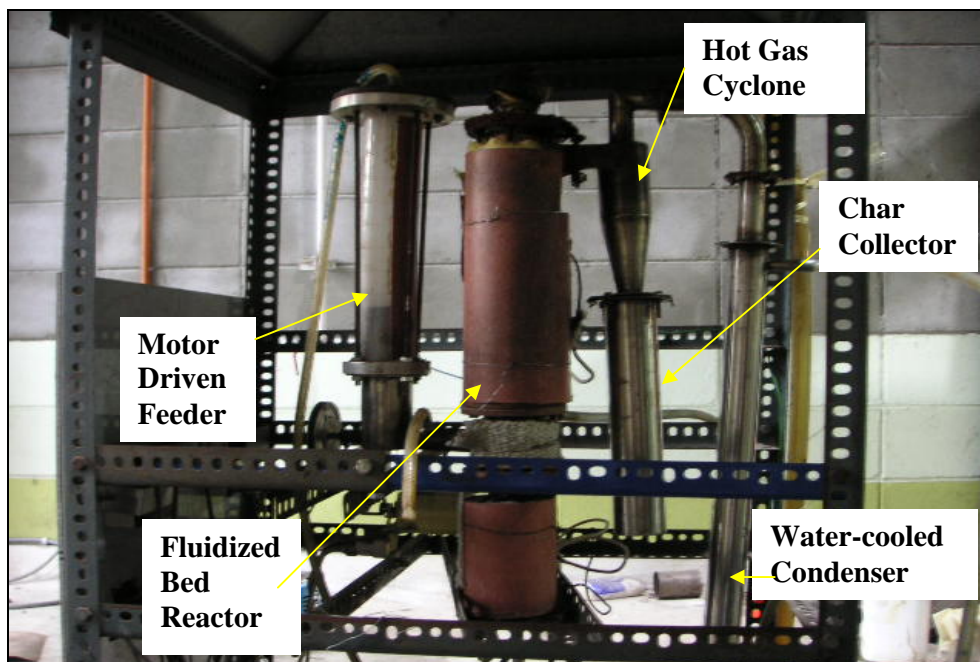


**Figure 3.4** Fluidized bed pyrolysis unit.

### 3.1.5 Characterization of Pyrolysis Oil

Physical and chemical analysis such as density, kinematic viscosity, pour point, heating value, flash point, acidity and miscibility were carried out to complete the characterization. The chemical composition in the pyrolysis oil was analyzed by FTIR and GC–MS. The methods tested on the physical properties of pyrolysis oil are showed as below. The process of which, has been detailed in the following subsections.

### 3.1.6 Density

The density was measured by using 50 ml pycnometer.

- a. Pycnometer was weighed,  $W_a$ .
- b. Pycnometer was then filled with sample.
- c. The mass of the pycnomer with sample was measured  $W_f$ .
- d. The density of sample was determined as follows:

$$\text{Density of sample} = (W_a - W_f) / 50 \text{ ml}$$

### 3.1.7 Kinematic Viscosity

The kinematic viscosity of pyrolysis oil was measured according to ASTM D 445. In this standard method the time was measured in seconds for a fixed volume of liquid to flow under gravity through the capillary of a calibrated at a closely controlled temperature. The model of the instrument used was Koehler KV 3000. The Koehler KV 3000 is shown in Figure 3.5.

The procedure for the measurement of kinematic viscosity is shown as follows:

- a. A calibrated viscometer was filled with sample.
- b. The viscometer was allowed to remain in the kinematic viscosity bath long enough to reach the test temperature, 40 °C. 30 minutes should be sufficient.
- c. The head level of the test sample was adjusted by using suction to a position in the capillary arm of the instrument about 7 mm above the first timing mark.
- d. The time required for the meniscus to pass from the first to second timing mark was measured in seconds to within 0.1 s as the sample flowing freely. If this flow time was less than 200 s, a viscometer with a capillary smaller diameter would be selected and operation would be repeated.
- e. The procedures from (a) – (d) were repeated to make a second measurement of flow time. Both measurements were recorded.
- f. If the two determined values of kinematic viscosity calculated from the flow time measurements agree within determinability of  $\pm 0.20$  %, the kinematic viscosity that calculated from the average of these determined values was reported. If not, the measurements of flow times were repeated after a thorough cleaning and drying of the viscometers until the calculated kinematic viscosity determinations agree with the stated determinability.



**Figure 3.5** Koehler KV 3000

### 3.1.8 Pour point

Pour point was determined according to ASTM D 97. The measurement of pour point is shown in Figure 3.6. The procedure for measurement of pour point is shown as follows:

- a. 50 ml of sample was filled in the test jar.
- b. The test jar was closed with the cork carrying the pour point thermometer. The position of the cork and thermometer was adjusted to fit tightly. The thermometer bulb was immersed to make sure the beginning of the capillary was 3 mm below the surface of the sample.
- c. The test jar was inserted into the jacket. The appearance of the sample was observed when the temperature of the sample was 9 °C above the expected pour point. The sample was cooled at a specific rate and examined at intervals of 3 °C for flow characteristics.

- d. The test jar was transferred to the next lower temperature bath in accordance with the following schedule:
- Sample was at +27 °C, move to 0 °C bath
  - Sample was at +9 °C, move to -18 °C bath
  - Sample was at -6 °C, move to -33 °C bath.
- e. The test jar was held on a horizontal position for 5 s as soon as the sample in the jar did not flow when tilted. If the sample showed any movement, the test jar was replaced into the jacket immediately and the test of flow was repeated at next temperature, 3 °C lower.
- f. The test was continued until the sample showed no movement when the test jar was held in a horizontal position for 5 s. The observed reading of the test thermometer was recorded.
- g. The temperature recorded in previous step was added with 3 °C and reported as pour point.

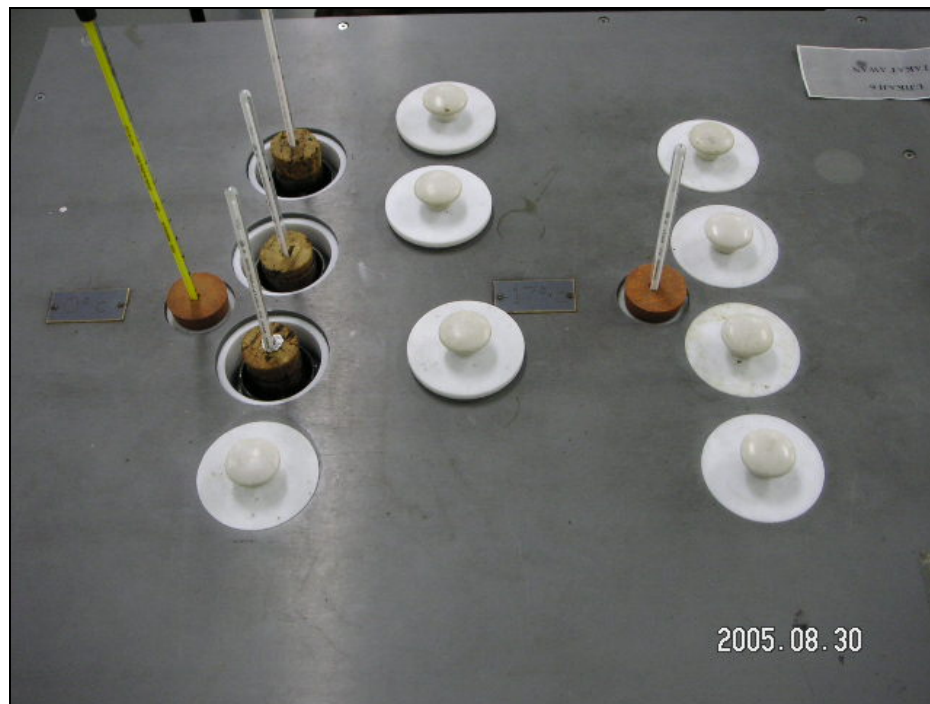


**Figure 3.6** Pour point measurements

### 3.1.9 Heating Value

The heating value was measured as calorimetric value by ASTM D 240. The procedure of measurement of heating value is shown as follows:

- a. The sample was weighed and added into the cup.
- b. The cup was placed in the curved electrode and the fuse wire was arranged to the central portion.
- c. The bomb was slowly charged with oxygen to 3.0 MPa gage pressure at room temperature after the test sample and fuse were in place.

The calorimeter reading was recorded

### 3.2 Flash point

The flash point was obtained according to ASTM D 3828 in a small scale closed-cup tester. The instrument used to determine flash point was Koehler Rapid Tester, model K 16491, as shown in Figure 3.7. The procedure of measurement of flash point is shown as follows:

- a. The temperature of the test cup and sample should be maintained at 3 °C below the expected flash point.
- b. A small portion (4 ml) of sample was introduced into the test cup.
- c. The test flame was lighted and adjusted it to a diameter of 4 mm.
- d. After a specified time (2 min), a test flame was applied and an observation made as to whether or not a flash occurred.
- e. The sample was removed from the test cup. The test cup was cleaned and the cup temperature was adjusted 5 °C lower or higher depending on whether or not a flash occurred previously.
- f. A fresh sample was introduced and tested. The procedure from (a) to (e) was repeated until the flash point was established within 5 °C.
- g. The procedure was then repeated at 1 °C intervals until the flash point was determined to the nearest 1 °C.





**Figure 3.7** Kohler rapid tester model K16491

### 3.2.1 Acidity

The pH of pyrolysis oils is low due to the volatile acids, mainly acetic and formic acid (Spila et al., 1998). These acids with water are the main reasons for the corrosiveness of pyrolysis oils especially at elevated temperatures (Aubin and Roy, 1980). The pH of pyrolysis oil was obtained by using pH meter model Orion 410A.

### 3.2.2 Infra-Red (IR) characterization

Perkin Elmer Spectrum One Fourier Transform Infra-Red (FTIR) spectrophotometer was used to characterize the pyrolysis oil produced from oil palm shell. The functional groups in the pyrolysis oil were determined from the infra-red spectrum. The absorption frequency spectra were recorded and plotted. The FTIR spectrophotometer provides the adsorption spectrum in percentage incident intensity,

along the wave numbers 4400 to 370  $\text{cm}^{-1}$ . The standard IR spectra of hydrocarbons were used to identify the functional group of the components of the derived liquids.

### 3.2.3 Miscibility

The miscibility of the pyrolysis oil with water and other solvents was tested.

- a. The following solvents were used.
  - Water
  - Methanol
  - Chloroform
  - Paraffin, alpha olefin (1-hexadecene)
  - NaOH (sodium hydroxide)
- b. 1 ml of solvent was added into pyrolysis oil at volume ratio of 1:1, the miscibility was observed.

### 3.2.4 GC–MS analysis

The GC–MS system used a J & W Scientific DB 1701 capillary column in a HP 5989x Hewlett Packard unit. Methanol was used as the standard solvent. The following conditions were used for the DB 1701 column. The library search was Wiley Database.

Column dimensions : 60 m x 0.25 mm

Film thickness : 0.25  $\mu\text{m}$

GC condition : Inlet system: split injector, He, 250  $^{\circ}\text{C}$ .

Oven temperature: 40  $^{\circ}\text{C}$  isotherm for 4 min, 3  $^{\circ}\text{C min}^{-1}$  to 280  $^{\circ}\text{C}$ . Detection: FID/MS, 280  $^{\circ}\text{C}$ .

### 3.3 Extraction of Phenols from Pyrolysis Oil

In this study, liquid-liquid extraction (solvent extraction) was used to extract the phenol and phenolic compounds from the pyrolysis oil. Evaporation method was used to remove the solvent being used. The procedure of extraction is outlined as follows:

1. 250 g of pyrolysis oil derived from oil palm shell was dissolved in 250 g of ethyl acetate with the oil to solvent in weight ratio of 1:1.
2. The mixture was filtered with Whatman filter paper of specification of 12.5 cm x 100 circles.
3. The filtered oil–ethyl acetate mixture was then collected in a separating funnel as shown in Figure 3.8.
4. A 5 wt % of sodium bicarbonate solution was prepared and the pH of the solution was maintained at approximately 8 – 9.5.
5. 500 g of 5 wt % sodium bicarbonate solution was mixed with the oil–ethyl acetate mixture in the separating funnel with the oil-ethyl acetate mixture to sodium bicarbonate solution in weight ratio of 1:1.
6. A resulting aqueous bicarbonate layer which contained strong organic acids and highly polar compounds was discharged. The ethyl-acetate soluble fraction contained phenol, phenolic compounds and neutral fractions.
7. The ethyl-acetate soluble fraction was then filtered.
8. The filtered ethyl-acetate soluble fraction was evaporated using E-01611-00 Economy Rotary Evaporator. The evaporation was carried out at 60 °C with rotation speed of 90 rpm.
9. The phenol and neutral fractions could be further fractionated into isolated phenolics and neutrals if desired. The ethyl-acetate soluble fraction from step 7 was added with 5 wt % sodium hydroxide solution in a 1:1 ratio by weight in a separating funnel. The 5 wt % sodium hydroxide solution was maintained at pH 12 – 13.
10. The funnel was shaken and phases were separated.

11. The alkaline aqueous solution contained phenols was acidified with a solution of sulfuric acid 50 % by weight to a pH near 6. Ethyl acetate was added into the neutralized aqueous solution in a 1:1 ratio by weight to extract the phenol and phenolic compounds.
12. The ethyl acetate soluble fraction from step 11 was then separated and evaporated by the evaporation technique mentioned in step 8.

The chemicals used are given in Appendix A. Table 3.1 shows the different extraction conditions set for the experiment run.



**Figure 3.8** Extraction of phenol from pyrolysis oil

**Table 3.1:** Different extraction conditions set

<b>Experiment No.</b>	<b>Weight of pyrolysis oil used, kg</b>	<b>Extraction</b>
1	0.2500	With NaOH
2	2.0000	With NaOH
3	0.5254	Without NaOH
4	0.6523	Without NaOH
5	0.3212	Without NaOH
6	0.6823	Without NaOH
7	0.8754	Without NaOH
<b>Total</b>	<b>5.3066</b>	

### 3.3.1 Sulfonation

The sulfonation method in this study was according to Berger *et al.* (2000). The method used the alkene sulfonic acid to alkylate and sulfonate phenol, alkylphenol, alkoxylated phenol to produce corresponding sulfonic acid. The alkene sulfonic acid used to alkylate and sulfonate phenolic compounds was produced from the falling film sulfonation unit.

### 3.3.2 Sulfonation of Alpha Olefin

The sulfonation unit which was employed to produce alkene sulfonic acid consisted of a 5 mm I.D. falling film reactor. The experiment was conducted at Advanced Oleochemical Technology Division (AOTD) of Malaysia Palm Oil Board (MPOB). The sulfonation unit was set up by research group of AOTD. The alkene sulfonic acids used were 1-tetradecene and 1-hexadecene. The schematic of the sulfonation unit is shown in Figure 3.9.

Operation procedure:

1. The heaters and circulators were switched on.
2. The bottle was filled up with oleum.
3. The pumping rate for oleum was set to be 0 g/min.
4. The peristaltic pump was switched on and the pumping rate of sample was adjusted to 600 g/hr.
5. Sample was allowed to flow through the thin film reactor for three minutes.
6. The nitrogen was flowed into the system. The amount of total of nitrogen pushed in was measured and adjusted to give the SO<sub>3</sub> diluted to 5 % weight in nitrogen by using manometer.
7. The weight balance of sample injected into the thin film reactor was measured in every minute and adjusted to the desired feed rate.
8. The oleum was injected and the peristaltic pump rate was adjusted to the desired feed rate.
9. The reaction could be observed by the change in the colour of sample. The sample was in dark colour after reaction had been taken place. The temperature was also increased during the reaction.
10. The weight of the sample and oleum was recorded in every minute.
11. The alpha olefin sulfonic acid was collected directly from the falling film sulfonation unit and chilled to 0 °C. It was then immediately transferred to a freezer for storage until used.

The calculations of the feed rate of sample, oleum and nitrogen are given in Appendix B and Appendix C.

### 3.3.3 Sulfonation and Alkylation of Extracted Pyrolysis Oil

Procedure:

1. 100 g of extracted pyrolysis oil was added to a 500 ml round-bottom flask equipped with magnetic stirrer, thermometer, and water condenser.
2. 30 g of C14 alpha olefin sulfonic acid was then added while the extracted pyrolysis oil was heated to 90 °C.

3. The mixture was held at 120 °C over a two hour period and periodically analyzed for increasing acid value (AV) until the value remained constant.
4. After the acid value remained constant the sample was cooled.
5. The final product was analyzed to determine the percentage of alkylphenol sulfonate produced from pyrolysis oil. CID titration using Hyamine 1622 is a method of determining surfactant activity of anionic materials.

The experiment showed above was also carried out on the extracted pyrolysis oil with different weight ratio of C14 alpha olefin sulfonic acid (100:30; 100:60; 100:90). The sulfonation process of extrated pyrolysis oil was then repeated using C16 alpha olefin sulfonic acid. Figure 3.10 shows the sulfonation and alkylation of extracted pyrolysis oil process.

The sulfonated and alkylated pyrolysis oil was then neutralized with 50 % sodium hydroxide solution. The neutralized product was then dried with evaporation method and tested for the anionic active matter and surface tension.

Seven different surfactants were produced. The types of surfactants are given in Table 3.2.

**Table 3.2:** Types of the surfactant used in the experiment

<b>Surfactant</b>	<b>Alkene sulfonic acid</b>	<b>Type</b>	<b>Extracted phenols: alkene sulfonic acid (weight ratio)</b>
SURF1	Tetradecene	Anionic	100:30
SURF2	Tetradecene	Anionic	100:60
SURF3	Tetradecene	Anionic	100:90
SURF4	Hexadecene	Anionic	100:30
SURF5	Hexadecene	Anionic	100:60
SURF6	Hexadecene	Anionic	100:90
SURF7	Tetradecene	Anionic	100:60 (not extracted phenol)

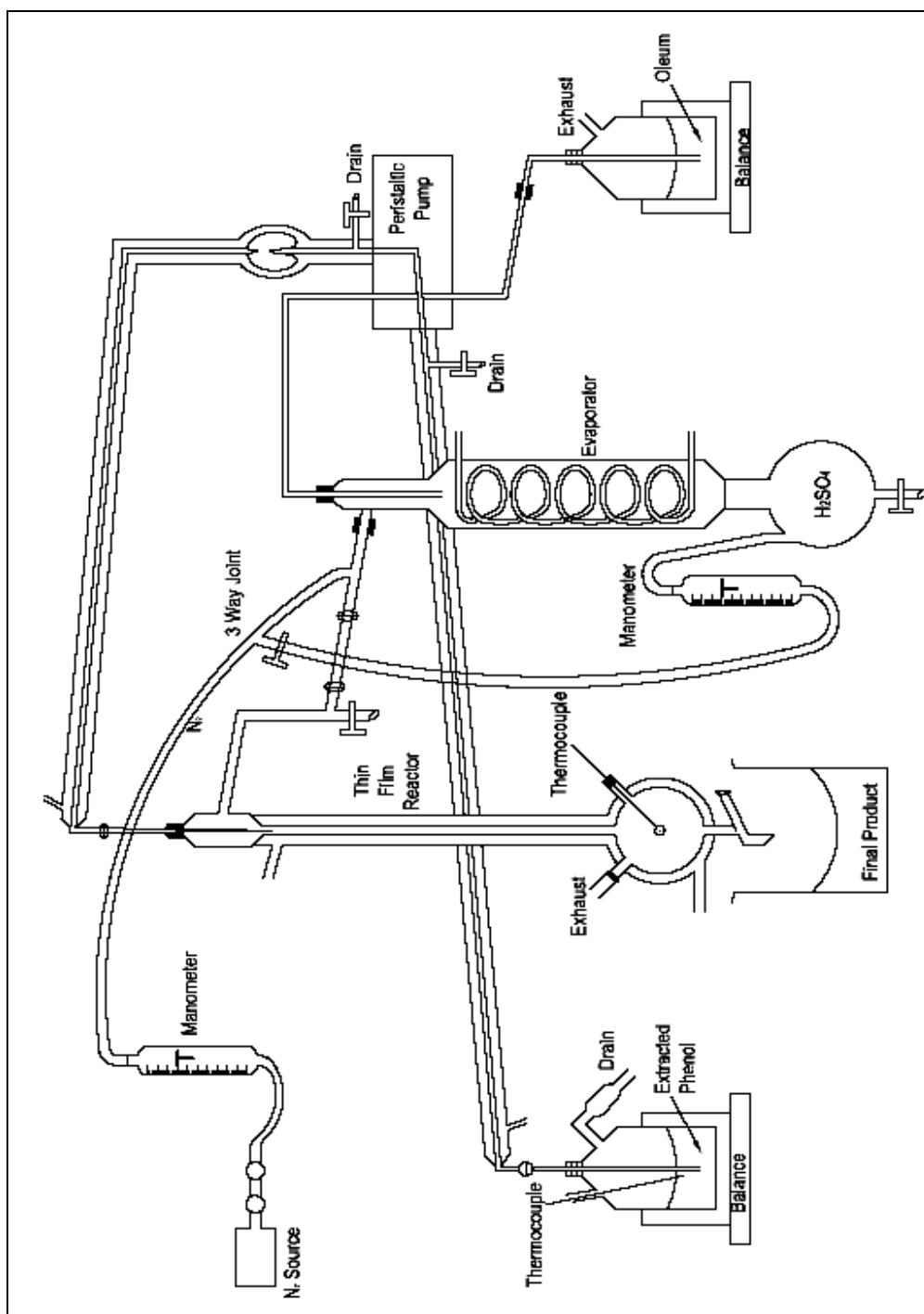


**Figure 3.9** Sulfonation unit with falling film reactor



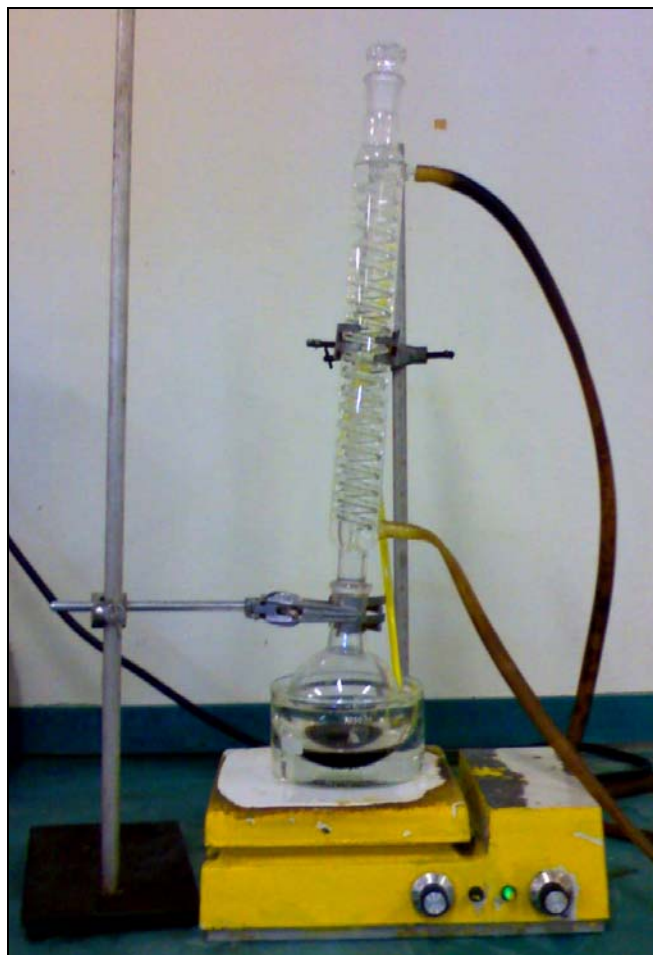


**Figure 3.10** Sulfonation and alkylation of extracted pyrolysis oil

#### 3.3.4 Analysis of Surfactant

The acid value (AV) and the surfactant activity of the sulfonation product were determined. The product from the sulfonation process was then analyzed by FTIR. The functional groups presence in the surfactant can be determined from the infra-red spectrum. The surfactant was first evaporated after neutralization prior to analysis. The dried surfactant was mixed with potassium bromide (KBr) and pressed under pressure to form a thin KBr disc that was then scanned on the FTIR model.

### 3.3.5 Acid Value

The following reagents were prepared:

- Reagent A: 2 g of sodium hydroxide was dissolved in 500 ml methyl alcohol. The actual normality was determined by neutralization with potassium hydrogen phthalate by using 1 % of phenolphthalein as the indicator accurately.
- Reagent B: 250 ml of isopropyl alcohol was added in the equal volumes of toluene. The mixture was then neutralized with reagent A by using 1 % of phenolphthalein as the indicator.

Procedure:

1. The size of sample was determined from the Table 3.3.

**Table 3.3:** Estimation of sample size for acid value determination

Acid value	Approx. wt of sample, g	Accuracy of weighing
0 – 5	20	$\pm 0.05$ g
5 – 15	10	$\pm 0.05$ g
15 – 30	5	$\pm 0.05$ g
30 – 100	2.5	$\pm 0.001$ g
100 and over	1.0	$\pm 0.001$ g

2. 1 g of sulfonated pyrolysis oil was weighed into Erlenmeyer flask. Approximately 100 ml of reagent B and 1 ml of indicator were added and mixed until the sample was completely dissolved.
3. The mixture from step 2 was titrated with the standard alkali solution which was reagent A mentioned above. It was shaken vigorously to the appearance of the first permanent pink colour of the same intensity as that of the neutralized solvent before addition. The colour must persist for 1 min. The formula for calculation of acid value is shown in Appendix D.

### 3.3.6 Hyamine Titration for Anionic Active Matter using Methylene Blue Indicator

The following reagents were used:

- Reagent A: Chloroform, reagent grade
- Reagent B: Ethanol, reagent grade, denatured was diluted to 50 % with deionised or distilled water
- Reagent C: Indicator solution was prepared by adding 0.03 g methylene blue HCl, 12 g of 96 wt% of sulfuric acid (reagent grade), 50 g of sodium sulfate (reagent grade) into 100 ml distilled water. The solution was then diluted to 1 liter with distilled water.
- Reagent D: 2.1g Hyamine 1622 was added into 1 litre distilled water for preparation of 0.0045 Molar Hyamine solution. The solution was then titrated with 99 wt % of sodium dodecylsulfate to determine the actual molarity.

Procedure:

1. The neutralized sulfonated pyrolysis oil was weighed into a 250 ml volumetric flask.
2. A little reagent B (2 to 5 ml) was dispersed into the sample and diluted to 250 ml with distilled water. 50 % ethanol was used to break foam as necessary. The aliquot was mixed well.
3. 10 ml of aliquot from step 2 was pipette into a 100 ml glass stopper cylinder.
4. 15 ml of reagent A and 25 ml of reagent C were added into the 100 ml glass stopper cylinder.
5. The sample was titrated with reagent D. It was shaking well between each addition.
6. The endpoint was reached when the intensity of the blue indicator was equal in the water and chloroform layers.
7. The methylene blue indicator would dissolved in the chloroform (bottom) layer until the endpoint was near and it would went completely into water

(upper) layer if the endpoint was passed. The formula for calculation of anionic active matter is shown in Appendix D.

### 3.3.7 Surface Tension Measurements

Surface tensions of different surfactant concentrations' solutions were measured by using a KRÜSS tensiometer at room temperature, 26 °C. The KRÜSS tensiometer K6 is shown in Figure 3.11.



**Figure 3.11** Tensiometer K6

### **3.4 Preparation of xanthan gum**

#### **3.4.1 Microorganism**

*Xanthomonas campestris* (NRRL B-1459) is the bacteria employed for xanthan production. *Xanthomonas campestris* was obtained from Northern Regional Research Laboratory, US Department of Agriculture. The bacteria were maintained on YM agar plates (3 g/L yeast extract, 3 g/L malt extract, 5 g/L peptone, 10 g/L glucose (dextrose), 20 g/L agar). Commercial xanthan gum was purchased from Fluka.

#### **3.4.2 Slant Culture Inoculum**

A lyophil preparation of *Xanthomonas campestris* was opened aseptically and suspended in 7 mL sterile YM (Figure 3.12). This suspension was incubated at 28° C for 24 hours and streaked on agar plates to check culture viability and purity (Figure 3.13) . Culture was grown on an agar slant and maintained at 4° C for future use. At two to three weeks intervals, the culture was transferred to a fresh YM agar slant, incubated for 20 to 24 hours and stored at 4° C.



**Figure 3.12** Stock cultures of *xanthomonas campestris* in 7 mL sterile YM



**Figure 3.13** Colonies of *xanthomonas campestris* on a streak plate

The 20 mL of 18-hour 50 mL culture was added with 10 % of glycerol (a cryogenic agent) divided into 20 microcentrifuge tubes and stored in the freezer at  $-4^{\circ}\text{C}$  as stock cultures (Figure 3.14)



**Figure 3.14** Stock cultures of *xanthomonas campestris* into microcentrifuge tubes

### 3.4.3 Culture Media

The inoculum growth medium was YM Broth : 3 g/L yeast extract, 3 g/L malt extract, 5 g/L peptone, 10 g/L glucose (dextrose). It was same as the glucose agar except agar was omitted. The production medium compositions are following : 5 g/L  $K_2HPO_4$ , 1.14 g/L  $NH_4NO_3$ , 0.1 g/L  $MgSO_4$ . The pH has to be adjusted to 7.0 – 7.2 by addition of  $H_2SO_4$ . Tap water was used to provide trace minerals. Media in laboratory glassware was autoclaved at 121° C. Sterilization time is 15 minutes. The formulas for yeast malt (YM) agar, YM broth and production medium recommended by United State Department of Agriculture's Northern Regional Research Laboratory (NRRL).

### **3.4.4 Local fruit juices shaker fermentations**

#### **3.4.4.1 Inoculum preparation**

Cultures were inoculated with a 10 % (v/v) inoculum prepared as follows. One standard loop fresh of cells grown on agar a plate was transferred to an Erlenmeyer flask 200 mL containing 20 mL of YM Broth. First-stage inoculated media was incubated for 24 hours at 200 rpm (rotary) at 28° C. The 24-hour 7 mL culture was transferred to Erlenmeyer flask 45 mL of YM broth in of Erlenmeyer 250 mL. Cultivation was carried out by shaking at 200 rpm and 28° C for 18 hours.

#### **3.4.4.2 Experimental methods**

Experiments were carried out using Erlenmeyer flask 1000 mL and Erlenmeyer flask 500 mL containing 20 mL of medium and 30 mL of sterilized of local fruit which were incubated with rotary shaking at 200 rpm for 2 days at  $28 \pm 1^{\circ}$  C. The amount of local carbon sources 15 % v/v used in the production medium. The fermentation conditions for the whole experiment at pH 7. Nevertheless dissolved oxygen was not controlled during incubation.

An Optic ivymen incubator was used to culture cells in liquid inoculum. A Hirayama<sup>TM</sup> autoclaved was used to sterilize the equipment. A Memmert<sup>TM</sup> incubator functioned as an oven to dry and sterilize the equipment. A Bench centrifuge superminor was used to precipitate the cells.

#### **3.4.4.3 Local Fruits**

Local fruits were obtained from supermarket which is containing pineapple, watermelon, papaya, sugarcane, honeydew, mango, coconut sap, guava, star fruit and



dragon fruit. Figure 3.15 shows the preparation of local fruits as local carbon sources for xanthan production.

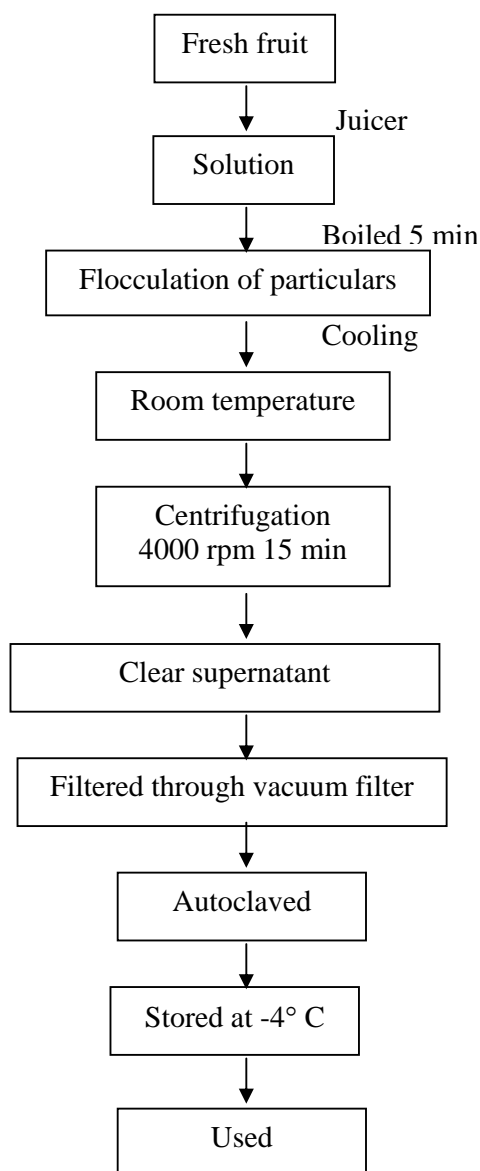


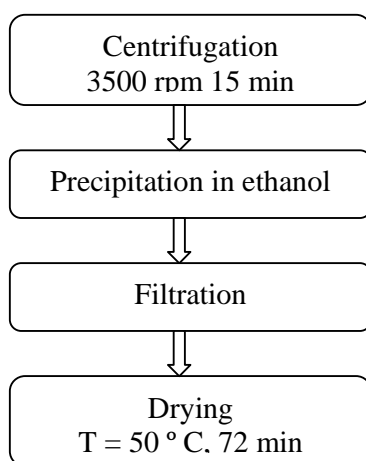
**Figure 3.15** Flow chart of preparation of local fruits

### 3.4.5 Analytical methods

#### 3.4.5.1 Extraction and purification process of Xanthan Gum

Xanthan gum was extracted and purification process according to the schematic in Fig 3.17. Xanthan gum was recovered from the cell-free supernatant by precipitation with three volumes ethanol (96 %). The precipitate formed was removed, lyophilized and weighed. The xanthan gum precipitated was dried in the oven at 50° C for 72 hours.

##### Extraction process



### **Purification process**

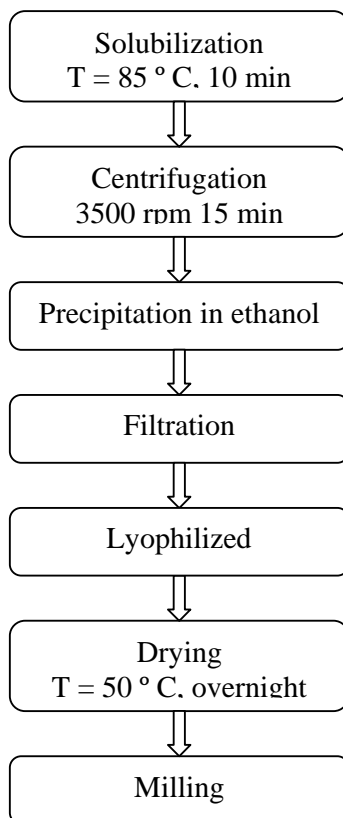


**Figure 3.16** Flow chart representatives of the extraction and purification process of xanthan gum produced using local carbon sources

#### **3.4.5.2 Pyruvate and acetate content**

Xanthan samples (1000 ppm) were hydrolyzed in 1 M HCl for 2 hours at 80° C. Then 10 mL of H<sub>2</sub>O was added to follow extraction with ethyl acetate (CH<sub>3</sub>CO<sub>2</sub>C<sub>2</sub>H<sub>5</sub>). The procedure was repeated three times. The organic phase was removed through evaporation and the residue was diluted in water, filtered through a 0.45 µm filter. A 0.2 M H<sub>3</sub>PO<sub>4</sub> solution was used as eluent at a flowrate of 0.8 mL/min. Pyruvate and acetate content were determined by HPLC using C18 column and the UV detector at 210 nm.

### **3.4.5.3 Gelatinization of refined xanthan gum**

Chromium (III) acetate was added into refined xanthan gum (1500 ppm) with ratio 10 : 1. The mixture was stirred slowly at room temperature until it is fully dissolved. The solution was added into small glass bottle. Then, solution was placed into oven at 60° C. The observation was done within for 9 days. The strength of gel based on gel strength code.

### **3.4.5.4 Viscosity measurements**

The viscosity of the cell-free fermentation broth was measured with a Brookfield Engineering Laboratories Inc. viscometer (Model CPS) using spindle 18 in the range of 0.1 – 120  $\text{S}^{-1}$ . Viscosity measurements were carried out at room temperature. The viscosity was then compared between xanthan gum commercial in distilled water and distilled water with 0.2 w/w % and 0.4 w/w % NaCl. The xanthan gums produced with concentration 1000 ppm were fully dissolved before viscosity was measured [12].

### **3.4.5.5 FTIR analysis**

The infrared spectra of xanthan gum were run in KBr discs using a Perkin Elmer spectrum one FTIR spectrophotometer in the frequency range of 4000 – 400  $\text{cm}^{-1}$ . The dry polymer was mixed with potassium bromide (KBr) and pressed into pellets under pressure to form a thin KBr disc. Differential spectra of xanthan gum purified were also recorded.

#### 3.4.5.6 Glucose Concentration

The glucose concentration of local fruit was determined by using a glucose analyzer ( **Model YHI 2700**). The fruit juices from local fruit were presented to the needle port for automatic sample injection. The analysis is based on membrane glucose.

#### 3.4.5.7 Solid-state NMR Spectroscopy

The molecular structure of xanthan gum produced was recorded using  $^{13}\text{C}$  NMR spectra. The  $^{13}\text{C}$  NMR spectra were acquired using **Bruker Avance 400**. The sample was packed in 4 mm zirconia rotors using Kel-F end caps and spun at speeds of 7 kHz.

#### 3.4.5.8 Oil Displacement Experiment

Brine and paraffin were used as the aqueous and oleic phases in the experiments. Brine was 3 wt % NaCl solution. Sand pack flooding was conducted at the ambient temperature. Sand pack holder of 2.4 cm in diameter and length of 30 cm were used. A Sage<sup>TM</sup> Pump – Model M362 and pressure gauge were used. For each test, 150 – 250  $\mu\text{m}$  of clean silica sand was packed. The silica sand was used only once for each run. The porosity of the sand pack was 44 – 49 %, and the absolute permeability to water was approximately 7.0 – 8.5 Darcy. The displacement tests were conducted horizontally. The polymer used in this study was xanthan from Fluka. The experiment included waterflooding succeeded by surfactant solution injection then followed by polymer flood. This was proposed to quantify the surfactant polymer flooding recovery as a tertiary method for water flooding.

The procedures are stated as follows (Babadagli *et al.*, 2002):

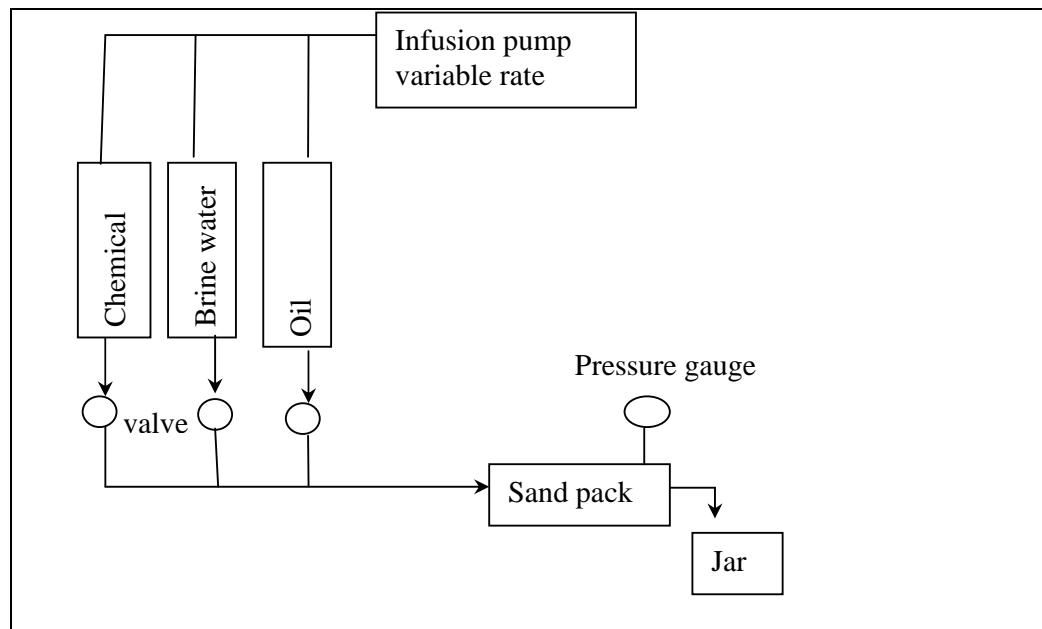
- a) The sand pack was injected with brine until it was 100 % saturated.
- b) The sand pack was then injected with oil to irreducible water saturation,  $S_{wi}$ . All the experiments were performed at a constant oil rate of 0.3 ml/min.
- c) The sand pack was aged for 1 day before starting the waterflooding.
- d) The sand pack was then flooded by brine solution. The experiment was continued until 100 % produced water cut was reached.
- e) The oil remaining in the sand pack after the waterflood was then subjected to various injections of surfactant solution for further oil recovery.
- f) 2 PV chemical slug of 5 wt % surfactant was injected into the sand pack and it was followed by 2 PV of 500 ppm xanthan flood.
- g) The brine was then injected into the sand pack at a constant rate of 0.3 ml/min.

Table 3.4 summarizes the information of the experiments. All the experiments were carried out at ambient temperature. Figure 3.17 is a schematic for the apparatus used in the displacement experiment.

**Table 3.4:** Details of the oil displacement experiments

Exp. No.	Chemical type and concentration	Experiment Type
1	SURF1 - 0.5 % , Xanthan 500 ppm	Brine + Surf.+ Polymer
2	SURF2 - 0.5 % , Xanthan 500 ppm	Brine + Surf.+ Polymer
3	SURF3 - 0.5 % , Xanthan 500 ppm	Brine + Surf.+ Polymer
4	SURF4 - 0.5 % , Xanthan 500 ppm	Brine + Surf.+ Polymer
5	SURF5 - 0.5 % , Xanthan 500 ppm	Brine + Surf.+ Polymer
6	SURF6 - 0.5 % , Xanthan 500 ppm	Brine + Surf.+ Polymer
7	SURF7 - 0.5 % , Xanthan 500 ppm	Brine + Surf.+ Polymer
8	Xanthan commercial- 500 ppm	Brine + Polymer
9	Xanthan produced – 500 ppm	Brine + Polymer
9	SURF1 - 0.5 %	Brine + Surfactant

- Surf. = surfactant
- Exp. = experiment



**Figure 3.17** Experimental apparatus for displacement experiment

## **CHAPTER 4**

### **RESULTS AND DISCUSSION**

This chapter presents the production of surfactant and xanthan gum as additives for enhanced oil recovery. It was also included the physical properties and the chemical compositional analysis of surfactant through fluidized bed reactor technology and xanthan gum through shaker fermentation. The extraction of phenolic compounds from pyrolysis oil and the production of surfactant are described. Next, the results of the analysis of the produced surfactant and xanthan gum are also presented. The analyses include the volumetric estimation of surfactant and the identification by FTIR. This chapter also describes the surfactant polymer flooding using the produced surfactants and xanthan gum. The results were evaluated in terms of the final oil recovery.

#### **4.1 Production of surfactants**

##### **4.1.1 Physical and Chemical Characterization of Pyrolysis Oil**

The products obtained from the pyrolysis oil palm shell were liquid, gas and char. The liquid yield was found to be 40 wt % of the dry feedstock. The pyrolysis



oil produced was dark in colour, viscous liquid with a smoky odour. No phase separation was observed in the pyrolysis oil. The pyrolysis gas was flared to the atmosphere. The gas and char had not been studied.

#### 4.1.2 Physical Properties of Pyrolysis Oil

Physical properties for the pyrolysis oil were determined using standard methods. The physical properties of the pyrolysis oil are summarized in the Table 4.1 and compared to the Islam *et al.*'s study (1999).

**Table 4.1:** Physical properties of palm shell pyrolysis oil and its comparison

Physical properties	Present study 2006	Islam <i>et al.</i> 's study 1999
Calorific value (MJ/kg) ASTM D240	16.2	22.1
Density (g/cm <sup>3</sup> )	1.17	1.20
Viscosity ( at 50 °C) (cSt) ASTM D 445	6.62	14.63
pH	2.3	2.7
Flash Point (°C)	60 (ASTM D 3828)	54 (ASTM D93)
Pour point (°C) ASTM D 97	-22	-10

When comparing the viscosity obtained from Islam *et al.* (1999) which was 14.63 cp, the viscosity of the pyrolysis oil in this study was lower (6.62 cp). The lower viscosity was due to the higher water content in the pyrolysis oil. The heating value of the pyrolysis oil was affected by the composition of the oil. The higher heating value of palm shell pyrolysis oil in this study was lower than previous study, which was 16.2 MJ/kg due to the presence of high percentage of moisture components. The water was not removed from the pyrolysis oil prior to the analysis. Extra cost is needed if fractionation of the oil was carried out. Pyrolysis oil contains low-boiling (below 100 °C) water-soluble compounds and hence conventional drying methods cannot be used. The amount of volatile water-soluble compounds in the pyrolysis oil is high and hence xylene distillation [ASTM D 95] in which the water is distilled away with a co-solvent, cannot be used too. (Oasmaa and Peacocke, 2001).

The density of pyrolysis oil was 1.167 g/cm<sup>3</sup>, which was relatively low as well. For the pyrolysis liquids analyzed the low viscosity was an indication of a low pour point. The lower viscosity, 6.62 cp at 50 °C, with a low pour point -22 °C, was explained by the high water content and lower proportional of water-insoluble of the oil. The pyrolysis oil had a low pH value of 2.3. The pH was affected mainly by volatile acids and the diluting effect of water. The flash point was 60 °C, which mean it can be stored safety at room temperature.

The pyrolysis oil was acidic, unstable when heated, had a low heating value and contained more water. The properties of the pyrolysis liquids analyzed vary a lot depending on the feedstock and the pyrolysis process conditions. The oil palm shell in this study was stored in open air condition prior to the pyrolysis process. Exposure of the raw material to the atmosphere can be attributed to the difference in the properties of feedstock, e.g., loss of some light compounds and oxygen to the air. In addition, Islam *et al.* (1999) obtained the pyrolysis oil at a fluidized bed temperature of 500 °C, which is different with the reaction temperature in this study, 450 °C. In this study, the fluidized bed temperature could not be increased due to the limitation of the maximum current that could be achieved by the system. The system would be unstable if the heater was overheated.

Four stages were observed when heating the pyrolysis oil.

1. First stage, the viscosity of the pyrolysis oil increased due to the polymerization reactions.
2. Second stage, an aqueous phase was separated out from the heavy lignin – rich phase. The liquid started boiling at 99 °C (below 100 °C).
3. Third stage, gummy formation from the heavy lignin – rich phase when the temperature was raised to about 150 °C.
4. Fourth stage, char or coke formation from the gummy phase at the temperature above 150 °C. The char or coke was a black shining material.

The observation above is in agreement with the work by Oasmaa and Peacocke (2001). The distillation curve was not reported. Flashing occurred immediately when giving away 50 % of the volume at 150 °C.

#### **4.1.3 Solubility with Water and Other Solvents**

The pyrolysis oil from oil palm shell was semi-soluble in water. Water was easily added into the pyrolysis oil from oil palm shell. However, black sticky material formed and stuck to the wall of the test tube when adding excess water into the oil. A phase separation occurred when adding more water to the pyrolysis oil. The water insoluble lignin derived fraction separated out of the aqueous phase. The physical appearance of the black sticky material showed that the water-insoluble fraction was separated.

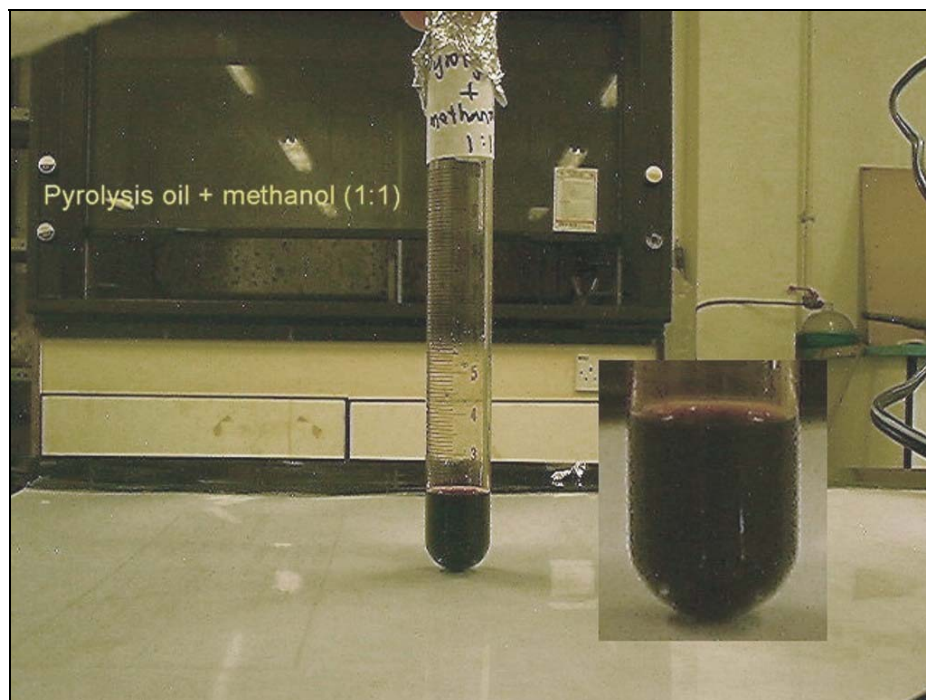


**Figure 4.1** The solubility of pyrolysis oil in methanol in 1:1 volume fraction



**Figure 4.2** The dissolubility of pyrolysis oil in hexadecene in 1:1 volume fraction

The solubility of pyrolysis oil in other solvents was affected by the degree of polarity. In this study, the pyrolysis oil fully dissolved in methanol and ethyl acetate, which were polar solvent. These solvents dissolved 100 % of the pyrolysis oil. The result is shown in Figure 4.1. Acetone was also a good solvent but not as effective as alcohols. It is believed that the pyrolysis oil contained high polarity compounds. The pyrolysis oil had high oxygen content due to aldehydes, ketones, carbohydrates, phenols, and lignin derived material. These compounds caused the polarity of pyrolysis oil and high solubility in polar solvent.

The pyrolysis oil did not dissolve in hydrocarbons like hexane, n-paraffin diesel fuels and polyolefins. It also did not dissolve in alpha olefin such as 1-hexadecene. Figure 4.2 shows the dissolubility of pyrolysis oil in hexadecene with 1:1 volume fraction. All the sample of pyrolysis oil produced in this study showed the same behaviour in the solubility tests.

#### **4.1.4 FTIR Characterization**

The functional groups of the pyrolysis oil were determined by absorption frequency spectra. All pyrolysis oils subjected to the FTIR analysis were derived from the same conditions: particle size 212 – 425  $\mu\text{m}$ , nitrogen flow rate of 1.26  $\text{m}^3/\text{hr}$  and operating temperature of 450  $^{\circ}\text{C}$ . Due to the limitation of the pyrolysis equipment, a large amount of the pyrolysis oil could not be produced through only one run. A total of 24 runs were carried out to collect the needed pyrolysis oil, approximately 6 kg. Therefore, in order to investigate the consistency of the equipment and the quality of the produced pyrolysis oil, four pyrolysis oils were taken from different production period and subjected to the FTIR analysis. They were labelled as pyrolysis oil A, B, C and D. The spectrums recorded after scanning on the FTIR are shown in Figure 4.3 to Figure 4.6. Same absorbance peak areas were found. It can be seen that their peak patterns were very similar, showing that their functional groups should be also similar.

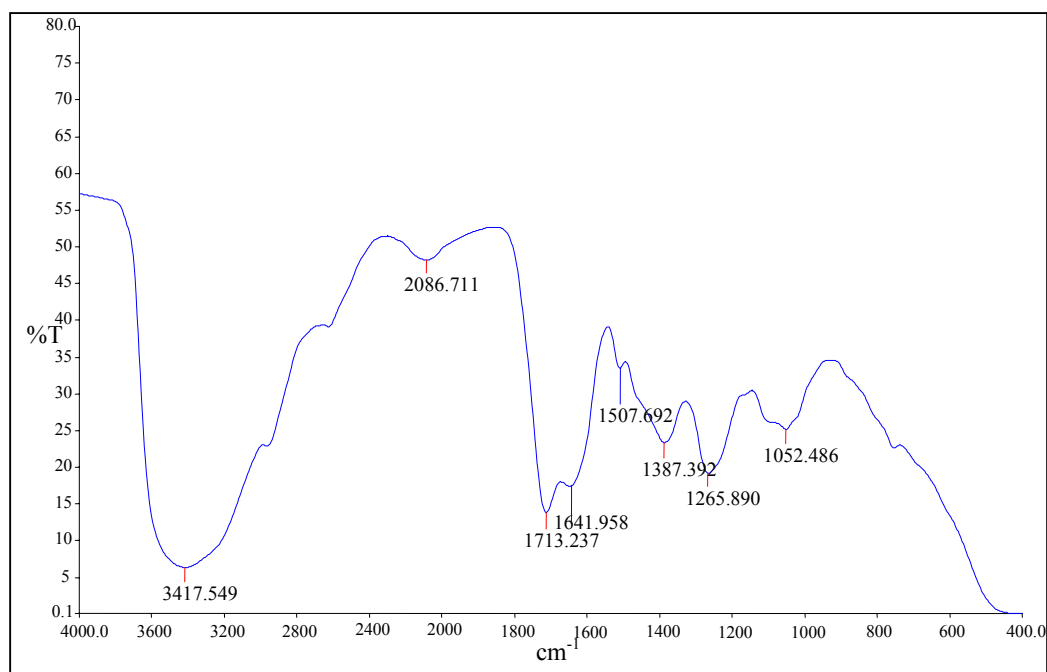


**Figure 4.3** Infra-red spectrum of pyrolysis oil A produced from oil palm shell

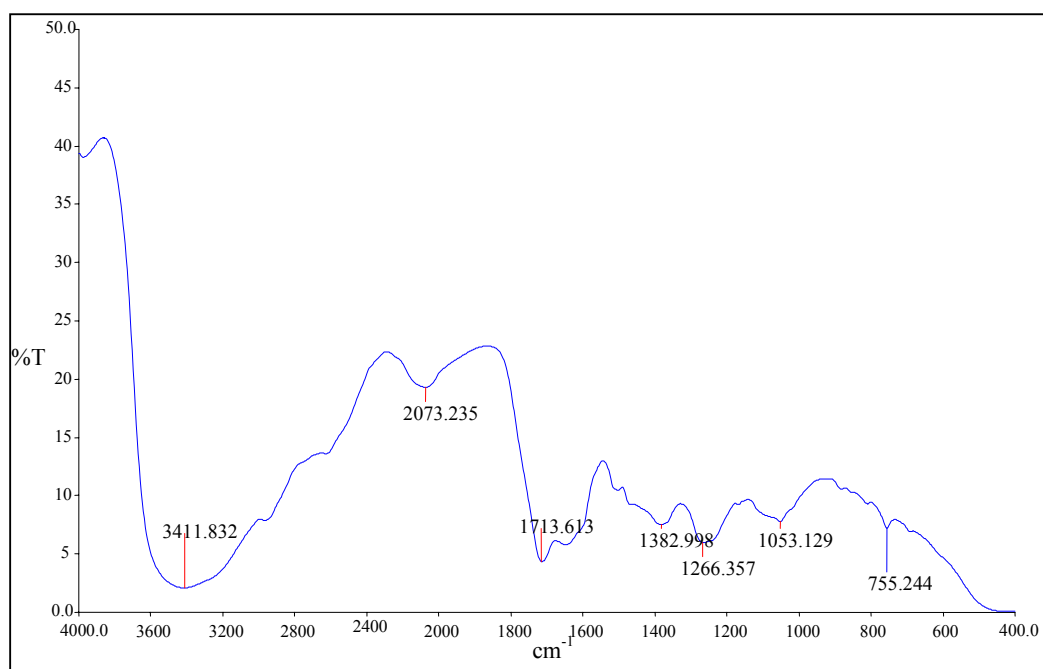


**Figure 4.4** Infra-red spectrum of pyrolysis oil B produced from oil palm shell

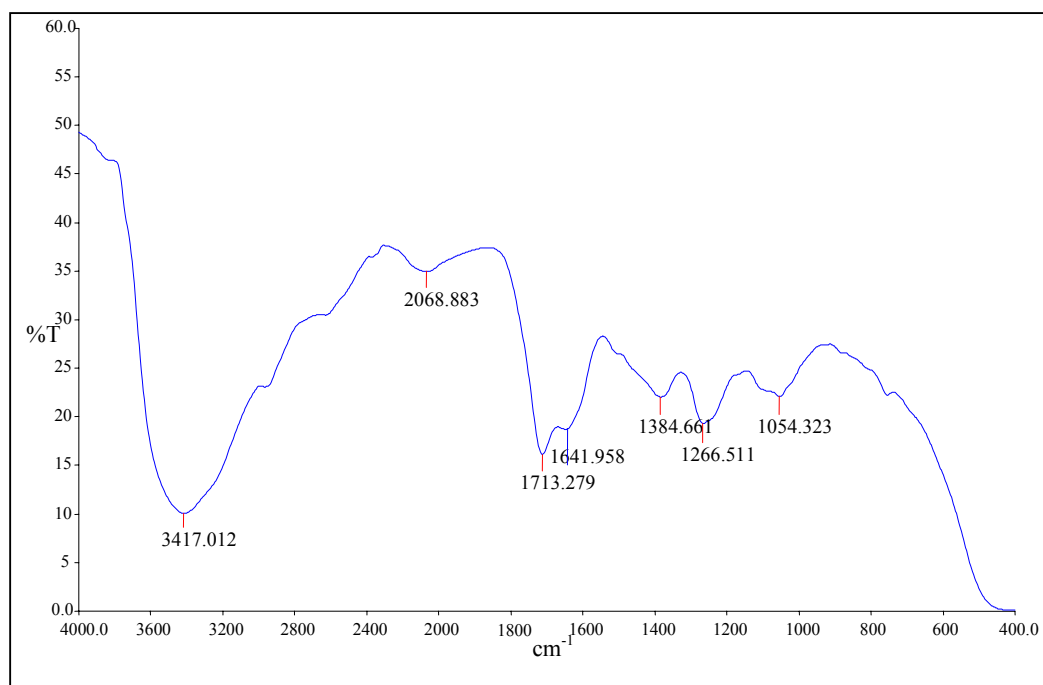


**Figure 4.5** Infra-red spectrum of pyrolysis oil C produced from oil palm shell

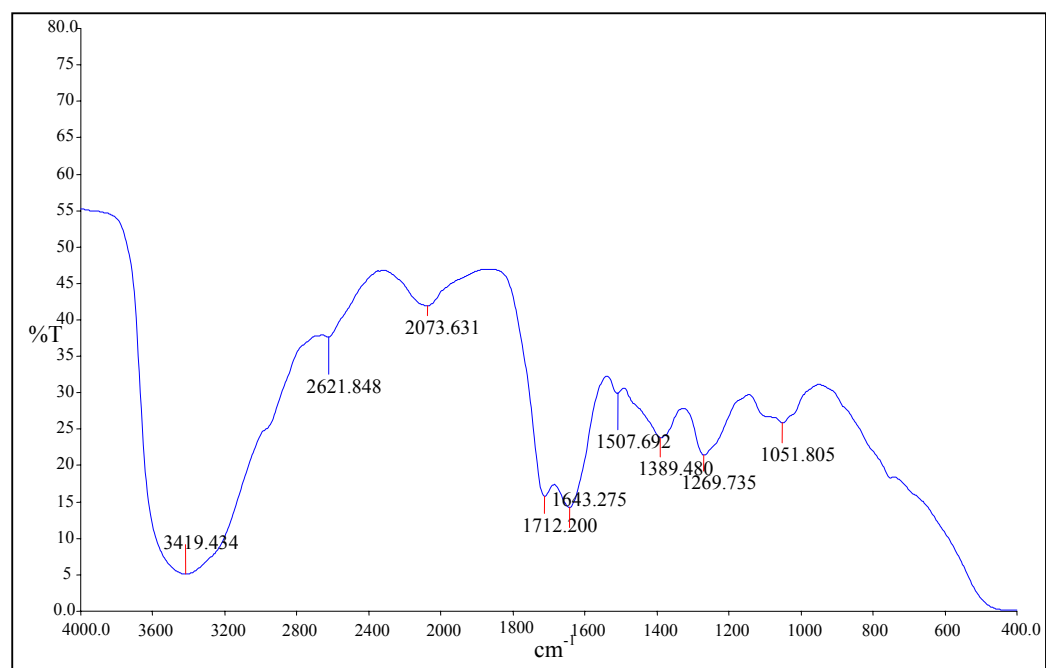


**Figure 4.6** Infra-red spectrum of pyrolysis oil D produced from oil palm shell

**Table 4.2:** FTIR functional groups and the indicated compounds of the pyrolysis oil

Frequency range ( $\text{cm}^{-1}$ )	Group	Family
3500 – 3200	O–H stretch	Alcohols, phenols (H-bonded)
3400 – 2400	O–H stretch	– COOH ( in carboxylic acids)
2000 – 1660	C=C stretch	Aromatics
1725 – 1705	C=O stretch	Ketones
1600 – 1450	C=C stretch	Aromatics
1475 – 1315	C–H bending	Alkanes
1260 – 1140	C–O stretch	Phenols
1300 – 1000	C–O stretch	Alcohols, esters, ethers, carboxylic acids, anhydrides
900 – 690	C–H out-of-plane bend	Aromatics

The compositional groups are presented in Table 4.2. The IR absorption bands were analyzed refer to the Chemical Analysis by Rubinson (1987). The IR spectra of alcohols and phenols gave characteristic broad O–H stretching absorptions in the region of 3600–3200  $\text{cm}^{-1}$ . The presence of alcohols and phenols (H –bonded) O–H stretch in pyrolysis oil was indicated by the absorbance peak of O–H stretching vibration between 3500–3400  $\text{cm}^{-1}$ . The carboxylic acid was indicated by the absorbance peak of O–H stretching in between 3400–2400  $\text{cm}^{-1}$ .

The absorbance peaks between 2000–1600  $\text{cm}^{-1}$  represented the C=C stretching vibration indicated the presence of C=C bond in aromatic ring (usually shows several peaks). The frequency range of 1725–1705  $\text{cm}^{-1}$  presented ketones of C=O stretching. The peaks in between 1600–1450  $\text{cm}^{-1}$  were another indication of the presence of aromatic ring due to the C=C stretching vibration. The possible presence of alkanes group was indicated by the strong absorbance peak of C–H bending in the regions 1615–1475  $\text{cm}^{-1}$ . The presence of the significant peaks at



1640 and 1700  $\text{cm}^{-1}$  could be ascribed to C=O (carbonyl) stretching vibrations indicative of the ketones, phenols or aldehydes, or represent C=C stretching vibrations indicative of alkenes and aromatics. Absorptions due to the C–O stretching for alcohols and phenols also occurs in the fingerprint region, but can sometimes be distinguished since they tend to be stronger than surrounding absorptions. They occurred in the regions 1260–1140  $\text{cm}^{-1}$  for phenols. C–H stretching and bending vibrations between 1475–1315  $\text{cm}^{-1}$  indicated the presence of alkane groups in pyrolysis oil. The band at 1389  $\text{cm}^{-1}$  was ascribable to bending vibrations for  $\text{CH}_3$  groups. The peaks between 1200–1000  $\text{cm}^{-1}$  were indication of the presence of primary, secondary, tertiary alcohols, ethers and esters due to C–O stretching. Absorbance peaks of C–H out of plane bending between 900–650  $\text{cm}^{-1}$  indicated the presence of single, polycyclic and substituted aromatic compounds.

#### **4.1.5 GC – MS Characterization**

The results of the FTIR were confirmed with the GC–MS analysis. Two samples were subjected to GC–MS for the chemical compound identification, which are pyrolysis oil A and B. Both were produced at the same conditions: particle size 212 – 425  $\mu\text{m}$ , nitrogen flow rate of 1.26  $\text{m}^3/\text{hr}$  and operating temperature of 450  $^\circ\text{C}$  but in different production period. GC–MS analysis was carried on these two samples in order to get an idea of the type of organic compounds in the pyrolysis oils which produced at the same conditions. Table 4.3 and Table 4.4 show the detailed analysis of the pyrolysis oil. The GC–MS chromatograms of the pyrolysis oils are given in Appendix E.

**Table 4.3:** Tentative GC–MS characterization of pyrolysis oil A from oil palm shell

Chemical compounds	Area percent, %
<b><u>Phenolics</u></b>	
Phenol	36.19
2 methoxy phenol (guaiacol)	4.58
2,6-dimethoxy phenol	4.57
2-methoxy-4 methyl phenol	2.40
4-ethyl -2 methoxy phenol	2.21
3-[(trimethylsilyl)oxy]-phenol	1.96
2-methoxy-4(1-propenyl ) phenol	1.48
2,6-dimethoxy-4-(2-propenyl) phenol	1.39
4-hydroxy-3-methoxy benzaldehyde (vanillin)	0.96
2-methyl phenol (o-cresol)	0.52
4-methyl phenol (p-cresol)	0.49
4-hydroxy-3,5-dimethoxy benzaldehyde	0.43
2-methoxy -4-propyl phenol	0.26
<b><u>Non- phenolics</u></b>	
Triphenylphosphine oxide	12.97
4-hydroxy benzoic acid	6.11
4-hydroxy -methyl ester benzoic acid	2.04
3-hydroxy-4 methoxy benzoic acid	1.91
2-methyl-ethyl ester propenoic acid	0.44
2 hydroxy-3-methyl-2 cyclopenten-1-one	1.36
3-ethyl-2-hydroxy-2-cyclopenten-1-one	0.26
1-(4-hydroxy-3-methoxyphenyl) - ethanone	0.42
Others	17.08

Due to the complexity of the chemical compositions in the pyrolysis oil, only the major peaks were selected from the chromatogram for the purpose of chemicals identification. From the chromatograms, it can be seen that the pyrolysis oils were such an unknown and complex mixture of organic compounds, therefore, there was no calibration of the MS detector was set due to the lack of an appropriate standard

mixture for calibration. Thus, the results of the chemical analysis can only be stated in area percent.

**Table 4.4:** Tentative GC–MS characterization of pyrolysis oil B from oil palm shell

Chemical compounds	Area percent, %
<b><u>Phenolics</u></b>	
Phenol	27.11
2 methoxy phenol (guaicacol)	8.47
2,6-dimethoxy phenol	6.16
2-methoxy -4 methyl phenol	5.45
2,6-dimethoxy-4-(2-propenyl) phenol	5.28
4-ethyl -2 methoxy phenol	4.59
2-methoxy -4(1-propenyl ) phenol	4.50
1,2 Benzenediol (pyrocatechol)	3.31
2-methyl phenol (o-cresol)	2.08
2-methoxy - 4-(2-propenyl) phenol	1.83
3-methoxy - 1,2 - benzenediol	1.22
2-methoxy -4-propyl phenol	1.13
4-hydroxy -3-methoxy benzaldehyde (vanillin)	1.04
2-methoxy - 4-vinylphenol	0.94
<b><u>Non – phenolics</u></b>	
n-hexadecanoic acid	5.69
Thiocamphor	3.80
Furfural	2.08
2,3,5 – trimethoxytoluene	2.00
2-chloro-1-phenyl-1-penten-3-ol	0.71
Others	12.64

The results from the GC-MS analysis are matched with the results of the FTIR analysis. Thus, FTIR analysis can be used as a fast screen technique to observe the chemical compositions in the pyrolysis oil. As expected, a lot of aromatics and oxygenated compounds were found in the pyrolysis oil, such as phenols, ketones,

and acids. The results are also in agreement with the work by Islam *et al.* (1999) which reported that the pyrolysis oil from oil palm shell was highly dominant with oxygenated compounds and contained a high concentration of phenolic compounds.

From Table 4.3 and 4.4, the phenol was found to be 36.19 area % and 27.11 area %, in the pyrolysis A and B, respectively. Although the pyrolysis oils were produced in the same pyrolysis conditions, however, it can be seen that the estimated amount of chemical compositions was different. The type of chemicals found in pyrolysis A was also slightly different from that found in pyrolysis B. Propanoic acid and benzoic acid were found in pyrolysis oil A but n-hexadecanoic acid was found in pyrolysis oil B. Some other oxygenates were found such as triphenylphosphine oxide, 2-hydroxy-3-methyl-2-cyclopenten-1-one, 3-ethyl-2-hydroxy-2-cyclopenten-1-one, 1-(4-hydroxy-3-methoxyphenyl)-ethanone in pyrolysis oil A but furfural, 2-chloro-1-phenyl-1-penten-3-ol in pyrolysis oil B. Pyrolysis oil was extremely complex and may be composed of hundreds of organic compounds, the minor peaks in GC-MS chromatograms were classified as other chemical compounds. Other unidentified compounds were 17.08 area % and 12.64 area % in the pyrolysis oil A and B, respectively. The unidentified compounds might be composed of some other aromatic and oxygenated compounds.

However, it can be confirmed that the phenolic compounds were the major components in the pyrolysis oil. Both pyrolysis oil A and B were composed of phenol, 2 methoxy phenol, 2,6-dimethoxy phenol, 2-methoxy -4 methyl phenol, 2,6-dimethoxy-4-(2-propenyl) phenol, 4-ethyl -2 methoxy phenol, 2-methoxy -4(1-propenyl ) phenol, 2-methyl phenol and 2-methoxy -4-propyl phenol. The results are consistent with the study reported by Wong (2002). Jamil *et al.* (2000) also reported the phenol and its derivatives were more than 43 wt% of the total pyrolysis oil from oil palm shell. As a matter of fact, the concentrations of the phenolic compounds were very high in pyrolysis oil from oil palm shell.

#### 4.1.6 Extraction of Phenolic Compounds

The chemical composition analysis of the pyrolysis oil showed that there were several chemical compounds in the pyrolysis oil, such as acids, ketones, phenolics and other oxygenated compounds. Since the phenolic compounds are the major constituents in the oil, they have been looked as a potential substitute for petroleum-based phenol and can be used as the starting material in the synthesis of surfactant.

#### 4.1.7 Liquid–liquid Extraction of Phenols from Pyrolysis Oil

As shown in Table 3.1 previously, experiment run no.1, liquid–liquid extraction was performed by using 5 wt % of sodium hydroxide in a weight ratio of 1:1 to isolate the phenolic and neutral fractions. The alkaline aqueous solution, containing the phenols, was acidified with 50 % sulphuric acid and lastly extracted with ethyl acetate. In the step of extraction with aqueous sodium bicarbonate solution, a precipitate was formed (5 wt %) along with the soluble acid fractions. The precipitate was the salt produced from the neutralization process where the strong organic acid reacted with sodium bicarbonate. Carbon dioxide gas was released during the extraction process.

**Table 4.5:** Yields of pyrolysis oil based on starting oil in experiment run no.1

Yields of pyrolysis oil based on starting oil, wt %			
	EtOAc Insol.	Organic Acids	Phenol
Pyrolysis oil	0	* Solids: 5	9.09

EtOAc Insol. = ethyl acetate insoluble

\* Not Determined

The results from the experiment run no.1 are given in Table 4.5. Since the objective of this experiment is to extract the phenolic compounds, therefore the acid and neutral fractions were not determined. The yield of the phenolics fraction in the extract was 9.09 wt % of the pyrolysis oil derived from oil palm, which was lower than expected (~ 30 to 40 wt %). It was believed that there were some losses when transferring pyrolysis oil during the extraction process. The experiment was therefore repeated by using a large quantity of pyrolysis oil to minimize the losses.

In experiment run no.2, 2 kg of pyrolysis oil derived from oil palm shell was used in the extraction process. In the extraction with sodium bicarbonate solution, a precipitate was formed (11.81 wt %) along with the soluble acids fraction. After extraction with a 5 wt % aqueous solution of sodium hydroxide and acidification to pH 6 with 50 % sulfuric acid, the yield of phenolic compounds was still low, 3.29 wt % based on starting pyrolysis oil. The results for the experiment run no.2 are given in the Table 4.6.

**Table 4.6:** Yields of pyrolysis oil based on starting oil in experiment run no.2

<b>Yields of Pyrolysis Oil Based on Starting Oil, wt%</b>			
	<b>EtOAc Insol.</b>	<b>Organic Acids</b>	<b>Phenol</b>
Pyrolysis oil	0	56.13	3.29

EtOAc Insol. = ethyl acetate insoluble

\* Not Determined

After utilizing 2 kg of pyrolysis oil derived from oil palm shell in the extraction, the total yield of phenol fractions was only 65.8 g. The results were unexpected and the step of extraction by using sodium hydroxide and acidification was unable to separate the phenol and neutral fraction efficiently. The concentration of sodium hydroxide (NaOH) used in this study was not strong enough to extract the phenolic fractions. According to previous study by Carlos *et al.* (1997), the recoveries of phenols after a single stage alkaline extraction with concentrated NaOH solution were higher than using five stages of cross-current extraction with diluted NaOH solution. They reported 70 wt % of phenol was extracted from Eucalyptus wood tar using a 5 M NaOH aqueous solution. In contrast, Chum *et al.*

(1990) suggested a 5 wt % of sodium hydroxide of solution in a volume ratio of 5:1 of solution: extract was used. Thus, it can be concluded that the low yield of extracted phenols could be attributed to low amount and concentration of NaOH solution had been utilized in this study. Furthermore, in the extraction with NaOH solution, the two separated phases were difficult to identify because both were dark in colour. It could not be easily distinguished by observation. The losses could have occurred when separating these two separated layers.

In the experiment run no.1 and no.2, the phenol extraction process ended only after the phenolic and neutral compositions were generally reduced to purified phenolics without any neutral fractions. However, the yield of the phenolics was found to be less than 10 wt % after extraction. In order to increase the yield of the extracted phenolic, a high concentration and volume of NaOH solution should be used. It should be noted that by using more solvent in the extraction process, the cost of extraction will increase. Hence, in the following experiment, the pyrolysis oil was extracted without using sodium hydroxide producing a combined phenolics and neutral fraction in pyrolysis oil.

In experiment no.3, the yield of the phenol/neutral fraction was 10.65 wt %. The experiments was continued by using different quantity of pyrolysis oil with the same method described in Chapter 3 but without the step of extraction process by NaOH solution. The yields of the extraction are given in Table 4.7.

**Table 4.7:** Yields phenol/neutral fraction from pyrolysis oil based on starting oil (without NaOH)

<b>Experiment no.</b>	<b>Pyrolysis oil, g</b>	<b>Phenol/neutral fraction, g</b>	<b>Phenol/neutral fraction, wt %</b>
3	525.41	55.97	10.65
4	652.27	223.38	34.25
5	321.18	43.90	13.67
6	682.28	257.16	37.69
7	875.39	189.69	21.67

total	3056.53	770.10	
		<b>average yield</b>	<b>25.20</b>

From the Table 4.7 shown above, the extraction scheme described above allowed the isolation of 10 to 38 wt % of the starting pyrolysis oil derived from oil palm shell as a phenol/neutral fraction.

#### 4.1.8 Identification and Quantification of Extracted Pyrolysis Oil

The phenol/neutral fractions in the extracted oil from raw pyrolysis oil were analyzed by FTIR and GC – MS. The results are shown as below.

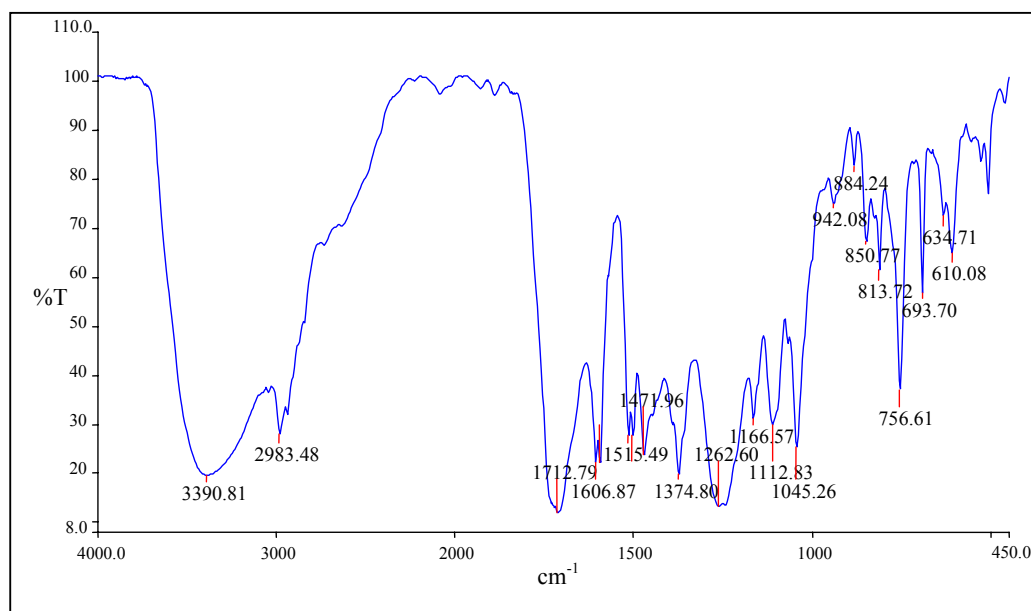


**Figure 4.7** Infra-red spectrums of extracted phenolic and neutral fractions

From the infra-red spectrum recorded, alcohols and phenols gave characteristic broad O–H stretching absorptions in the region of 3600–3200 cm<sup>-1</sup>. The presence of alcohols and phenols (H –bonded) O–H stretch in pyrolysis oil was indicated by the absorbance peak of O–H stretching vibration between 3500 – 3400



$\text{cm}^{-1}$ . Phenols showed absorption due to the C–O stretching and –OH deformation vibrations in the regions 1260–1140  $\text{cm}^{-1}$ . Adsorption due to the C–O stretching for alcohols and phenols also occurred in the fingerprint region. The absorbance peaks between 2000–1600  $\text{cm}^{-1}$  represented the C=C stretching vibration indicated the presence of C=C bond in aromatic ring (usually shows several peaks). Absorbance peaks of C–H out of plane bending between 900–650  $\text{cm}^{-1}$  indicated the presence of single, polycyclic and substituted aromatic compounds. Ketones showed a strong absorption in the region from 1725–1705  $\text{cm}^{-1}$ . This band, usually the most intense in the spectrum, was due to C=O stretching vibration. Aliphatic groups were found in the extracted pyrolysis oil as well. The vibration modes were the C–H stretching around 3000  $\text{cm}^{-1}$  and the –CH deformation modes around 1460  $\text{cm}^{-1}$  and 1380  $\text{cm}^{-1}$ .

The results were then confirmed with GC-MS analysis. Table 4.8 shows the phenolic compounds were extracted while the organic acids were being removed. The extracted oil contained 50.2 area % of phenols. The overall total concentration of phenol and phenolic compounds was up to 93.79 area % in the extracted oil. Besides the phenolic compounds, the extracted oil also contained about 6.72 area % of impurities. These impurities included 4.10 area % of thiocamphor and 2.11 area % of 2, 3, 5 – trimethoxytoluene which were the neutral compounds. These results show that liquid-liquid extraction process in this study was success to improve the purity of phenol and phenolic compounds in the pyrolysis oil from oil palm shell. The GC–MS chromatogram of the extracted oil is given in Appendix F.

**Table 4.8:** Identification of chemical compounds in extracted oil (without NaOH)

Compounds (major peaks)	Area percent of total ,%
<b><u>Phenolics</u></b>	
Phenols	50.20
2 - methoxy phenol	12.05
2,6-dimethoxy phenol	9.86
2-methoxy - 4-methyl phenol	6.32
2-methoxy -4(1-propenyl ) phenol	5.03
4-ethyl -2 methoxy phenol	4.21
2 - methyl phenol (o-cresol)	2.03

3- allyl - 6 methoxy phenol	1.67
2- methoxy -4-propyl phenol	0.86
3 - methoxy - 1,2 - benzenediol	0.65
1,2 Benzenediol	0.48
2- methoxy - 4-vinylphenol	0.44
<b><u>Non - phenolics</u></b>	
Thiocamphor	4.10
2,3,5 - trimethoxytoluene	2.11

#### 4.1.9 Sulfonation of Alpha Olefin

In this study, the alpha olefin sulfonic acid (AOS acid) from the reaction of an alpha olefin and  $\text{SO}_3$ , before neutralization, was used to simultaneously alkylate and sulfonate the phenolic compounds in the extracted oil from pyrolysis oil of oil palm shell.

The alpha olefin sulfonic acid was produced by the sulfonation of an alpha olefin using a thin film  $\text{SO}_3$  reactor. The alpha olefin sulfonic acid produced was a mixture of alkene sulfonic acid and sultone. AOS acids produced were based on C14, and C16 alpha olefin, which were 1- tetradecene and 1- hexadecene. Two types of AOS acids were produced, they were C14 AOS acid and C16 AOS acid.

##### 4.1.9.1 Sulfonation of 1 – Tetradecene ( $\text{C}_{14}\text{H}_{28}$ ) using 1.2 Mole Ratio of $\text{SO}_3$

The C14 AOS acid was first produced from extracted pyrolysis oil and pyrolysis, followed by C16 AOS from extracted pyrolysis oil only. The calculations of the feed rate of tetradecene and oleum are given in Appendix B.

At the first run of sulfonation of tetradecene, the amount of  $\text{SO}_3$  utilized in the experiment was 0.21 mols of  $\text{SO}_3$  per mole of olefin. It was found that the actual mole ratio sample to  $\text{SO}_3$  was 1 to 0.21 in the experiment. The theoretical value should be 1 to 1.2. Analysis of the final product gave 1.8985 mg KOH/g oil acid value, which was too low. The first run of the sulfonation of tetradecene failed due to the non-functional of evaporator of the  $\text{SO}_3$  thin film reactor. The evaporator was used to evaporate the oleum to release the gas  $\text{SO}_3$  for reaction. After repair, the sulfonation of 1- tetradecene was repeated.

In the second run of sulfonation of tetradecene, the actual mole ratio of the sample to  $\text{SO}_3$  was found to be 1 to 1.39. The actual mole ratio in the experiment was similar to the theoretical value (1 to 1.2). The difference was trivial. The data recorded during the experiment is shown in the Appendix B.

Analysis of the final product, C14 AOS acid gave acid value of 127. The acid value is shown in Table 4.9. The acid value of 127 was used in the calculation of the degree of sulfonation. 62.23 % of C14 AOS acid was produced by assuming MW of 275. A 0.5055 g of the acid/sultone product was analyzed after neutralization. The C14 AOS acid was neutralized with 50 % NaOH and the analysis showed the anionic active matter of the reaction product was 47.3 % active.

**Table 4.9:** Acid value of C14 AOS acid

wt of sample, g	ml of titrant	AV
0.5218	2.48	130.0
0.5957	2.70	123.9
	average	<b>127.0</b>

The IR spectrum of the C14 AOS acid showed the presence of sultone bands at 1330 – 1360. The IR spectrum also showed the unsaturated sulfonic acid peaks at 1720, 1163, 1040 and 900  $\text{cm}^{-1}$ . It can be concluded that C14 AOS acid was successful being produced. The IR spectrums of tetradecene and C14 AOS acid are given in Appendix G.

#### 4.1.9.2 Sulfonation of 1 – Hexadecene (C<sub>16</sub>H<sub>32</sub>) using 1.2 Mole Ratio of SO<sub>3</sub>

Reaction product of 1 – Hexadecene and SO<sub>3</sub> was obtained with conditions where oleum was pumped at the rate of 16.04 grams per minute or approximately 1.2 moles of SO<sub>3</sub> per mole of olefin. The calculations of feed rate of Hexadecene and oleum are given in Appendix C.

Factor calculated in this experiment was same to the theoretical which was 1 to 1.18. The results indicated the actual mole ratio of SO<sub>3</sub> per mole of Hexadecene was 1.18 to 1 in the reaction. Analysis of C16 AOS acid gave 96.46 AV. The acid value is shown in Table 4.10. The acid value of 96.46 was used in the calculation of the degree of sulfonation and 47.97 % of alkene sulfonic acid was produced by assuming MW of 279. A 0.5088 g of the acid/sulfone product was analyzed after neutralization. The C16 AOS acid was neutralized with 50 % NaOH and the analysis showed the anionic active matter of the reaction product was 40.4 % active.

**Table 4.10:** Acid value of C16 AOS acid

wt of sample, g	ml of titrant	AV
0.1737	2.78	98.81
0.2375	3.62	94.10
	Average	<b>96.46</b>

The IR spectrum of the starting material, 1 – Hexadecene (Figure 4.8) and the final product, C16 AOS acid (Figure 4.9) showed the loss of C=C stretch at 1642 cm<sup>-1</sup>. The presence of sulfone bands at 1330 – 1360, 810 – 818 cm<sup>-1</sup> and unsaturated sulfonic acid peaks at 1711, 1161, 1040 and 902 cm<sup>-1</sup> indicated the conversion of 1 – Hexadecene into alkene sulfonic acid. A broad hydroxyl band centring at 3482 cm<sup>-1</sup> from the hydroxyalkane sulfonate was found. The results confirm the formation of C16 AOS acid and sulfone.

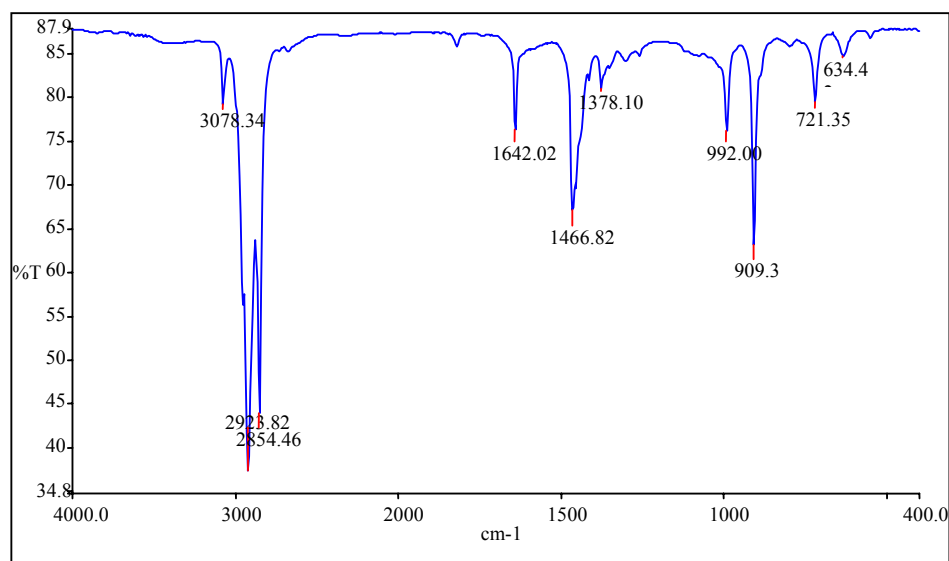


**Figure 4.8** Infra-red spectrum of 1 – Hexadecene

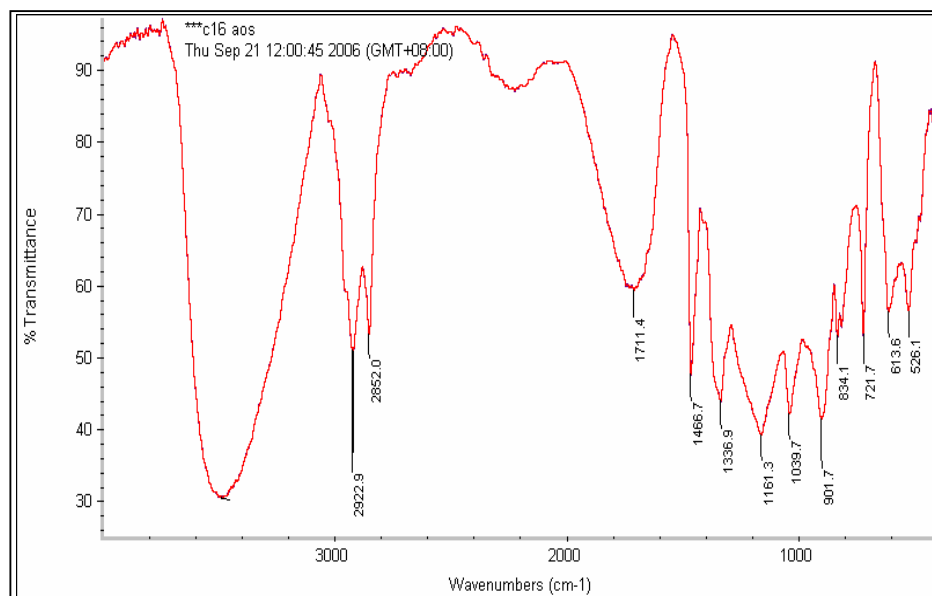


**Figure 4.9** Infra-red spectrum of C16 AOS acid

#### 4.1.9.3 Alkylation and Sulfonation of the Extracted Oil using Alpha Olefin Sulfonic Acid

The phenolic compounds in extracted pyrolysis oil was alkylated and sulfonated in one step using alpha olefin sulfonic acid (AOS acid) to synthesize the desired surfactants. There were six surfactants produced in this study using different type and weight ratio of alpha olefin sulfonic acid. The surfactants produced are shown in Table 4.11.

**Table 4.11:** Experiment details for alkylation and sulfonation by AOS acid

Exp. No.	Type of AOS acid used	Weight ratio	Surfactant Name
S1	C14	100:30	SURF1
S2	C14	100:60	SURF2
S3	C14	100:90	SURF3
S4	C16	100:30	SURF4
S5	C16	100:60	SURF5
S6	C16	100:90	SURF6

In the experiment of alkylation and sulfonation of extracted pyrolysis oil, the sampling was repeated every hour until the reaction was complete and the acid value was remained constant. Table 4.12 shows the acid value of C14 sulfonated pyrolysis oil and Table 4.13 shows the acid value of C16 sulfonated pyrolysis oil.

In Table 4.14, it is found that the anionic active matter of SURF 1 was the highest (40.4 % active) and the critical micelle concentration (CMC) was found to be the lowest (0.22 wt %) among all the surfactants. The determination of CMC of the surfactants is given in Appendix H. The surface tension of SURF 3 at concentration of 5 wt % was 33.2 mN/m, which is achieved the lowest value among these six different surfactants. These values indicated the SURF 3 was a good surfactant.

As shown in Table 4.14 and Table 4.15, analysis of SURF 4 gave the lowest value of anionic active matter (20.55 % active). The CMC and surface tension were found to be the highest at 0.28 wt % and 36.2 mN/m, respectively. SURF 4 was the poorest surfactant among the surfactants produced from pyrolysis oil.

**Table 4.12:** Acid value of C14 sulfonated pyrolysis oil

Time @ 90°C	Acid Value (AV) (using C14 AOS acid in different weight ratio)		
	100:30 (SURF 1)	100:60 (SURF 2)	100:90 (SURF 3)
0 hour	111.0	118.8	119.8
1 hour	133.2	215.8	230.9
2 hours	158.6	224.7	445.6
3 hours	194.5	372.5	631.0
5 hours	308.3	372.5	660.5

**Table 4.13:** Acid value of C16 sulfonated pyrolysis oil

Time @ 90°C	Acid Value (AV) (using C16 AOS acid in different weight ratio)		
	100:30 (SURF 4)	100:60 (SURF 5)	100:90 (SURF 6)
0 hour	140.3	187.0	190.0
1 hour	180.3	233.8	250.0
2 hours	240.3	294.3	288.0
3 hours	374.0	327.3	450.0
5 hours	374.0	558.0	589.0

**Table 4.14:** Anionic active matter and CMC of surfactants produced

Type of Surfactant	Percentage of anionic active matter, % active	CMC, wt %
SURF 1	40.40	0.22
SURF 2	28.80	0.24
SURF 3	39.09	0.24
SURF 4	20.55	0.28
SURF 5	32.79	0.28
SURF 6	36.00	0.24

**Table 4.15:** Surface tension of surfactants in concentration of 5 wt %

Type of Surfactant	Surface tension, mN/m
SURF 1	34.0
SURF 2	33.5
SURF 3	33.2
SURF 4	36.2
SURF 5	34.0
SURF 6	35.0

#### 4.1.9.4 Alkylation and Sulfonation of the Pyrolysis Oil using Alpha Olefin Sulfonic Acid

The pyrolysis oil was alkylated and sulfonated in one step using alpha olefin sulfonic acid (AOS acid) to synthesize the desired surfactants. There was only one surfactant produced in this experiment using weight ratio of alpha olefin sulfonic acid (100 : 60). The surfactants produced are shown in Table 4.16.



**Table 4.16:** Experiment detail for alkylation and sulfonation by AOS acid

Exp. No.	Type of AOS acid used	Weight ratio	Surfactant Name
S7	C14	100:60	SURF7

In the experiment of alkylation and sulfonation of pyrolysis oil, the sampling was repeated every hour until the reaction was complete and the acid value was remained constant. Table 4.17 and Table 4.18 shown analysis of SURF7 which is gave value of anionic active matter (29.90 % active). The CMC and surface tension were found at 0.22 wt % and 33.0 mN/m respectively.

**Table 4.17:** Anionic active matter and CMC of surfactants produced

Type of Surfactant	Percentage of anionic active matter, % active	CMC, wt %
SURF 7	29.90	0.22

**Table 4.18:** Surface tension of surfactants in concentration of 5 wt %

Type of Surfactant	Surface tension, mN/m
SURF 7	33.0

#### 4.1.9.5 FTIR Characterization of Produced Surfactants

The surfactant produced from pyrolysis oil of oil palm shell was characterized by using FTIR. The IR spectrums recorded of the seven produced surfactants from the pyrolysis oil show a similar pattern. The results indicate that chemical structure for these seven surfactants were similar. The spectrum recorded after scanning on the FTIR of surfactant SURF 1 is shown in Figure 4.10. The IR

spectrums of the other five types of surfactant (SURF 2, SURF 3, SURF 4, SURF 5 SURF 6 and SURF7) are given in Appendix I.

The presence of phenols O–H stretch was indicated by the absorbance peak of O–H stretching vibration between  $3500 - 3400 \text{ cm}^{-1}$ . The absorbance peaks between  $3000 - 2850 \text{ cm}^{-1}$  represented the C–H stretching vibration. It showed the loss of sultone bands at  $1330 - 1360 \text{ cm}^{-1}$  and alkene group at 1711, 1161, 1040 and  $902 \text{ cm}^{-1}$  indicating the conversion of alpha olefin sulfonic acid into alkylated, alkylphenol sulfonate. The peaks in between  $1200 - 1140$  were another indication of the presence of sulfonate groups due to the S=O stretching vibration. The region from  $2000$  to  $1500 \text{ cm}^{-1}$  is where C=O, C=N, and C=C bonds absorb. An adsorption in the range from  $1660 - 2000 \text{ cm}^{-1}$  shows the combination of a phenol with an olefinic group.

## **4.2 Production of xanthan gum from local fruits**

### **4.2.1 Dry weight of xanthan gum produced**

The growth of *Xanthomonas campestris* had come to death phase after 48 hours fermentation process. The dry weight of the xanthan gum was obtained after dried for 72 hours at  $50^{\circ} \text{C}$ . Figure 4.10 shows the result obtained for dry weight of xanthan gum produced from local fruits. It is found that the honeydew produced the higher yield of xanthan gum with 8.3550 g/L followed by xanthan gum from papaya and dragon fruit which is yield of xanthan 7.6850 g/L and 6.1230 g/L respectively. While the lower yield of xanthan gum from star fruit (3.5120 g/L).

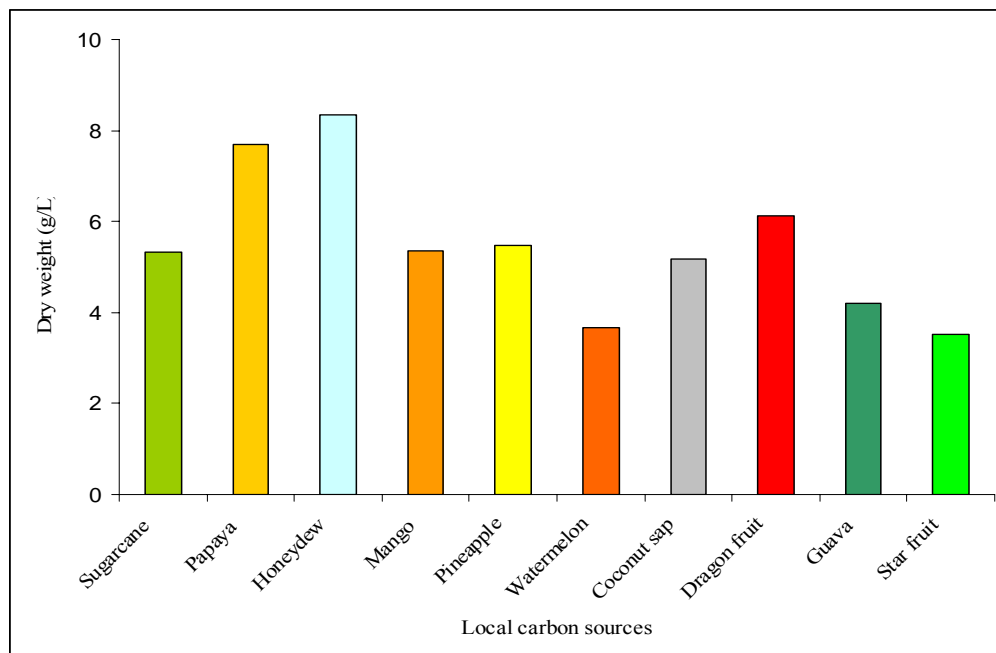


**Figure 4.10** Dry weights (g/L) of produced Xanthan gum

## 4.2.2 FTIR Characterization of Produced xanthan gums

### 4.2.2.1 Unrefined xanthan gum produced

The producing of xanthan gum from local fruits juice was confirmed by IR spectroscopy. The FTIR spectra recorded under same conditions. From the FTIR spectra [Fig. (a), (b), (c), (d), (e), (f), (g), (h), (i),(j)]. The spectra are summarized in Table 4.19 It is evident that xanthan gum shows a broad absorption peak at  $3422\text{ cm}^{-1}$  (commercial xanthan gum), which is the region for the hydrogen-bonded OH groups. All of spectra for xanthan production from local fruits which is similarity with commercial xanthan gum. Two peaks, one around  $1125$  and the other at  $1051\text{ cm}^{-1}$ , are attributed to the  $\text{-C-O-C-O-C-}$  acetal for xanthan gum from coconut sap only. It was differ from the others local fruits. The vibration peak of  $\text{-CH}_2$ , no appears in the spectra of xanthan gum from sugarcane and papaya and the peak of  $\text{-C-O-C-}$  in the spectra of xanthan gum from dragon fruit, guava and star fruit. It is

found that the vibration peak of C<sub>1</sub>-H of  $\beta$ -pyranose at 800 cm<sup>-1</sup> appears in the spectra of xanthan gum from watermelon only.

**Table 4.19 FTIR Spectra Data (cm<sup>-1</sup>) of xanthan gum unpurified**

V, cm <sup>-1</sup>											Assignment
XG	pine apple	water melon	sugar cane	papaya	honey dew	mango	coconut sap	dragon fruit	guava	star fruit	
3422	3419	3416	3424	3426	3441	3433	3415	3411	3422	3429	O-H
2908	2924	2924	-	-	2930	2924	2929	2936	2929	2929	-CH <sub>2</sub>
1626	1648	1625	1642	1641	1638	1636	1647	1642	1643	1639	-C=O of pyruvate, $\delta$ OH
1407	1401	1397	1394	1406	1399	1396	1407	1424	1407	1421	-COO <sup>-</sup>
1264	1245	-	1250	1259	1297	1256	1251	-	-	-	-C-O-C-, $\delta$
1089	1083	1071	1081	1081	1119	1120	1125 1051	1123	1124	1116	-C-O-C-O- C- acetal
-	-	800	-	-	-		-	-	-	-	C <sub>1</sub> -H of $\beta$ - pyranose

#### 4.2.2.2 Refined xanthan gum produced

The purification process seems efficient to eliminate impurities, leading to products of food quality. The xanthan gum produced from local fruits is collected after harvest via shaker fermentation at 28 ° C for 48 hours where it's purified through a total controlled sterilizing process with chemical added and recovery with three volumes of 96 % ethanol. The FTIR spectra of refined xanthan gum recorded under the same conditions. The spectra are summarized in Table 4.16.

It is found that the vibration peak of  $\text{-OH}$  at  $3569\text{ cm}^{-1}$  and  $3607\text{ cm}^{-1}$  appears in the spectra of refined xanthan gum from coconut sap and guava respectively. Compared with that of unrefined xanthan gum coconut sap and guava ( $3415\text{ cm}^{-1}$  and  $3422\text{ cm}^{-1}$ ) (Table 4.20), the peak of refined xanthan gum shifts to high wave number, suggesting that the intermolecular interaction between unrefined xanthan gum molecules is stronger than that between refined xanthan gum. From the observation, xanthan gum from watermelon only appears the vibration peaks of the acetal at  $1107\text{ cm}^{-1}$  of refined xanthan gum are stronger than those of unrefined xanthan gum at  $1071\text{ cm}^{-1}$ , inferring that the chemical modifier reacts with the  $\text{-OH}$  of the unrefined xanthan gum to form the acetal. These results indicate that when refined xanthan gum dissolves in water, the attraction of the molecular cluster of the solid phase to the refined xanthan gum surface molecules at the surface of the swollen layer is much weaker, causing the refined xanthan gum surface molecules which swell completely to diffuse into the water phase more easily. Only refined xanthan gum from honeydew exhibited the vibration peak of  $\text{C}_1\text{-H}$  of  $\beta$ -pyranose at  $803\text{ cm}^{-1}$  compared than others refined xanthan gum produced.

**Table 4.20 FTIR Spectra Data ( $\text{cm}^{-1}$ ) of xanthan gum purified after dry at  $50^\circ\text{C}$**

V, $\text{cm}^{-1}$										Assignment
pine apple	water melon	sugar cane	papaya	honey dew	mango	coconut sap	dragon fruit	guava	star fruit	
3422	3419	3416	3417	3426	3437	3607	3399	3569	3404	O-H
2924	2920	2930	2936	2930	2924	2924	2923	2919	2929	$\text{-CH}_2$
1646	1634	1635	1631	1645	1633	1648	1631	1646	1638	$\text{-C=O}$ of pyruvate
1402	1396	1393	1401	-	1399	1401	1399	1399	-	$\text{-COO}^-$
1250	1264	1253	1253	-	1245	1245	1263	-	-	$\text{-C-O-C-}$
1072	1107	1079	1098	1108	1117	1067	1115	1122	1117	$\text{-C-O-C-}$ O- C- acetal
-	-	-	-	803	-	-	-	-	-	$\text{C}_1\text{-H}$ of $\beta$ -pyranose

Table 4.17 shows the weight of refined xanthan gum after purification process. It is found that refined xanthan gum from sugarcane and honeydew gives higher percentage yield of xanthan, which is 79 % and 78 % respectively compared to other local fruits. While refined xanthan gum from dragon fruit exhibited lower percentage yield of xanthan after purification process.

**Table 4.17** Weight of refined xanthan gum after purification process

<b>Bil</b>	<b>Xanthan gum</b>	<b>Before (g)</b>	<b>After (g)</b>	<b>Percentage</b>
1	Pineapple	0.5048	0.3806	75.4
2	Watermelon	0.3449	0.2525	73.2
3	Papaya	0.5036	0.3779	75.0
4	Sugarcane	0.5066	0.4048	79.9
5	Honeydew	0.5054	0.3955	78.3
6	Mango	0.5038	0.3655	72.5
7	Coconut sap	0.5045	0.3550	70.4
8	Guava	0.5000	0.3100	62.0
9	Star fruit	0.5000	0.3100	62.0
10	Dragon fruit	0.5000	0.3000	60.0

#### 4.2.2.3 Viscosity measurement

The viscosities and shear stress of unrefined xanthan gum and refined xanthan gum in distilled water and NaCl were measured at different shear rate. 0.1 gram of dried xanthan gum was dissolved in 100 mL of distilled water. While for brine solution, 0.2 % w/v and 0.4 %w/v of NaCl was added into the solutions. The solutions were prepared by first adding water to the xanthan gum and NaCl powder and gently mixing until all xanthan gum appeared dissolved.

The result of the viscosities and shear stress measurement indicates that the unrefined xanthan gum from local fruits more viscous than commercial xanthan gum at room temperature (Figure 4.11 and 4.12) . This shows that unrefined xanthan gum contributed to a better characteristic compared commercial xanthan gum. The difference characteristic may due by dissimilarity content of sucrose, glucose and others. Local fruits juice sources contain polysaccharide and disaccharide and need to hydrolyze to become monosaccharide for metabolism process in order to grow. When the demand of glucose for the metabolism process is fulfilled, the microbe will transform the remaining starches into xanthan gum as energy storage. Thus, it can be noticed that the substrates used would affect the properties and the structure of the produced biopolymer.

The comparison of the unrefined xanthan gum in 0.2 % w/v and 0.4 % w/v NaCl, the viscosities and shear stress was shown as Figure 4.13, 4.14, 4.15 and 4.16. Meanwhile refined xanthan gum in 0.2 % w/v and 0.4 % w/v of NaCl, for their viscosities and shear stress was shown in Figure 4.17, 4.18, 4.19 and 4.20. In general, unrefined xanthan gum and refined xanthan gum in 0.2 % w/v of NaCl was higher compared than 0.4 % w/v of NaCl. Conversely it does not show significant difference for their viscosities and shear stress at any time.

The viscosities and shear stress of refined xanthan gum solutions from all of local fruits was higher than that of unrefined xanthan gum in distilled water and NaCl at any time as shown in Figure. It was also found that the refined xanthan gum dispersed very rapidly to give lump free solution.

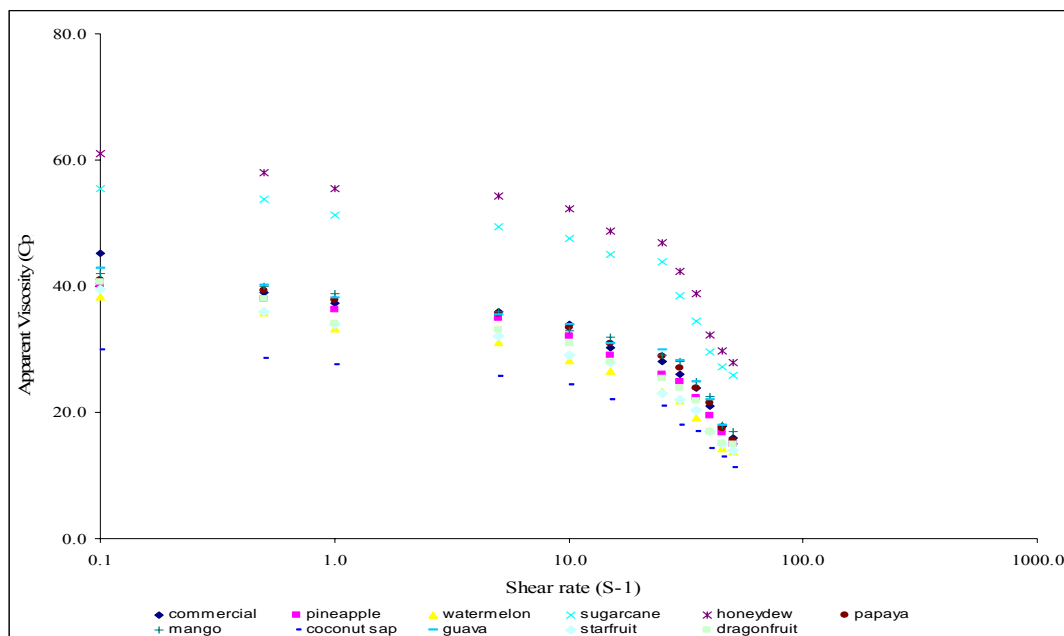


**Figure 4.11** Comparison viscosity graph for xanthan gum commercial and unrefined in distilled water (DW)

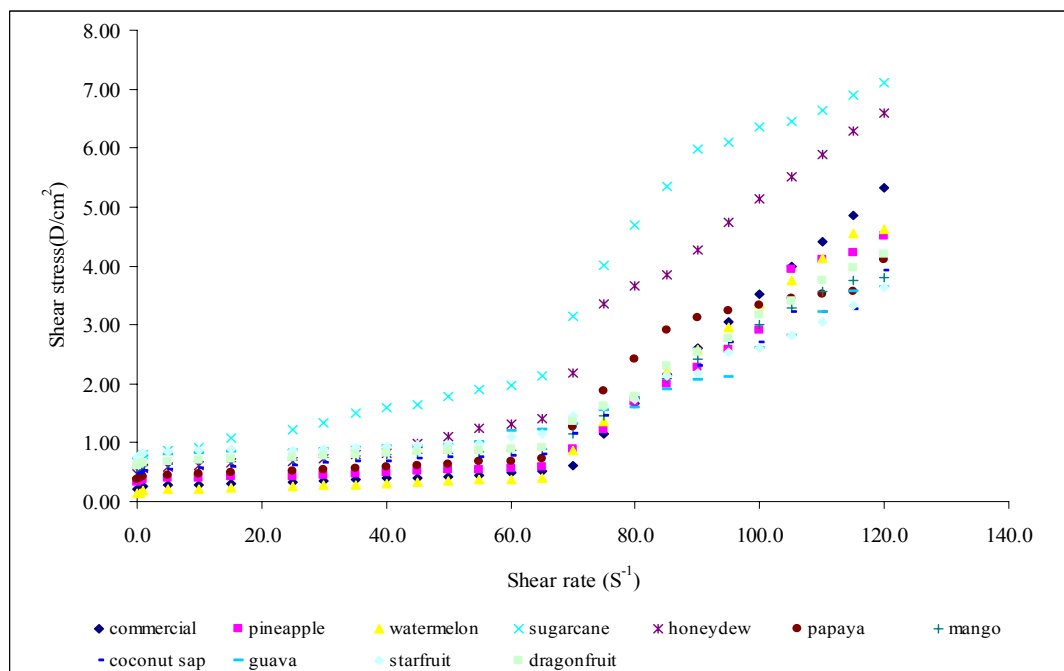


**Figure 4.12** Comparison shear stress graph for xanthan gum commercial and unrefined xanthan gum in distilled water (DW)



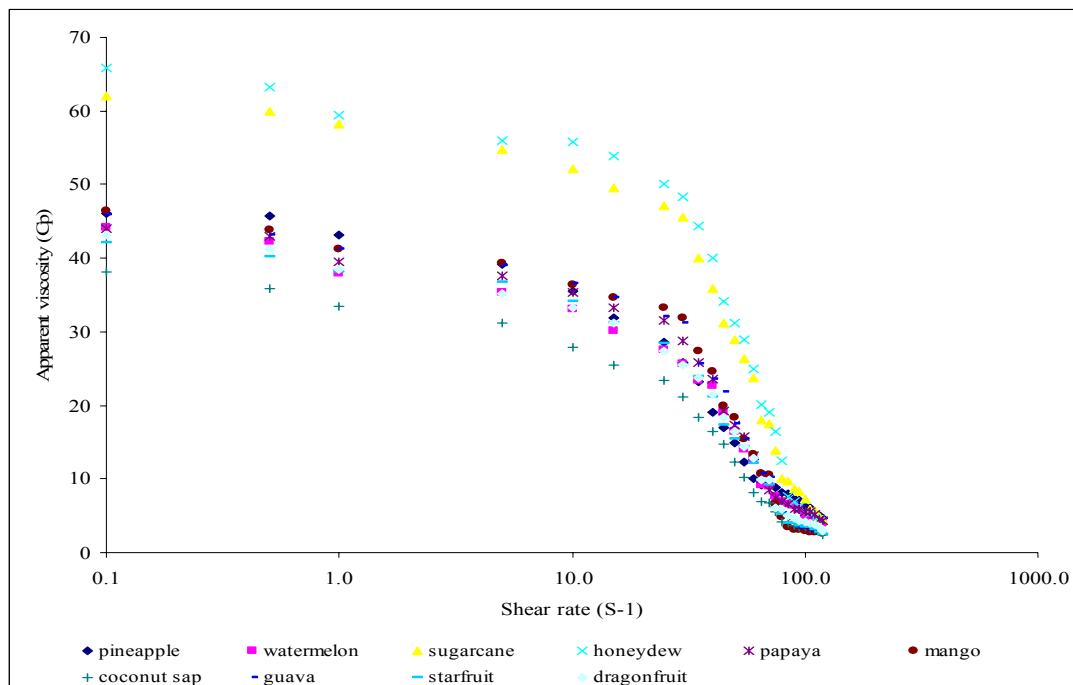


**Figure 4.13** Comparison viscosities of unrefined xanthan gum in 0.2 % w/v NaCl

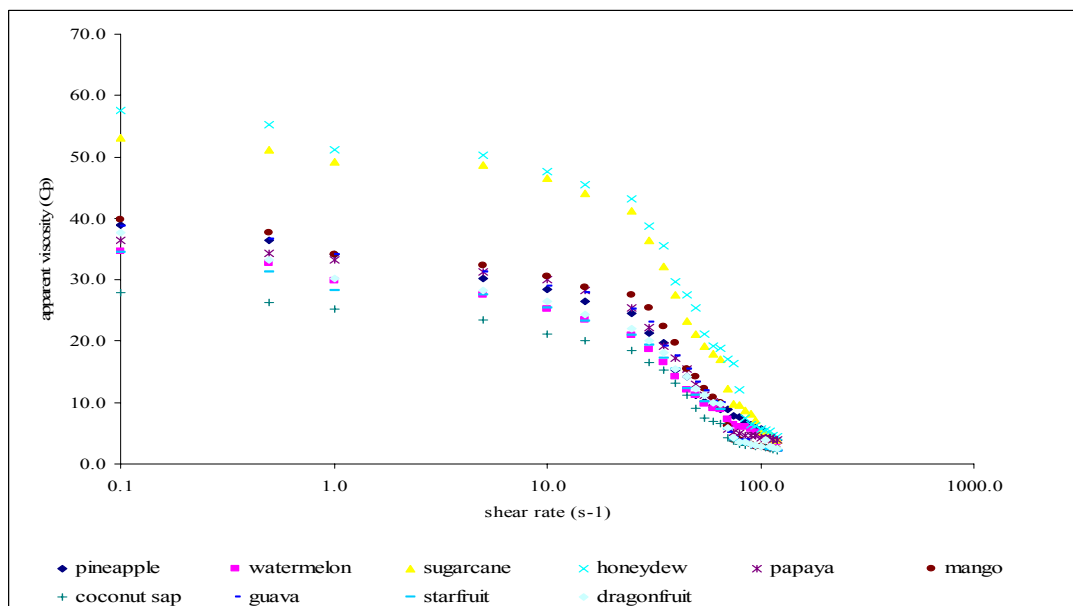


**Figure 4.14** Comparison viscosities of unrefined xanthan gum in 0.4 % w/v NaCl

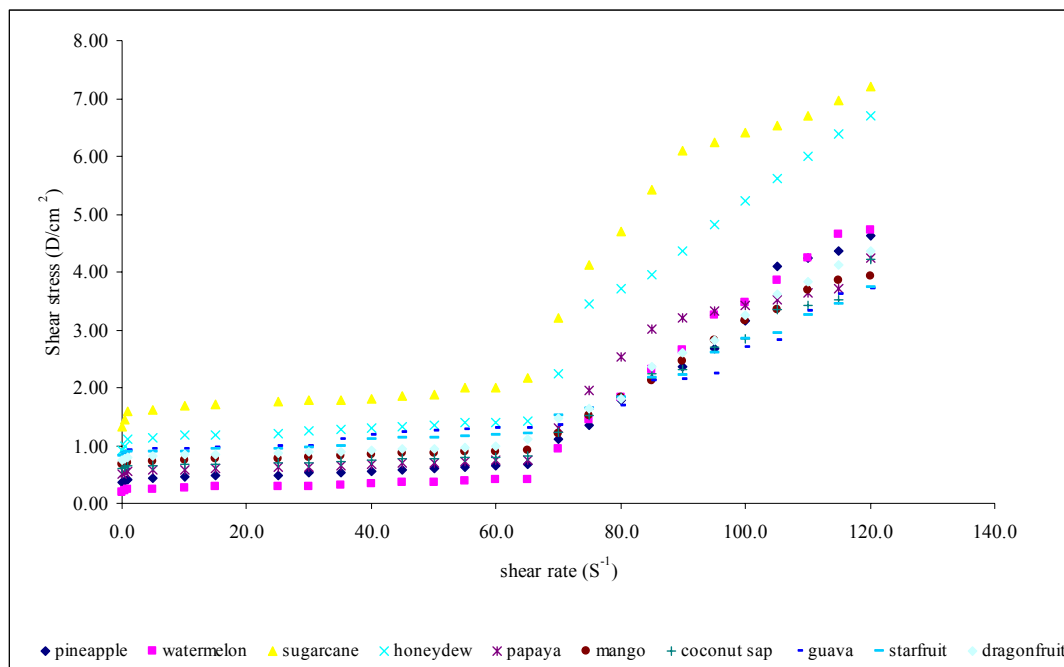


**Figure 4.15** Comparison shear stress graph for unrefined xanthan gum in 0.2 % w/v NaCl

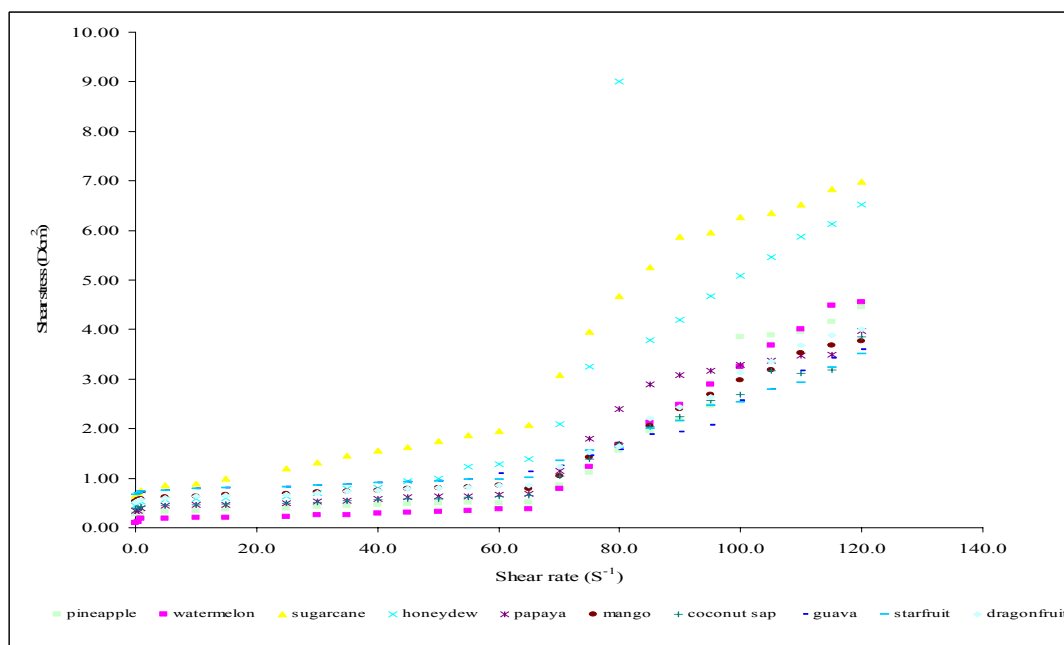


**Figure 4.16** Comparison shear stress graph for unrefined xanthan gum in 0.4 % w/v NaCl

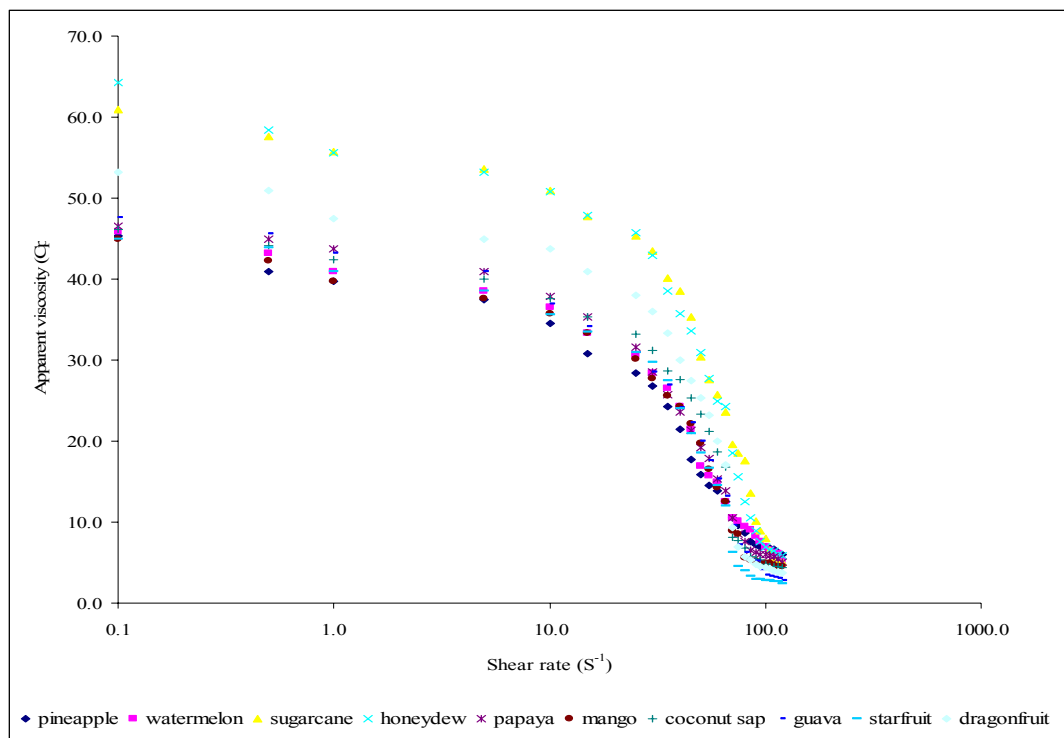


**Figure 4.17** Comparison viscosity graph for refined xanthan gum in distilled water (DW)

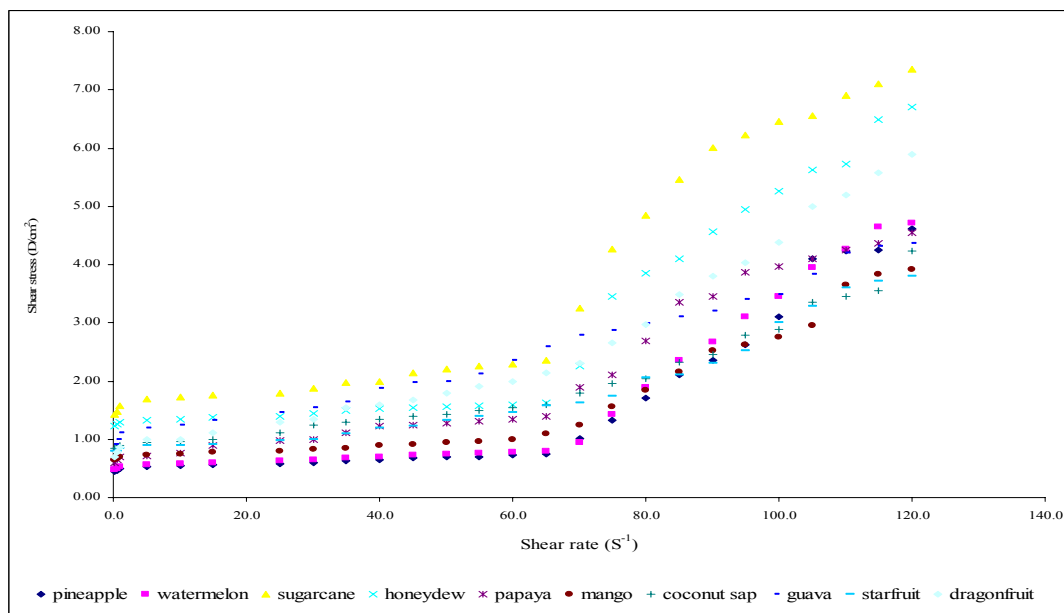


**Figure 4.18** Comparison shear stress graph for refined xanthan gum in distilled water (DW)

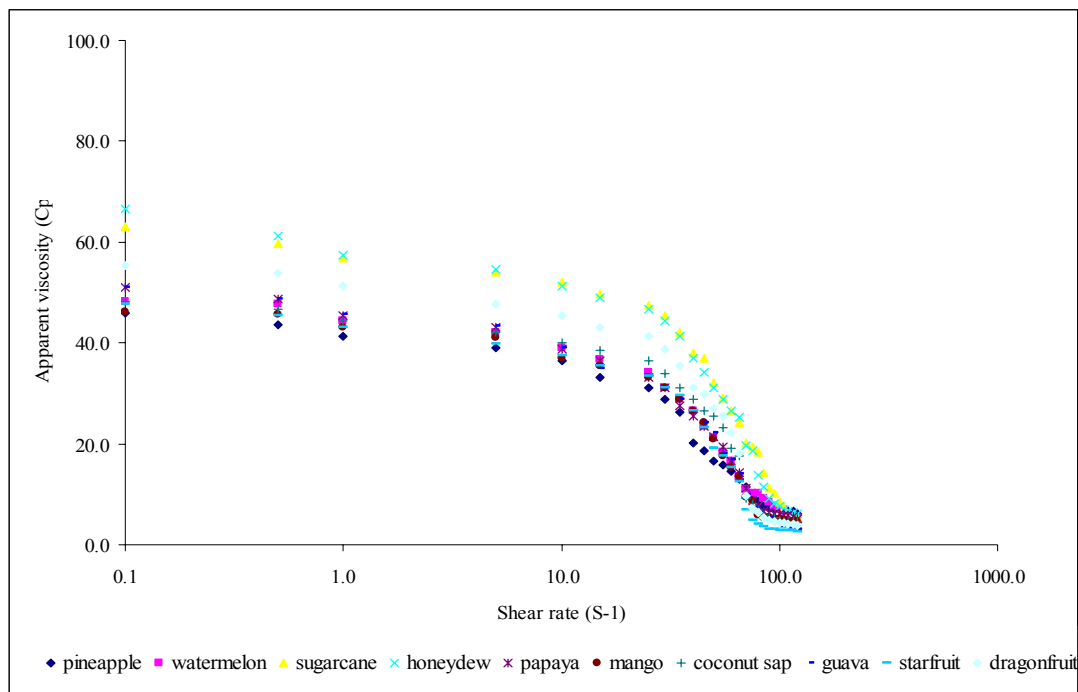


**Figure 4.19** Comparison viscosities of refine xanthan gum in 0.2 % w/v of NaCl

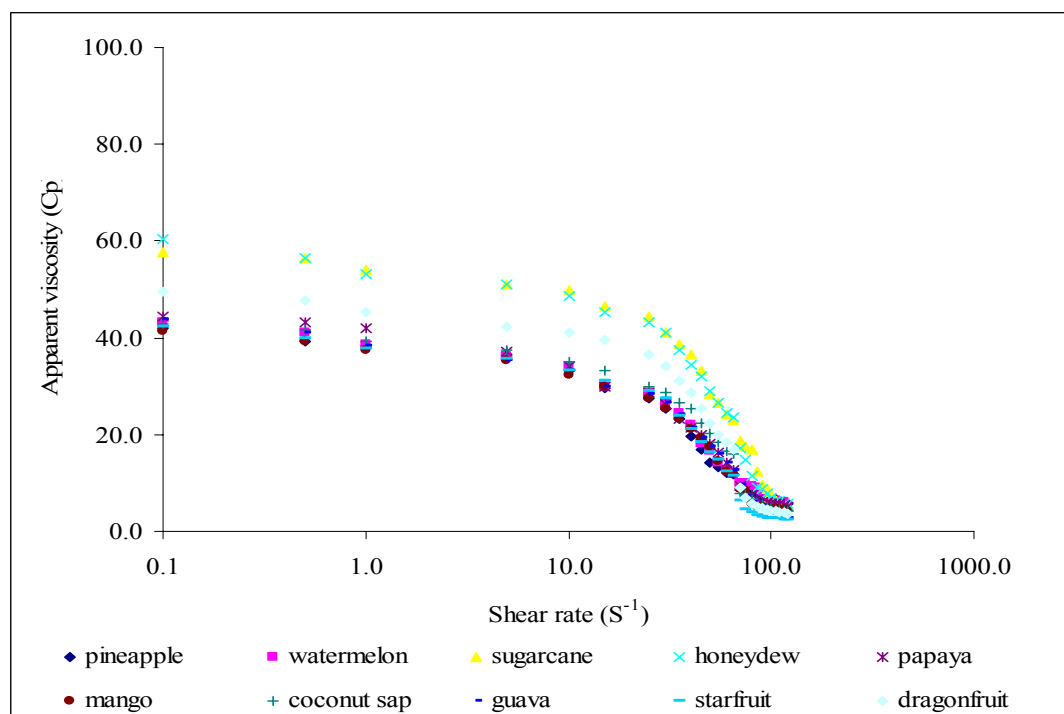


**Figure 4.20** Comparison viscosities of refine xanthan gum in 0.4 % w/v of NaCl

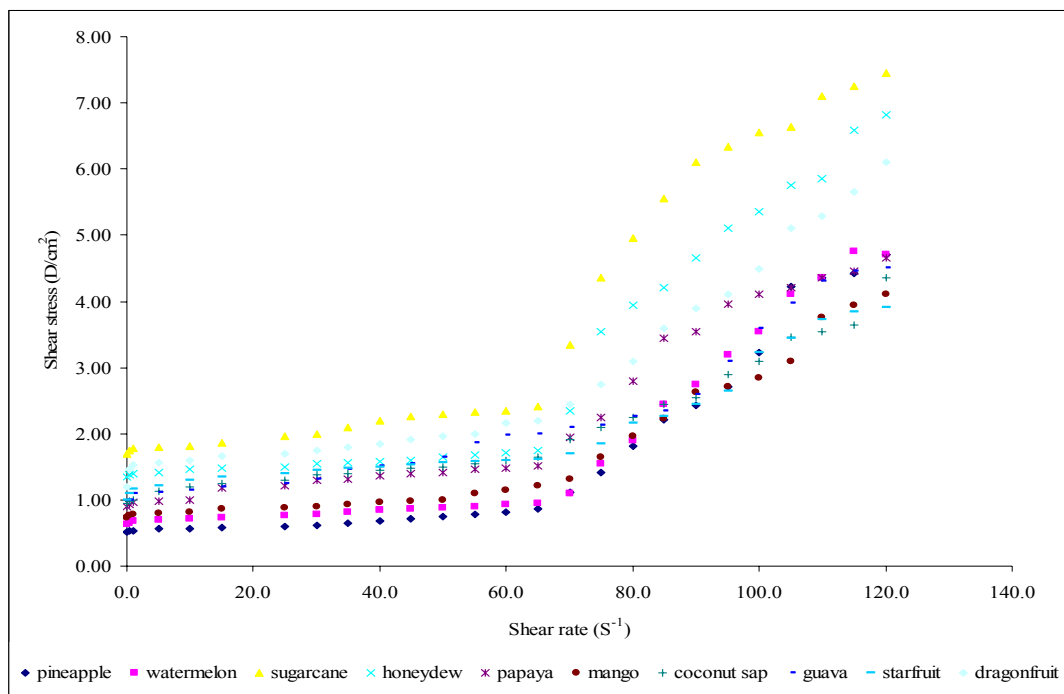


**Figure 4.21** Comparison shear stress graph for refined xanthan gum in 0.2 % w/v of NaCl

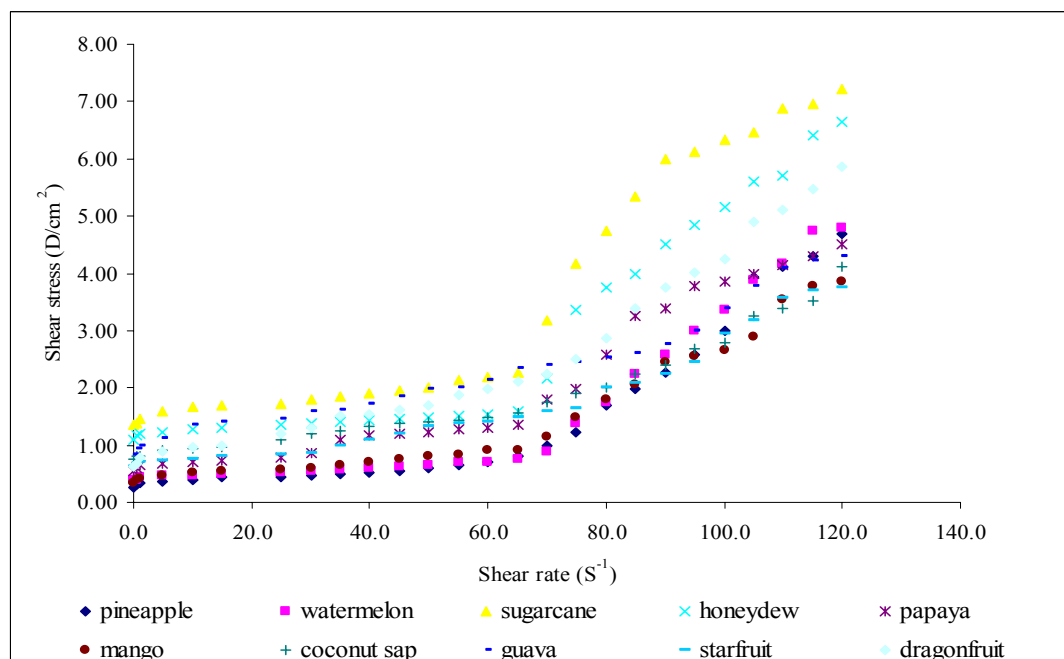


**Figure 4.22** Comparison shear stress graph for refined xanthan gum in 0.4 % w/v of NaCl

#### 4.2.2.4 Gelatinization of refined xanthan gum

The gelling of refined xanthan gum was performed using bottle experiment. Refined xanthan gum with concentration 1500 ppm placed in the oven at 60 °C for days. The gelling of refined xanthan gum was observed based on gel strength code (Figure 4.23).

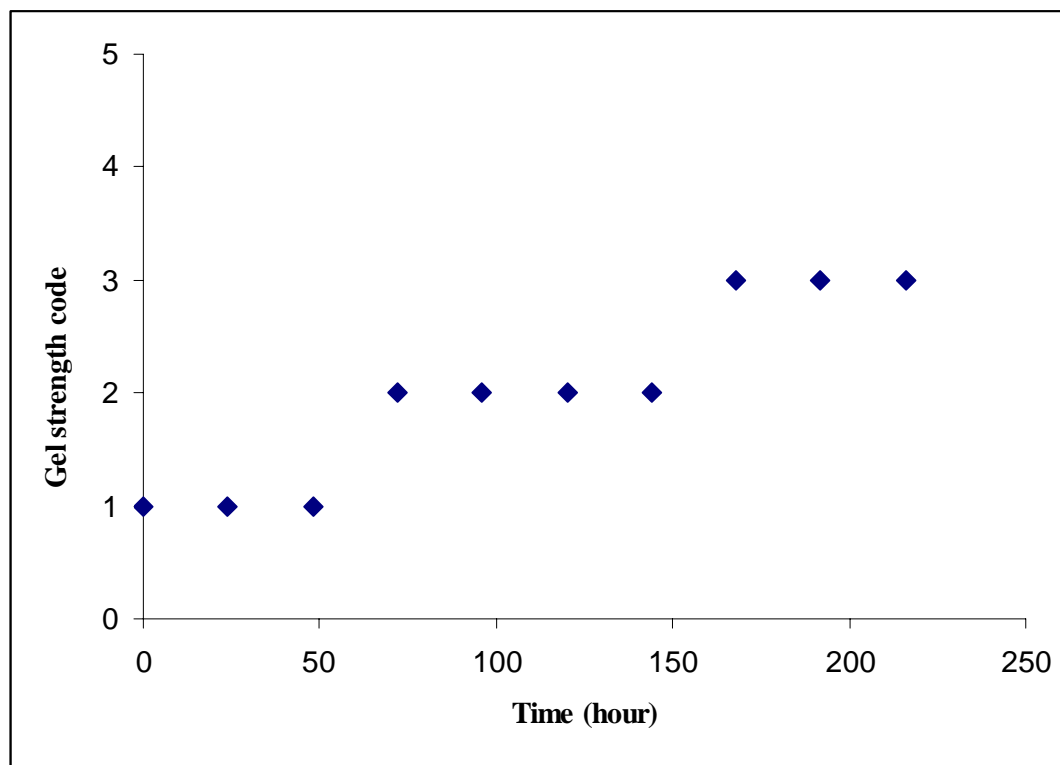


**Figure 4.23** The gelling of refined xanthan gum {1500 ppm, 10 : 1 ratio of XG to Cr (III)}



**Figure 4.24** Gelling of refined xanthan gum after 2 days at 60° C



**Figure 4.25** Gelling of refined xanthan gum after 6 days at 60° C

#### 4.2.2.5 Glucose concentration of fruits juice

The concentration of glucose used as the carbon sources during shaker fermentation at 28° C as can be seen in Figure 4.26. It is found that local honeydew gives highest glucose content of 61.2 g/L and the lowest concentration of glucose which is watermelon is 12.8 g/L only. From the observation, it was concluded that the yield of produced xanthan gum relies on the glucose concentration of local fruits.

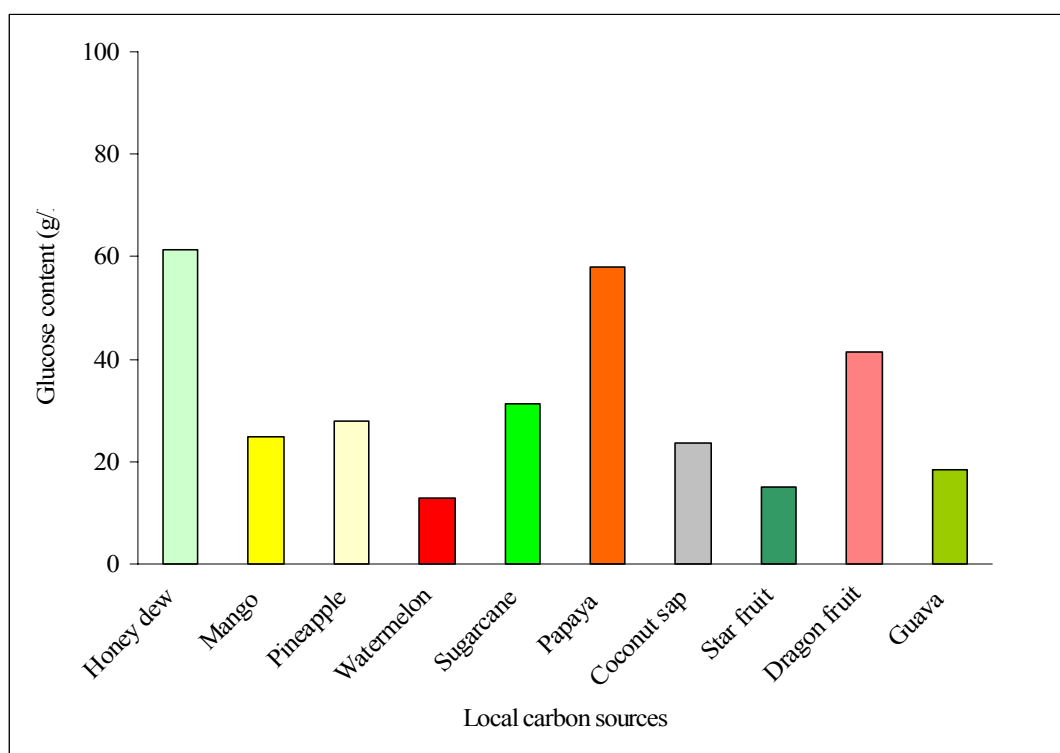


**Figure 4.26** Glucose concentration of fruits juice as carbon sources

#### 4.2.2.6 Pyruvate and acetate content

Xanthan gum is used extensively for enhanced oil recovery as a mobility control agent, in drilling operations to increase the suspension capacity of the drilling mud, and in gels to improve the volumetric sweep efficiency. Flow properties,



injectivity, and adsorption characteristics depend on acetate and pyruvate content of xanthan. The degree of pyruvilation and acetylation of xanthan gum was determined using High Performance Liquid Chromatography (HPLC). There is no significant difference in the acetate and pyruvate content of different local carbon sources as shown in Figure 4.27 and Figure 4.28 respectively. It shows that xanthan gum produced from papaya and mango refined exhibited highest content of acetate with 0.07 g/mL. Meanwhile the lowest of acetate content which is xanthan gum produced from pineapple and honeydew with 0.01 g/mL. It was similar with pyruvate content from xanthan gum refined from local fruits. From the observation, xanthan gum produced from sugarcane exhibited highest of pyruvate with 1.12 g/mL and followed by xanthan gum produced from pineapple with 0.66 g/mL. While xanthan gum produced from papaya exhibited lowest concentration of pyruvate with 0.45 g/mL.

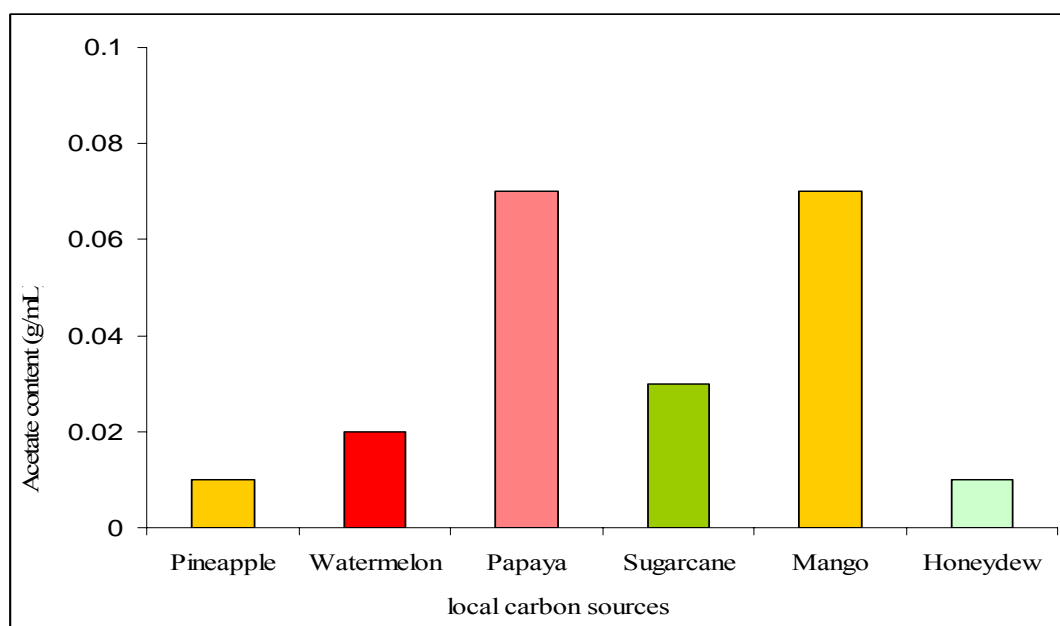


**Figure 4.27** Acetate content of 72 h xanthan samples from shaker fermentor

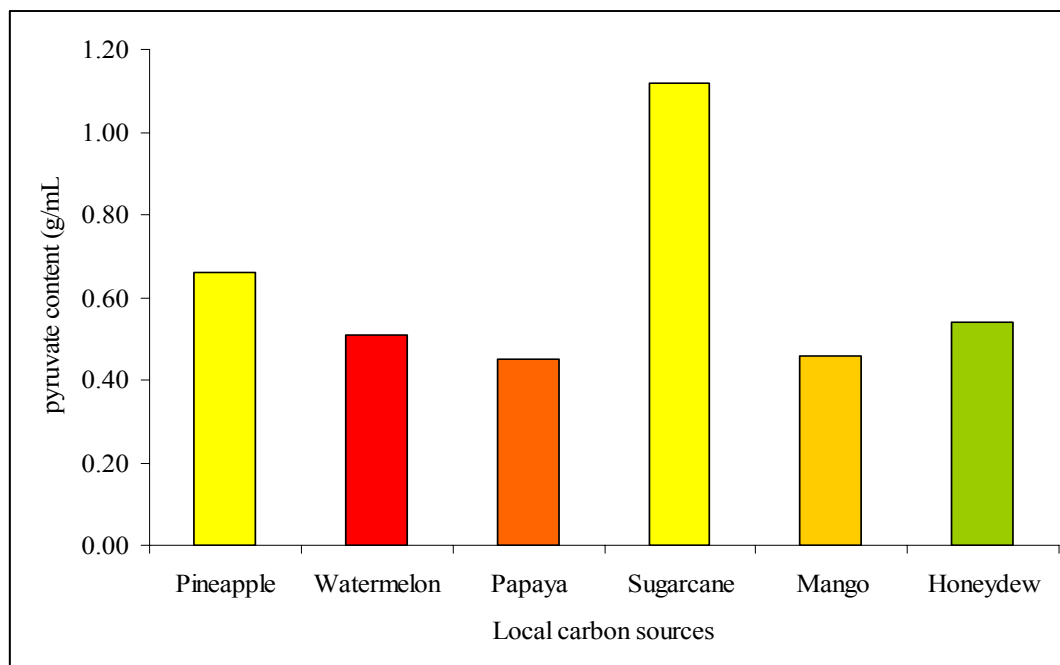


**Figure 4.28** Pyruvate content of 72 h xanthan samples from shake fermentor

#### 4.2.2.6 Solid state $^{13}\text{C}$ NMR

Solid state  $^{13}\text{C}$  NMR spectroscopy was used to investigate the structure of xanthan gum. The spectra can be divided into five main regions. In general, chemical shift signal at 180 ppm is due to carbonyl groups. The chemical shift signals at 108 ppm which originated from the C-1 carbon of mannose (acetyl and pyruvate group) and the resonance at 45 ppm, it is from glucuronic acid. Meanwhile chemical signal at 79 ppm is due to  $\text{sp}^3$ -hybridized carbons bonded to either nitrogen or oxygen. Furthermore chemical shifts from 27 – 35 ppm are due to  $\text{sp}^3$ -hybridized carbons attached to carbons and/or hydrogens. Conversely the entire of resonances from xanthan gum purified from honeydew juice were higher compared than xanthan gum purified from mango juice. The breadth and shape of the peaks in the spectra indicates that both forms of biopolymer are amorphous.

### 4.3 Dry weight of xanthan gum produced from local starches via shaker fermentation

The growth of *Xanthomonas campestris* had come to death phase after 48 hours fermentation process. The dry weight of the xanthan gum was obtained after dried for 72 hours at 50° C. Figure 4.29 shows the result obtained for dry weight of xanthan gum produced from local fruits. It is found that sago produced the higher yield of xanthan gum with 9.9690 g/L followed by xanthan gum from sweet potato and tapioca which is 8.7370 g/L and 6.3255 g/L respectively. While the lower yield of xanthan gum from rice starch (5.5190 g/L).

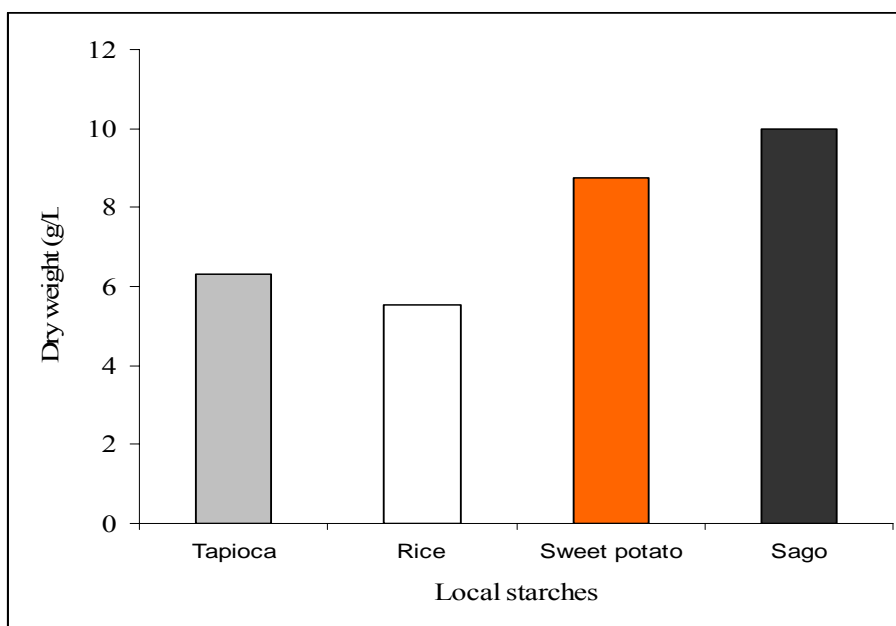


**Figure 4.29** Dry weights (g/L) of produced xanthan gum from starches

### 4.3.1 IR spectroscopy

#### 4.3.1.1 Unrefined xanthan gum produced

The producing of xanthan gum from local starches was confirmed by IR spectroscopy. The FTIR spectra recorded under same conditions. From the IR spectra [Fig. (a), (b), (c), (d)]. The spectra are summarized in Table 4.18. It is evident that xanthan gum shows a broad absorption peak at  $3422\text{ cm}^{-1}$  (commercial xanthan gum), which is the region for the hydrogen-bonded OH groups. Conversely no peak absorption of  $\text{C}_1\text{-H}$  of  $\beta$ -pyranose at  $850\text{ cm}^{-1}$  for commercial xanthan gum compared than xanthan gum produced. All of spectra for xanthan production from local starches which is similarity with commercial xanthan gum.

**Table 4.18 FTIR Spectra Data ( $\text{cm}^{-1}$ ) of xanthan gum unpurified**

V, $\text{cm}^{-1}$					Assignment
XG	Rice	Tapioca	Sweet potato	Sago	
3422	3386	3408	3390	3400	O-H
2908	2915	2915	2915	2922	$-\text{CH}_2$
1626	1646	1650	1650	1646	$-\text{C}=\text{O}$ of pyruvate
1407	1410	1399	1406	1381	$-\text{COO}^-$
1264	1145	1126	1141	1115	$-\text{C}-\text{O}-\text{C}-$
1089	1026	1022	1016	1024	$-\text{C}-\text{O}-\text{C}-\text{O}-$ C- acetal
-	850	850	850	853	$\text{C}_1\text{-H}$ of $\beta$ -pyranose

V, cm <sup>-1</sup>					Assignment
XG	Rice	Tapioca	Sweet potato	Sago	
3422	3401	3389	3397	3404	O-H
2908	2930	2930	2915	2915	-CH <sub>2</sub>
1626	1650	1653	1650	1650	-C=O of pyruvate
1407	1421	1429	1418	1418	-COO <sup>-</sup>
1264	1134	1134	1134	1119	-C-O-C-
1089	1021	1020	1022	1024	-C-O-C-O- C- acetal
-	850	853	853	857	C <sub>1</sub> -H of $\beta$ -pyranose

#### 4.3.1.2 Refined xanthan gum produced

The purification process seems efficient to eliminate impurities, leading to products of food quality. The xanthan gum produced from local starches is collected after harvest via shaker fermentation at 28 ° C for 48 hours where it's purified through a total controlled sterilizing process with washed 3 times of 99 % of ethanol. The FTIR spectra of refined xanthan gum recorded under the same conditions. The spectra are summarized in Table 4.19.

It is found that the entire of the vibration peak of the spectra of refined xanthan gum from rice, tapioca and sago only which is shifts to high wave number if comparing with unrefined and refined of xanthan gum.. It is suggesting that the intermolecular interaction between unrefined xanthan gum molecules is stronger than that between refined xanthan gum. It is also causes of inferring that the chemical modifier reacts. It is different with xanthan gum produced from sweet

potato. The commercial xanthan gum also no vibration peak of C<sub>1</sub>-H of  $\beta$ -pyranose at 850 cm<sup>-1</sup>, even though after process purification of xanthan gum.

**Table 4.19 FTIR Spectra Data (cm<sup>-1</sup>) of xanthan gum purified after dry at 50° C**

V, cm <sup>-1</sup>					Assignment
XG	Rice	Tapioca	Sweet potato	Sago	
3422	3401	3389	3397	3404	O-H
2908	2930	2930	2915	2915	-CH <sub>2</sub>
1626	1650	1653	1650	1650	-C=O of pyruvate
1407	1421	1429	1418	1418	-COO <sup>-</sup>
1264	1134	1134	1134	1119	-C-O-C-
1089	1021	1020	1022	1024	-C-O-C-O- C- acetal
-	850	853	853	857	C <sub>1</sub> -H of $\beta$ - pyranose

#### 4.3.1.3 Viscosity measurement

The viscosities and shear stress of unrefined xanthan gum and refined xanthan gum from local starches in distilled water and sodium chloride were measured at different shear rate. 0.1 gram of dried xanthan gum was dissolved in 100 mL of distilled water. While for brine solution, 0.2 % w/v and 0.4 %w/v of NaCl was added into the solutions. The solutions were prepared by first adding water to the xanthan gum and NaCl powder and gently mixing until all xanthan gum fully dissolved.

The result of the viscosities and shear stress measurement indicates that the unrefined xanthan gum from local starches in distilled water (DW) more viscous

than commercial xanthan gum at room temperature (Figure 4.30 and 4.31). This shows that unrefined xanthan gum contributed to a better characteristic compared to commercial of xanthan gum. The difference characteristic may due by dissimilarity content of sucrose, glucose and others. Local starches sources contain polysaccharide and disaccharide and need to hydrolyze to become monosaccharide for metabolism process in order to grow. When the demand of glucose for the metabolism process is fulfilled, the microbe will transform the remaining starches into xanthan gum as energy storage. Thus, it can be noticed that the substrates used would affect the properties and the structure of the produced biopolymer.

The comparison of the refined xanthan gum in between 0.2 % w/v and 0.4 % w/v of NaCl, the viscosities and shear stress was shown as Figure 4.32, 4.33, 4.34 and 4.35 respectively. In general, refined xanthan gum in 0.2 % w/v of NaCl was higher viscous compared than refined xanthan gum in distilled water (DW) and 0.4 % w/v of NaCl. Conversely it does not show significant differences for their viscosities and shear stress at any time.

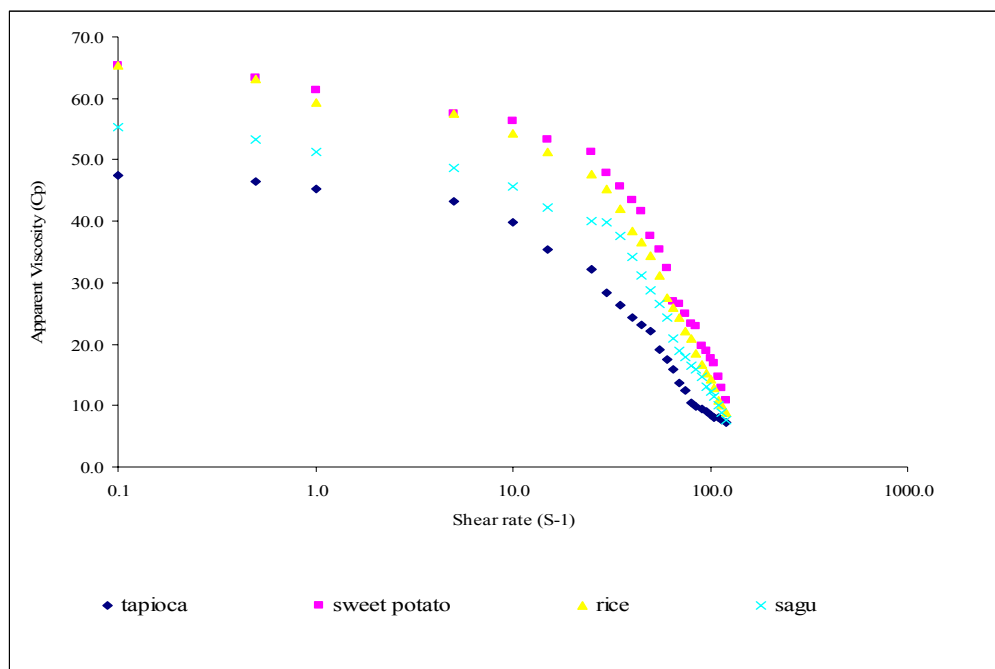


**Figure 4.30** Comparison viscosity graph for xanthan gum refined in distilled water (DW)

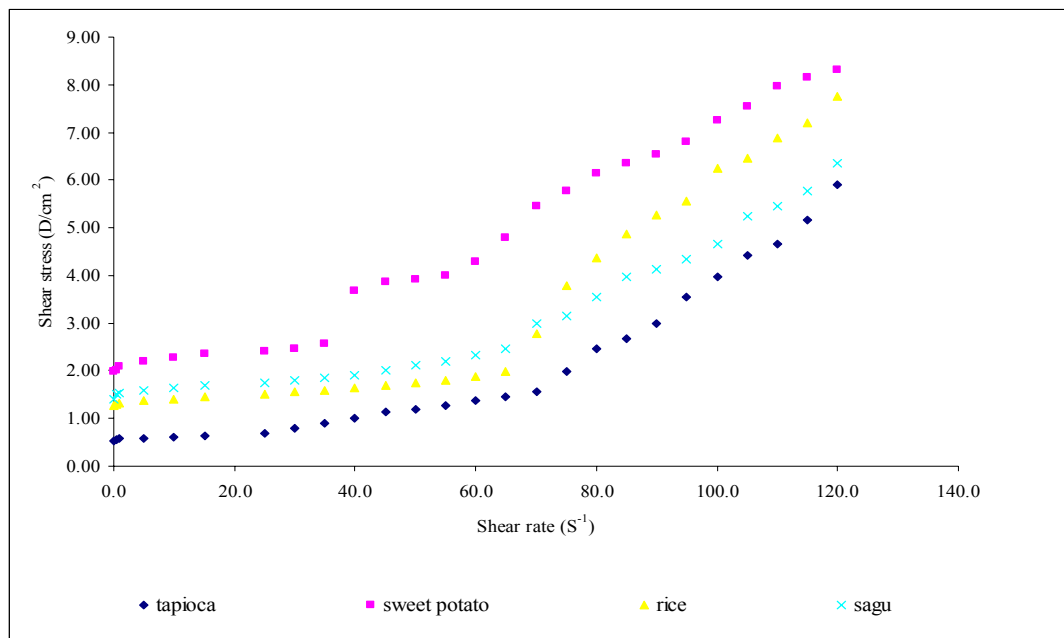


**Figure 4.31** Comparison shear stress graph for xanthan gum refined xanthan gum in distilled water (DW)

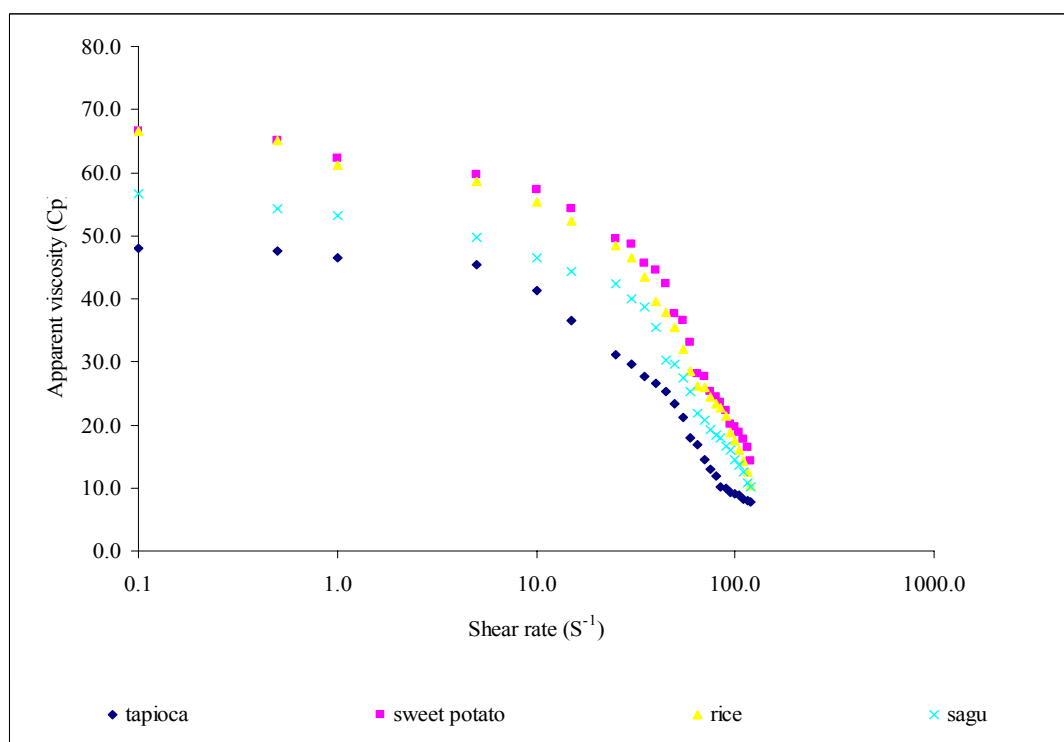


**Figure 4.32** Comparison viscosities of refined xanthan gum in 0.2 % w/v NaCl



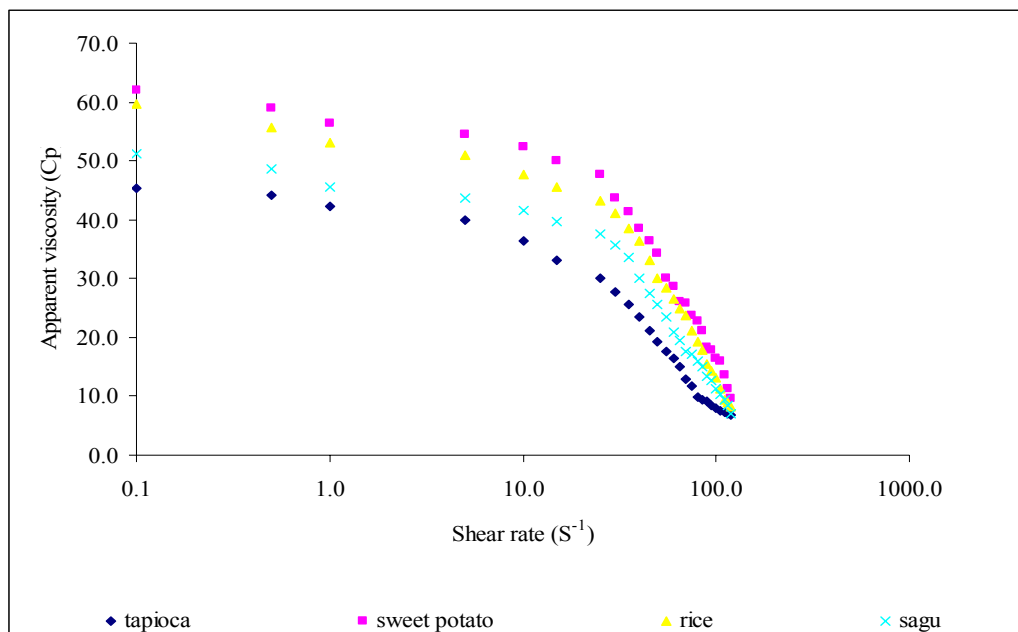


**Figure 4.33** Comparison viscosities of refined xanthan gum in 0.4 % w/v NaCl

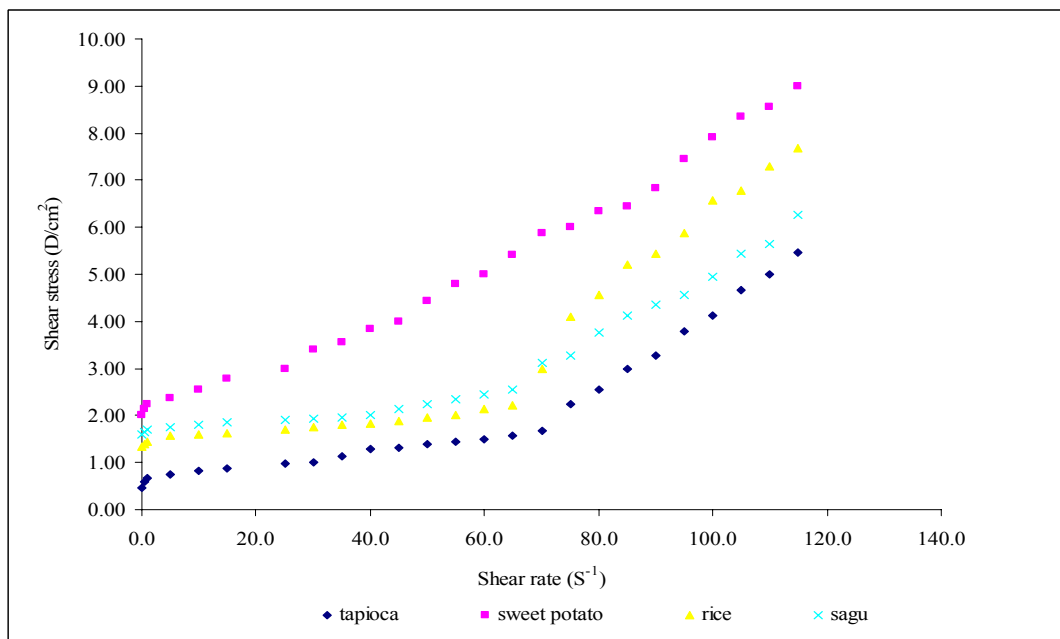


**Figure 4.34** Comparison shear stress graph for refined xanthan gum in 0.2 % w/v NaCl

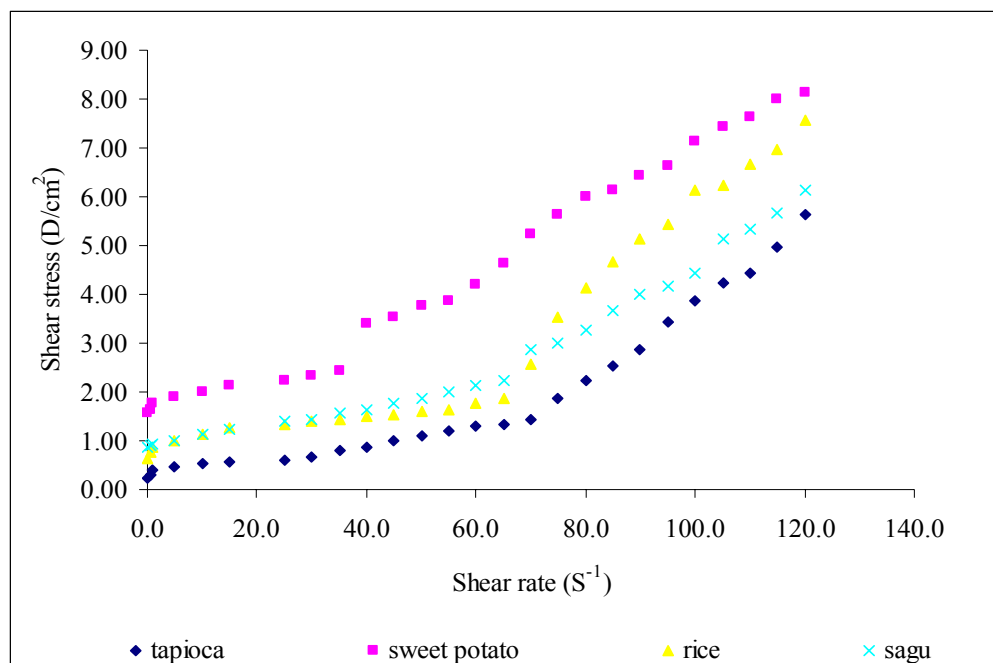


**Figure 4.35** Comparison shear stress graph for refined xanthan gum in 0.4 % w/v NaCl

#### 4.3.1.4 Pyruvate and acetate content

Xanthan gum is used extensively for enhanced oil recovery as a mobility control agent, in drilling operations to increase the suspension capacity of the drilling mud, and in gels to improve the volumetric sweep efficiency. Flow properties, injectivity, and adsorption characteristics depend on acetate and pyruvate content of xanthan. The degree of pyruvilation and acetylation of xanthan gum was determined using HPLC (Figure 4.36 and 4.37).

There is no significant difference in the acetate and pyruvate content of difference local starches. It shows that refined xanthan gum produced from sweet potato exhibited highest content of acetate with 0.08 g/mL. Meanwhile refined of xanthan gum from sago, rice and tapioca starches were exhibited the lowest of acetate content which is with 0.01 g/mL respectively.

It was similar with pyruvate content from xanthan gum refined from local starches. From the observation, xanthan gum from rice starch exhibited highest of pyruvate with 0.54 g/mL and followed by xanthan gum produced from sweet potato and tapioca starches with 0.49 g/mL and 0.46 g/mL respectively. While xanthan gum from sago starches was exhibited lowest concentration of pyruvate with 0.30 g/mL.

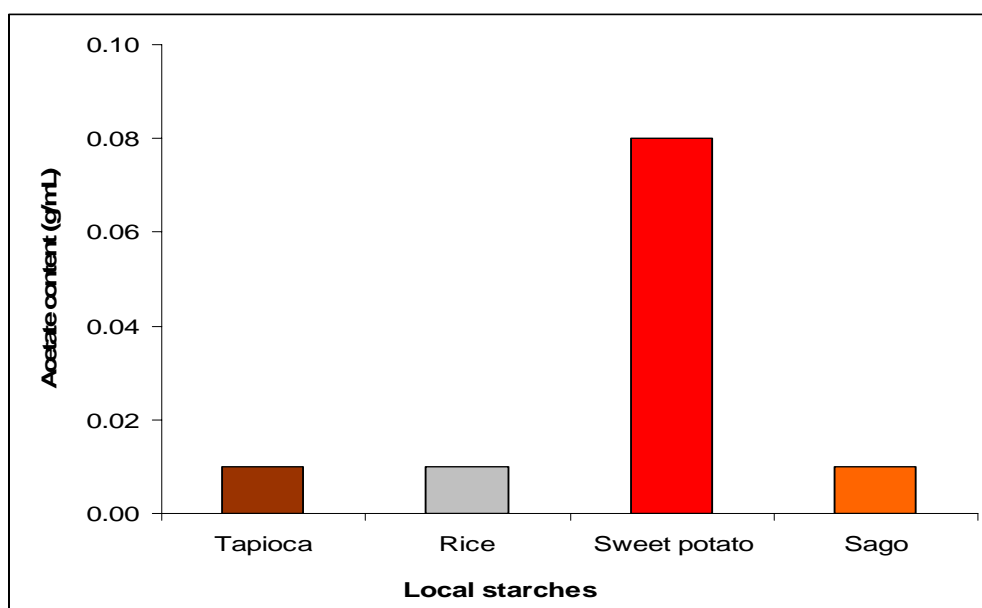


**Figure 4.36** Acetate content of 72 h xanthan samples from shaker fermentor

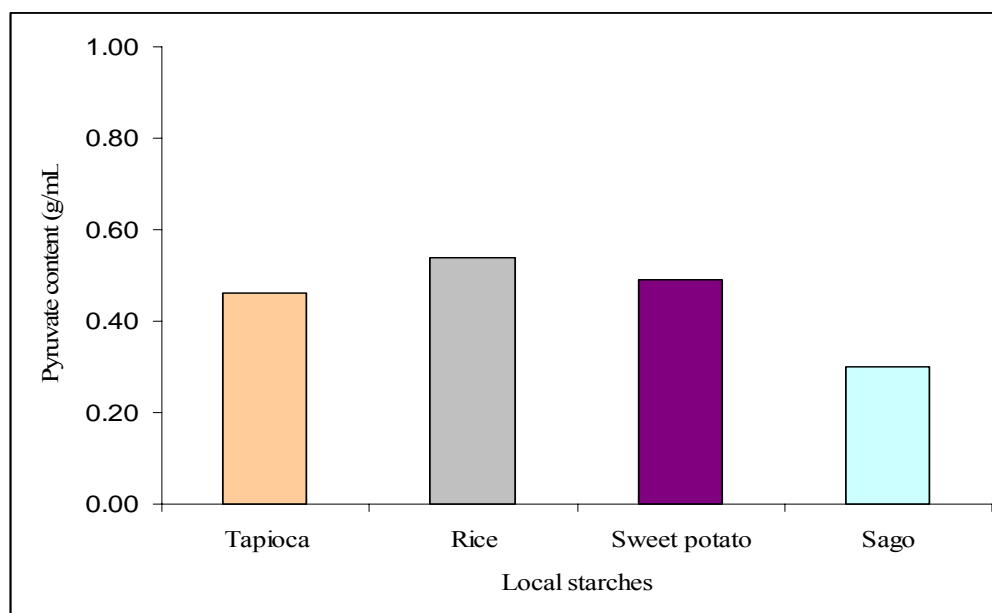


**Figure 4.37** Pyruvate content of 72 h xanthan samples

#### 4.3.1.5 Gelatinization of refined xanthan gum

The gelling of refined xanthan gum was performed using bottle experiment. Refined xanthan gum with concentration 1500 ppm placed in the oven at 60 °C for days. The gelling of refined xanthan gum was observed based on gel strength code (Figure 4.38).

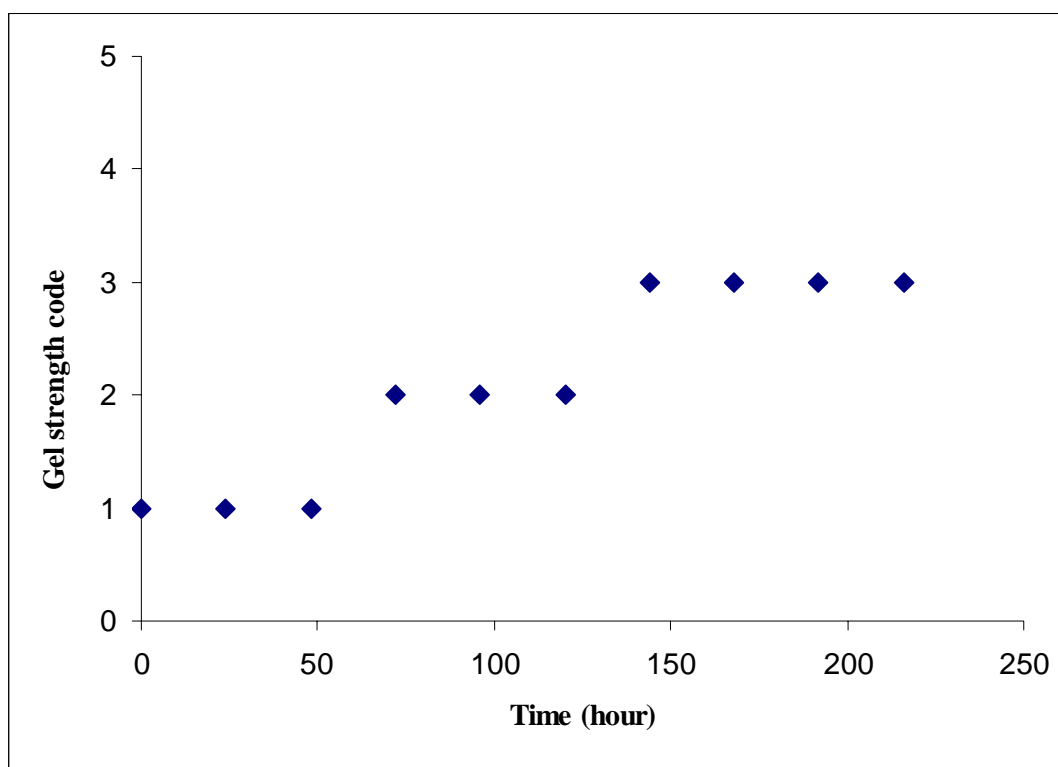


**Figure 4.38** The gelling of refined xanthan gum {1500 ppm, 10 : 1 ratio of XG to Cr (III)}



**Figure 4.39** Gelling of refined xanthan gum after 2 days at 60° C



**Figure 4.40** Gelling of refined xanthan gum after 5 days at 60° C

#### 4.3.1.6 Measurement of amylose and amylopectin using TGA

The amylose and amylopectin contents in starches from tapioca, rice, sweet potato and sago were determined by Thermal Gravimetric Analysis (TGA) under nitrogen at  $20^{\circ}\text{C min}^{-1}$  between  $25 - 950^{\circ}\text{C}$  as shown in Figure 4.41 – 4.44. Many studies have attempted to determine exact of amylose and amylopectin. Methods have been based on structural or functional differences between the two theoretical macromolecules present in starch. L. Yu and G. Christie (2001), investigated the starches transitions using differential scanning calorimetry (DSC). T.S.Gibson et.al. (1997) used Concanavalin A to measure amylose in cereal starches and flours They were found that advantages of this method which is no further purification. In this study, the values of amylose and amylopectin which is based on the thermal degradation of starches ( % weight loss) using TGA.

The TG plot shows the percentage loss in weight as a function of temperature. Three distinct zones can be seen

- a – Represents the evaporation of water and other volatile materials below  $150^{\circ}\text{C}$
- b – The main degradation zone
- c – The propagation reaction

Table 4.20 gives the temperatures of degradation which are represented as  $T_i$ ,  $T_p$ ,  $T_f$ . where  $T_i$ ,  $T_p$ ,  $T_f$  refers to initial, peak and final temperature.

**Table 4.20** Thermogravimetric analysis of starches

Samples	$T_i$ °C	$T_p$ °C	$T_f$ °C
Amylose	250	315	350
Amylopectin	250	325	400

The TGA curves presented a mass loss at 25-174 °C related to the water elimination. Thermal behaviour of starches at 250 – 350 °C can be related to the degradation of amylose, whereas the thermal degradation of amylopectin in starches at 250 – 400 °C. A carbonaceous residue has been described for thermal degradation of starches at 500°C under nitrogen.

Values of the amylose and amylopectin content were obtained from TGA curves presented in Table 4.21. Based on the degradation temperature (% weight loss) of starches, the amylose contents are 32.19, 53.49, 31.59 and 43.15 % for tapioca, rice, sago and sweet potato respectively. Meanwhile the amylopectin contents are 60.67, 64.25, 68.38 and 68.81 % for tapioca, rice, sago and sweet potato respectively

**Table 4.21** Thermal degradation of starches using TGA

Starches	Temperature range/° C	Cellulose	Mass loss/ %
Tapioca	251.92 - 351.92	Amylose	32.19
	251.92 – 391.92	Amylopectin	60.67
Rice	252.98 – 352.98	Amylose	53.49
	252.98 – 392.98	Amylopectin	64.25
Sago	252.72 – 352. 72	Amylose	31.59
	252.72 – 392. 72	Amylopectin	68.38
Sweet potato	256.42 – 356. 42	Amylose	43.59
	256. 42- 396.42	Amylopectin	68.81

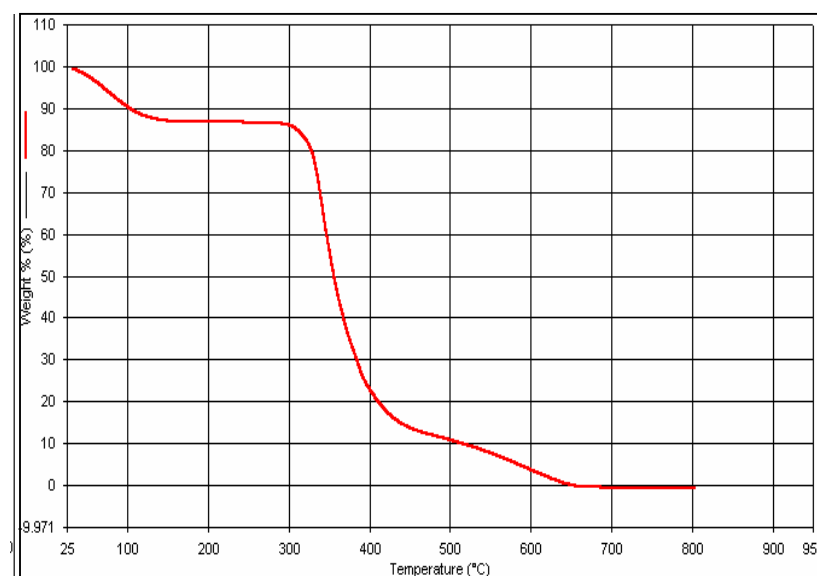


**Figure 4.41** Thermogravimetric curves for tapioca starch measured at heating rate of  $20^{\circ}\text{C min}^{-1}$  under nitrogen

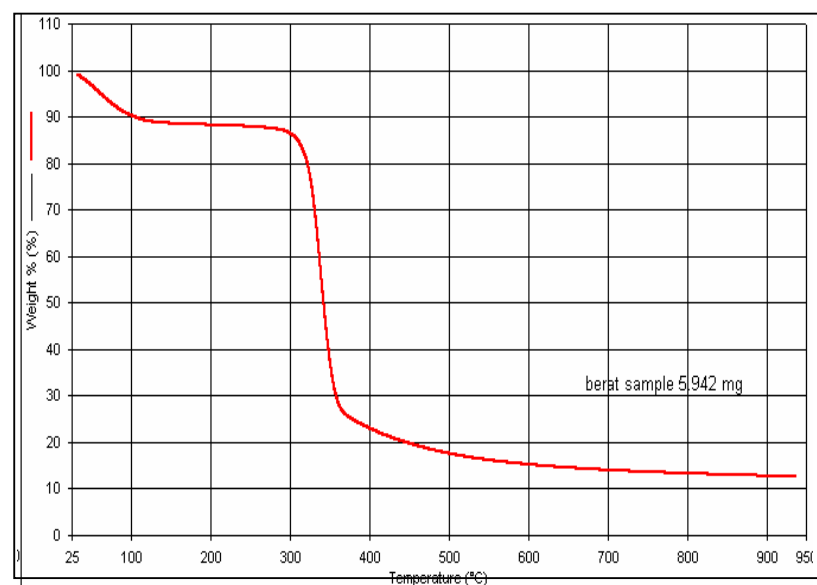


**Figure 4.42** Thermogravimetric curves for rice starch measured at heating rate of  $20^{\circ}\text{C min}^{-1}$  under nitrogen



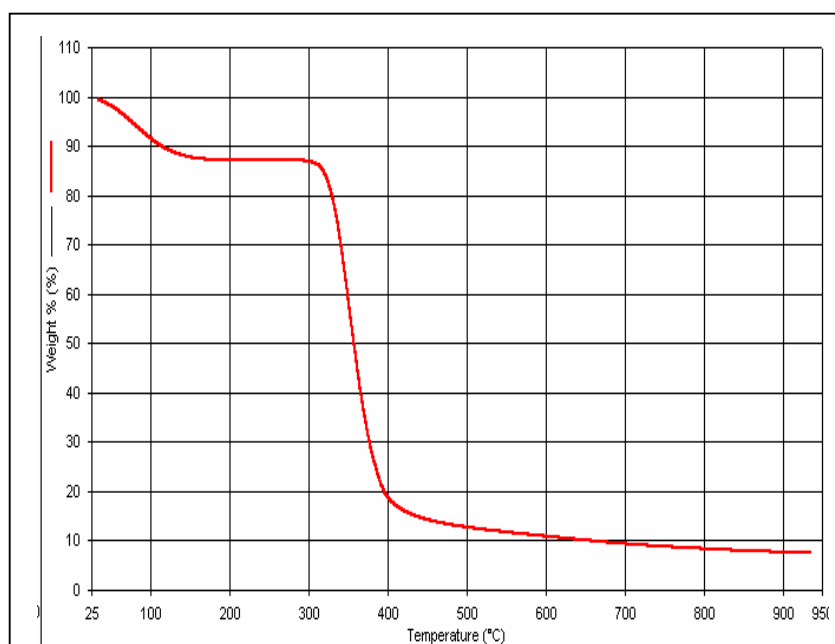


**Figure 4.43** Thermogravimetric curves for Sago starch measured at heating rate of  $20^{\circ}\text{C min}^{-1}$  under nitrogen

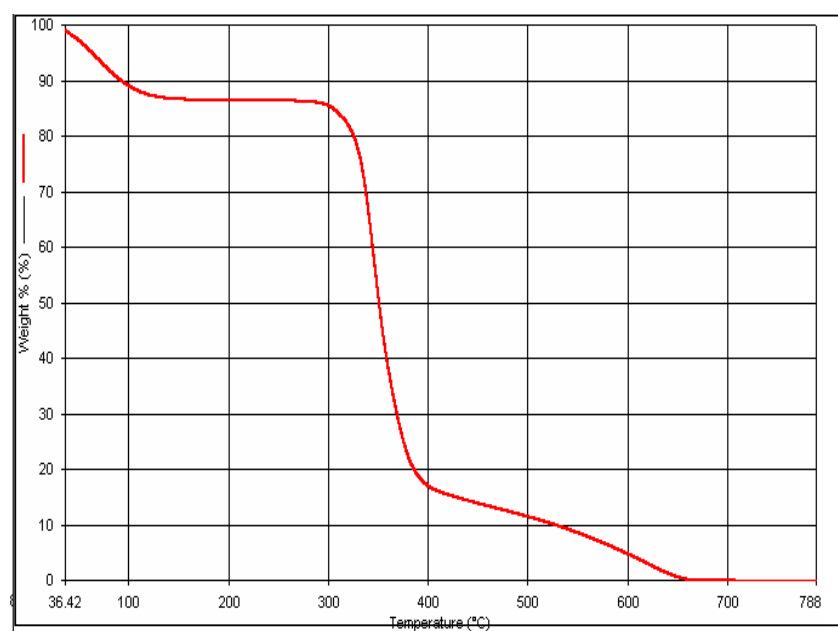


**Figure 4.44** Thermogravimetric curves for Sweet potato starch measured at heating rate of  $20^{\circ}\text{C min}^{-1}$  under nitrogen

### 4.3.2 Surfactant Polymer Flooding

#### 4.3.2.1 Surfactant produced and polymer commercial as additives

Seven displacement experiments were carried out by using seven different types of surfactants. The types of surfactants are given in Table 4.45 previously. Table 4.23 summarizes the information about the experiments in this study. All the experiments were carried out at ambient temperature. The details of the experiment are shown in the Table 3.4 previously.

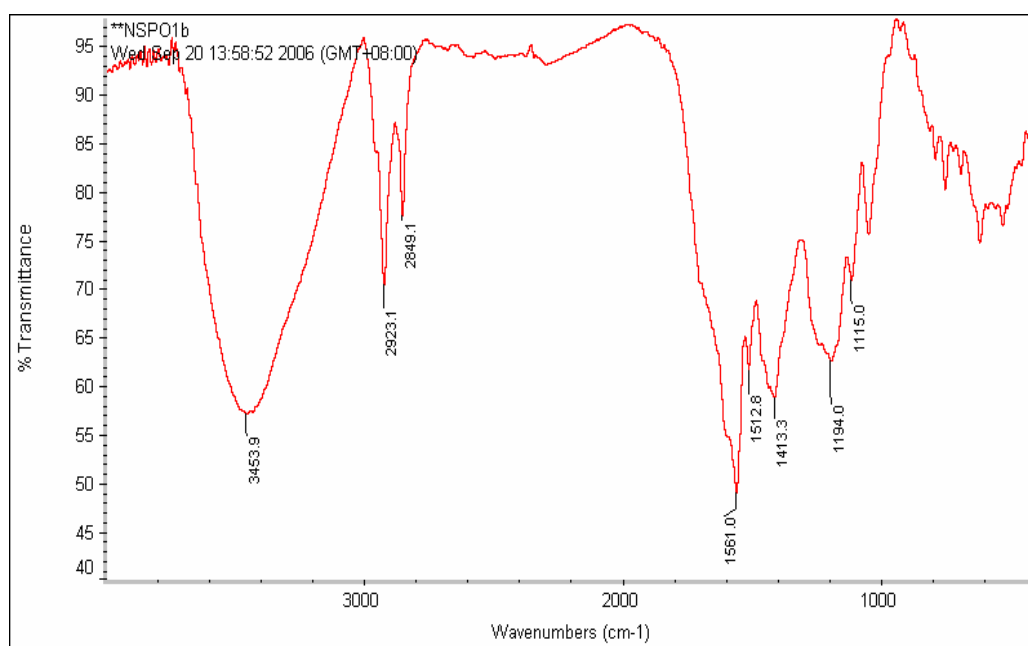


**Figure 4.45** Infra-red spectrum of SURF 1

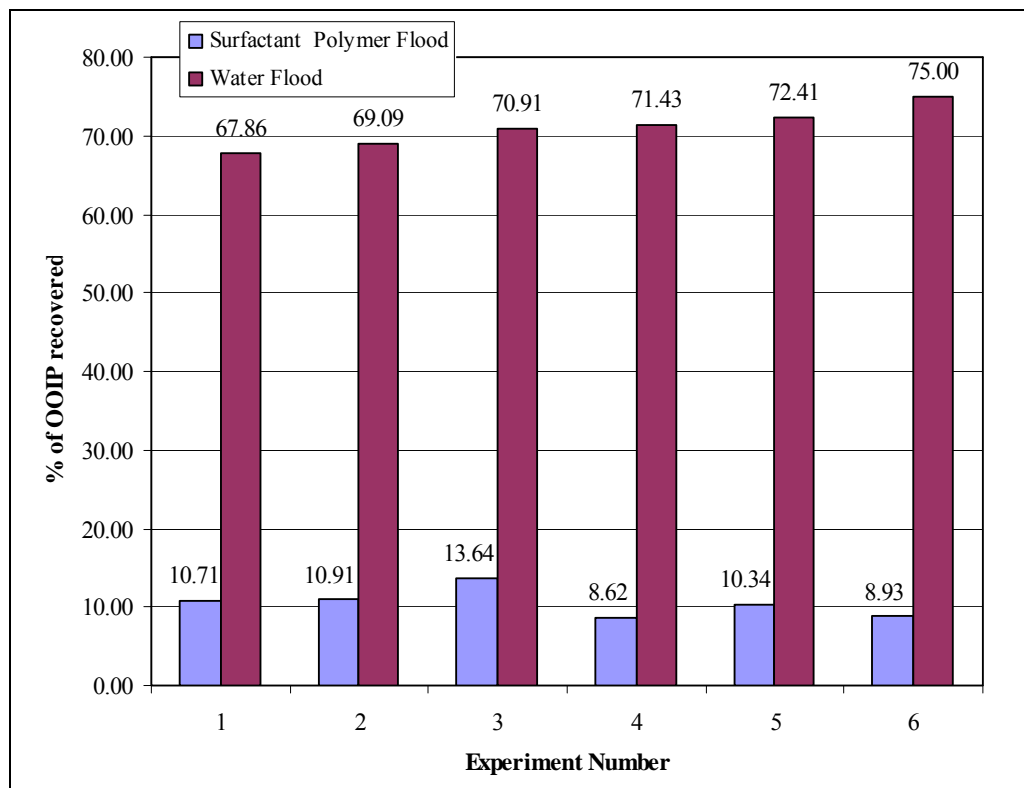


**Figure 4.46** The oil recoveries due to waterflooding and subsequent surfactant polymer flooding

The oil recovery by waterflooding and the additional recovery due to tertiary surfactant polymer flooding are shown in the Figure 4.46. The graph was plotted in terms of the recovery of OOIP (original oil in place). Experiment no 1 and no 2 resulted in 67.86 % and 69.09 % of water flooding recovery, respectively. But 10.71 % and 10.91 % of OOIP were obtained by tertiary surfactant polymer injection, respectively, which were not the highest oil recovery. On the other hand, the highest water flooding recovery was obtained in the experiment no 6, which was 75 %. It yielded additional recovery by surfactant polymer injection of 8.93 % OOIP, which was not the lowest tertiary recovery. Obviously, the performance of the surfactant polymer flooding depends on the surfactant type. There was no relation of the previous water flood history on the surfactant polymer recovery.

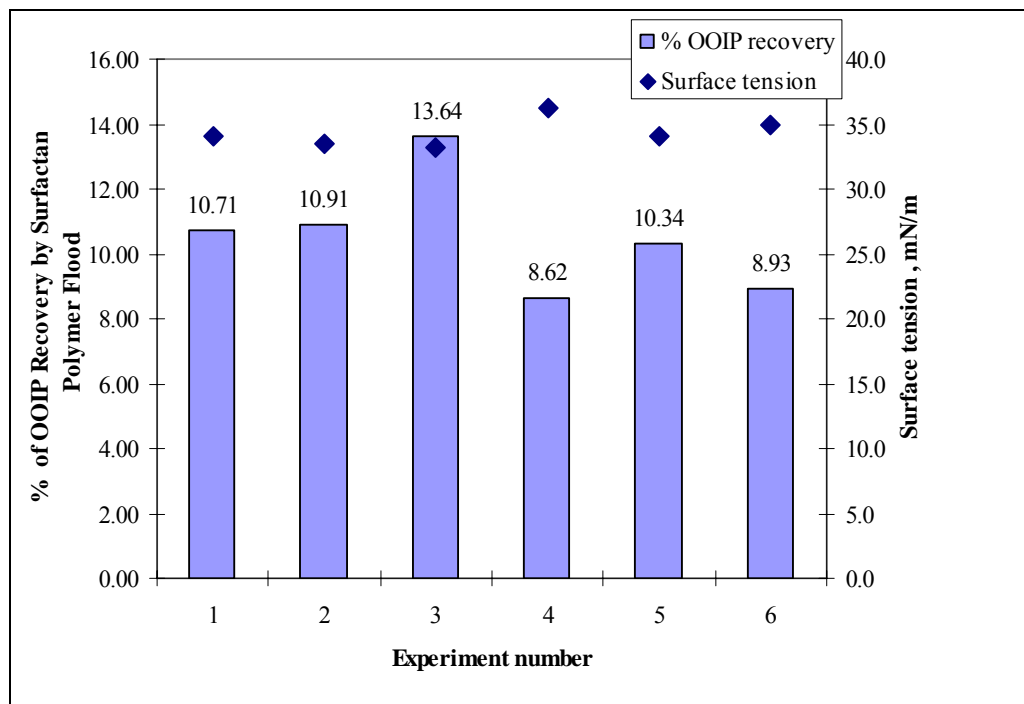


**Figure 4.47** The performance of waterflooding succeeded by surfactant polymer flooding

For evaluation of the additional recovery due to surfactant polymer flooding, the percentage of original oil in place recovered was plotted in Figure 4.47. The recovery of OOIP was plotted because each experiment had different initial water saturation. The highest recovery (13.64 % of OOIP) was obtained from experiment no 3. Surfactant type SURF 3 gave highest oil recovery. The lowest recovery was from surfactant type SURF 4 which yielded 8.62 % of OOIP. The lower surface tension yielded higher recovery for the surfactant used. From Figure 4.47, for surfactant type SURF 3 which had lowest surface tension of 33.2 mN/m resulted highest tertiary recovery (13.64 % of OOIP). SURF 4 which had highest surface tension of 36.2 mN/m gave lowest tertiary recovery (10.71 % of OOIP).

The surfactant performance was shown from the tertiary oil recovery. The descending order of the performance of surfactant would be SURF 3, SURF 2, SURF 1, SURF 5, SURF 6 and SURF 4. It is interesting to note that the surfactant types SURF 3, SURF 2 and SURF1 result in higher oil recovery were produced from sulfonating and alkylating pyrolysis oil by C14 alpha olefin sulfonic acid.

Because of the complexity of the chemical compound in the extracted phenols, the molecular weight of the extracted phenols in this study was not determined. If reactants are not mixed in the right mole ratio, yield is limited by one of the reactants. It is believed that complete reaction occurred in producing SURF 3 (extracted phenol: C14 sulfonic acid, 100: 90 in weight ratio) and SURF 5 (extracted phenol: C16 sulfonic acid, 100: 60 in weight ratio). A complete reaction is one which proceeds completely to the right; it is a reaction which will use up all reactants completely if they are present in stoichiometrically equivalent amounts. There might be some moles of the reactant in excess left over after the reaction has gone to completion in producing SURF 6 (extracted phenol: C16 sulfonic acid, 100: 90 in weight ratio). Thus, it affected the purity and the quality of the surfactant produced.

To determine whether the flooding with surfactant polymer is more effective than without surfactant and polymer, two further experiments were conducted. One was surfactant flooding without using polymer and the other one was polymer flooding without surfactant. The results were compared in Table 4.22.

**Table 4.22:** Displacement recovery performance of different surfactants

Surfactant type and concentration	Tertiary recovery ( % OOIP)	Experiment type
SURF1 - 0.5 %	10.71	Brine + Surf.+ Polymer
SURF2 - 0.5 %	10.91	Brine + Surf.+ Polymer
SURF3 - 0.5 %	13.64	Brine + Surf.+ Polymer
SURF4 - 0.5 %	8.62	Brine + Surf.+ Polymer
SURF5 - 0.5 %	10.34	Brine + Surf.+ Polymer
SURF6 - 0.5 %	8.93	Brine + Surf.+ Polymer
-	8.33	Brine + Polymer
SURF1 - 0.5 %	3.57	Brine + Surfactant

It was found that the polymer flooding obtained 8.33 % of OOIP only. The oil recovery for surfactant flooding without using polymer was found to be 3.57 % OOIP. Field practice has shown that polymer flooding can increase recovery by more than 12% OOIP (Tabary and Bazin , 2007). Obviously, it yielded lower oil recovery if single chemical was used. Surfactant was required to reduce the interfacial tension between the residual oil while mobility control by polymer was also strongly required for better displacement and sweep efficiency. It is technically possible to perform a low tension water flood at 5 wt % of surfactant produced from oil palm shell by using 500 ppm polymer to control the mobility. From the experiments, the surfactant polymer flooding recovered the original oil saturation in the range of 8 – 14 %. In field application, surfactant polymer flooding has been used extensively worldwide and has been successful in recovering an additional 10 to 20 % of OOIP (Yassin, 1988). The results in this study are matched with the theoretical results.

#### 4.3.2.2 Surfactant and polymer produced from local starches as additives

Displacement experiments were carried out by using four different polymer and surfactant. All the experiments were carried out at ambient temperature. Table 4.23 illustrated that the summary of sandpack flood tests.

**Table 4.23** Summary of sandpack flood tests

Test number	Waterflood recovery (% IOIP)	Final recovery (% OOIP)	Experiment type
P1 (sago)-500 ppm	52.69	15.43	Brine + Polymer
P2 (tapioca)-500 ppm	50.00	16.56	Brine + Polymer
P3 (sweet potato)-500 ppm	54.96	18.67	Brine + Polymer
P4 (rice)-500 ppm	51.34	15.76	Brine + Polymer
SURF7- 0.5 %	64.29	10.76	Brine + Surfactant
SURF7 – 0.5 % P3 – 500 ppm	70.50	20.21	Brine + Surf.+ Polymer

The oil recovery by water flooding and the additional recovery due to tertiary surfactant polymer flooding are shown in the Fig.4.48 and 4.49. The graph was plotted in terms of the recovery of OOIP (original oil in place). Experiment P1, P2, P3 and P4 was resulted in 52.69 %, 50.00 %, 54.96 % and 51.34 % of water flooding respectively. Conversely 15.43 %, 16.56 %, 18.67 % and 15.76 % were obtained by tertiary polymer injection respectively, which were not the highest oil recovery. It was also found that the oil recoveries of polymer produced for polymer flooding more highest compared than polymer commercial which is only 8.33 % of OOIP. It yielded lower oil recovery if single chemical was used.

Surfactant was required to reduce the interfacial tension between the residual oil while mobility control by polymer was also strongly required for better displacement and sweep efficiency. Furthermore the oil recovery for surfactant flooding without using polymer was 3.76 % OOIP and 64.29 % of water flooding. In order that the highest water flooding recovery was obtained in the experiment SURF7P3 which is 70.50 %. It yielded oil recovery by surfactant-polymer injection of 20.21 % of OOIP. Obviously the performance of the polymer surfactant flooding depends on the polymer type. There was no relation of the previous water flood history on the surfactant-polymer recovery.

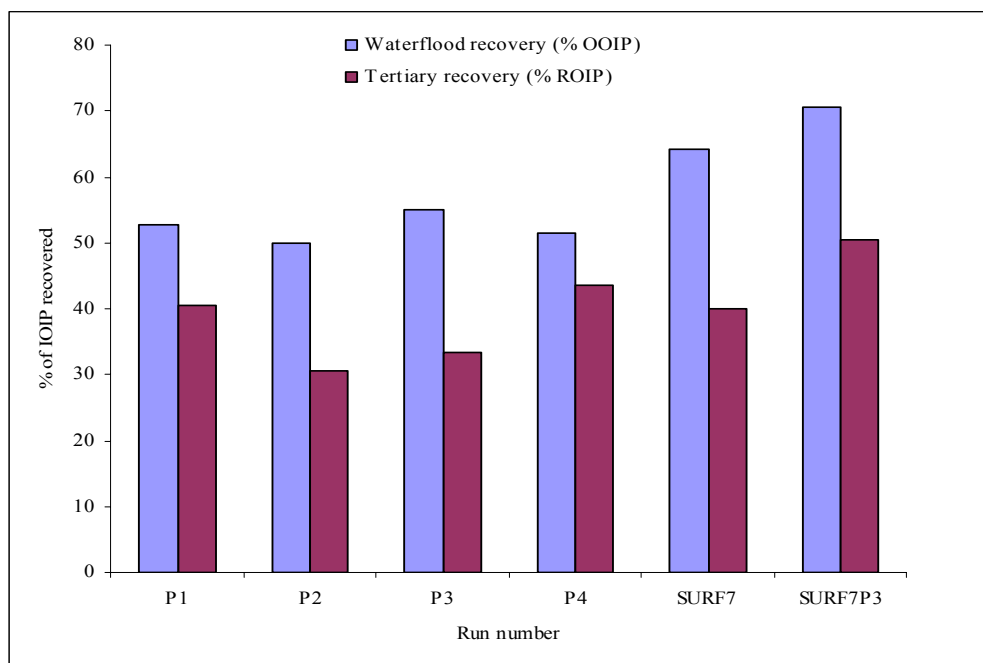


**Figure 4.48** The performance of waterflooding succeeded by surfactant polymer flooding

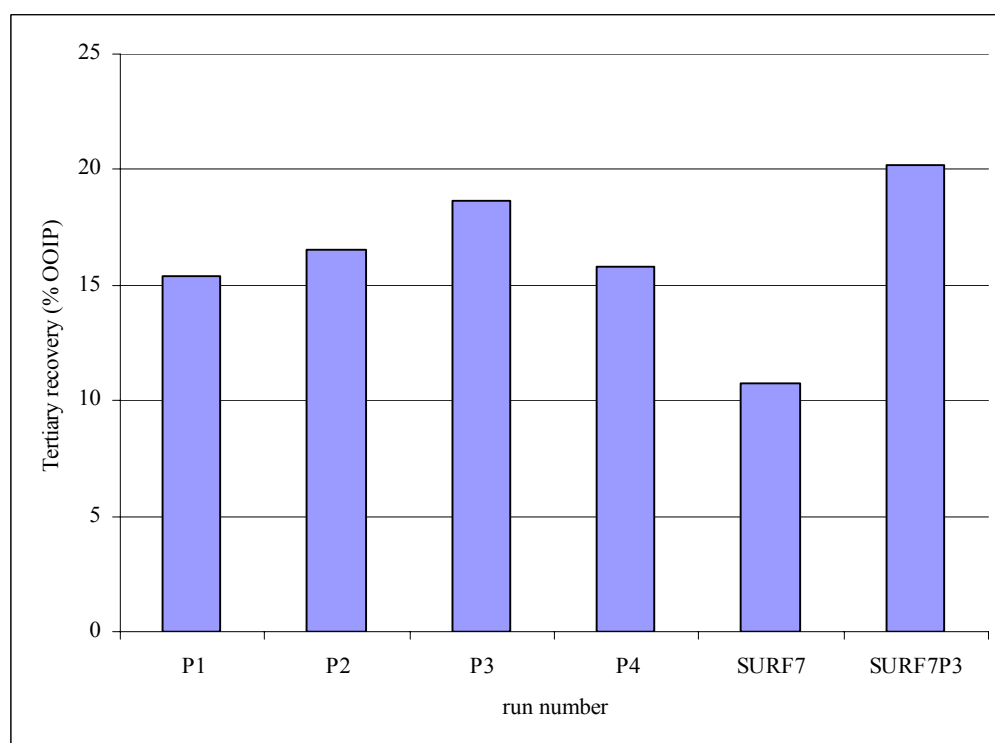


**Figure 4.49** The oil recoveries due to waterflooding and subsequent surfactant polymer flooding



### 4.3.2.3 Surfactant and polymer produced from local fruits as additives

Displacement experiments were carried out by using ten different polymer and surfactant. All the experiments were carried out at ambient temperature. Table 4.24 illustrated that the summary of sandpack flood tests.

**Table 4.24** Summary of sandpack flood tests

<b>Test number</b>	<b>Waterflood recovery (% IOIP)</b>	<b>Final recovery (% OOIP)</b>	<b>Experiment type</b>
PO1(watermelon)-500 ppm	57.69	19.23	Brine + Polymer
PO2 (pineapple)-500 ppm	50.00	17.24	Brine + Polymer
PO3 (dragon fruit)- 500 ppm	62.96	14.81	Brine + Polymer
PO4 (coconutsap)- 500 ppm	60.00	20.00	Brine + Polymer
PO5 (honeydew)- 500 ppm	69.30	15.38	Brine + Polymer
PO6 (papaya)- 500 ppm	62.50	16.67	Brine + Polymer
PO7 (starfruit)- 500 ppm	60.00	16.00	Brine + Polymer
PO8 (guava)- 500 ppm	53.85	15.38	Brine + Polymer
PO9 (mango)- 500 ppm	59.26	14.51	Brine + Polymer
PO10 (sugarcane)- 500 ppm	53.70	18.52	Brine + Polymer
SURF7 – 0.5 %	64.29	3.76	Brine + Surfactant
SURF7- 0.5 % PO4- 500 ppm	72.50	21.10	Brine + Surf.+ Polymer

The oil recovery by water flooding and the additional recovery due to tertiary surfactant polymer flooding are shown in the Fig.4.50 and 4.51. The graph was plotted in terms of the recovery of OOIP (original oil in place). Experiment P5 was resulted higher compared than others which is 69.32 % of water flooding respectively. Conversely 50 % were obtained by tertiary polymer injection respectively, which were not the highest oil recovery. It was also found that the oil recoveries of polymer produced for polymer flooding more highest compared than polymer commercial which is only 8.33 % of OOIP. It yielded lower oil recovery if single chemical was used. Surfactant was required to reduce the interfacial tension

between the residual oil while mobility control by polymer was also strongly required for better displacement and sweep efficiency. Furthermore the oil recovery for surfactant flooding without using polymer was 14.29 % OOIP. In order that the highest water flooding recovery was obtained in the experiment SURF7PO4 which is 72.50 %. It yielded oil recovery by surfactant-polymer injection of 21.10 % of OOIP. Obviously the performance of the polymer surfactant flooding depends on the polymer type. There was no relation of the previous water flood history on the surfactant-polymer recovery.

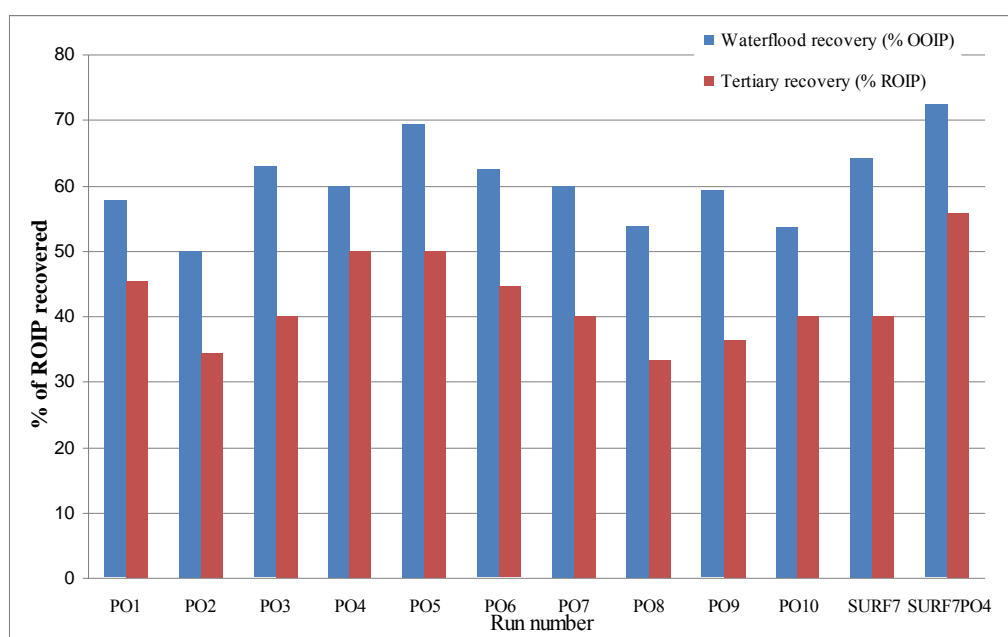


**Figure 4.50** The performance of waterflooding succeeded by surfactant polymer flooding

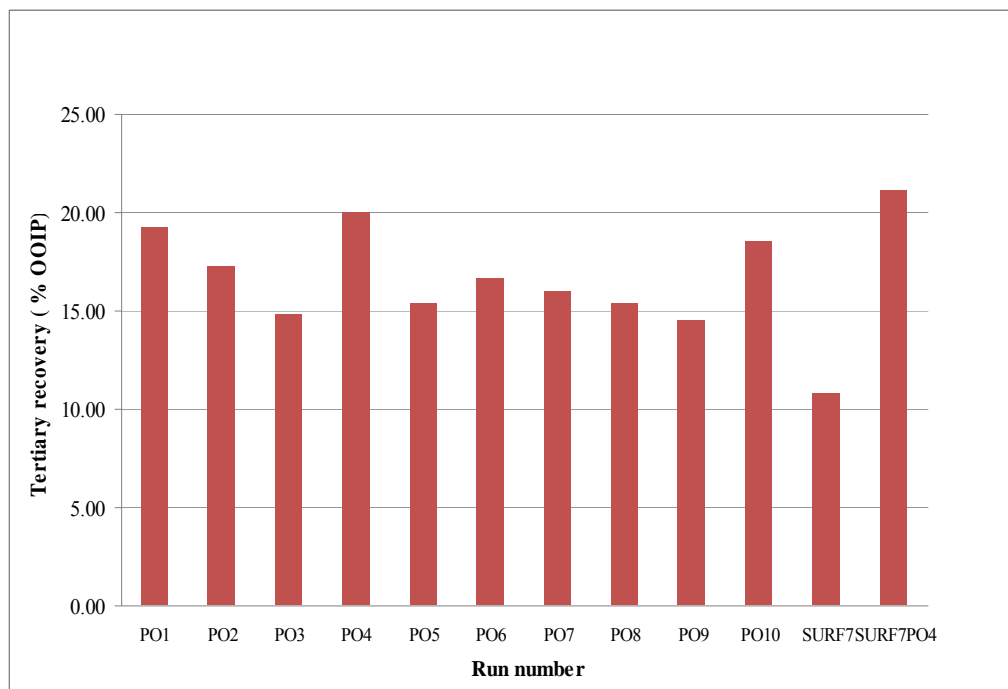


**Figure 4.51** The oil recoveries due to waterflooding and subsequent surfactant polymer flooding

Figure 4.52 and Figure 4.53 show the photos of the sand pack before and after water flooding followed by surfactant polymer flooding. The oil dyed red was injected into the sand pack as shown in Figure 4.13. As shown in the Figure 4.14, the surfactant polymer flooding gave good displacement performance in this study. The oil dyed red in the sand pack was displaced by the injected surfactant and polymer. The surfactant produced pyrolysis oil yielded the good performance in oil displacement test, and therefore it is a good candidate for enhanced oil recovery.

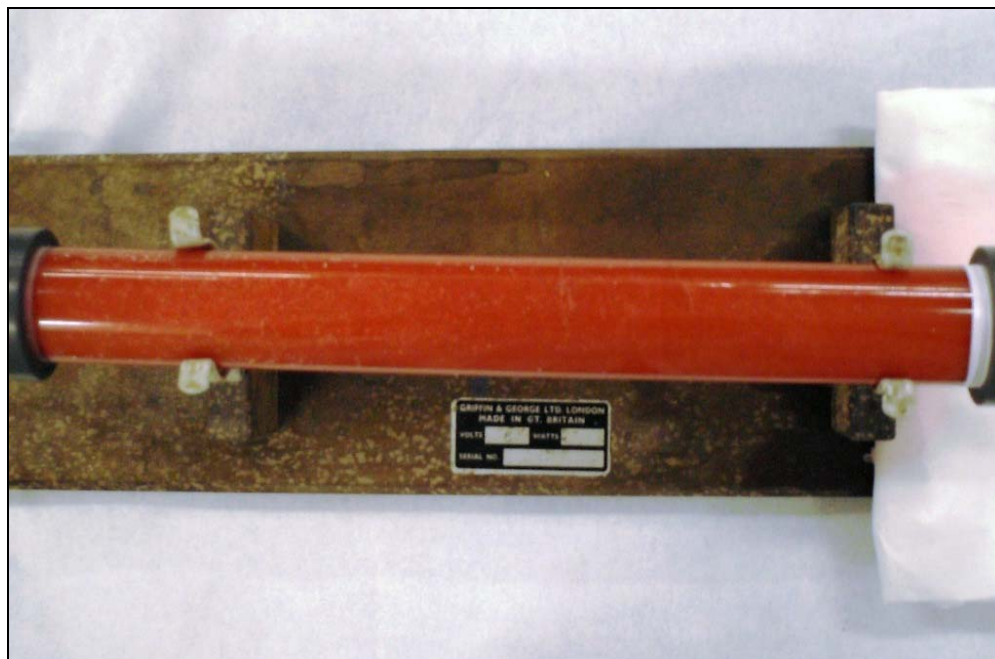


**Figure 4.52** The sand pack saturated with oil dyed red (before flooding)



**Figure 4.53** The sand pack after waterflooding succeeded by surfactant polymer injection

## **CHAPTER 5**

### **CONCLUSIONS AND RECOMMENDATIONS**

#### **5.1 Conclusions**

The main objective of this study was to produce additives surfactant and polymer from local sources for enhanced oil recovery. The following conclusions are drawn from this study:

1. The pyrolysis oil from oil palm shell contained high percentage of phenol and its derivatives more than 50 %.
2. The extraction technique using alkaline solution was able to extract the phenol fraction and yielded an average of 25.20 wt %.
3. Surfactant type SURF3 which was produced by sulfonation of extracted phenols of pyrolysis oil with C14 alpha olefin sulfonic acid (weight ratio of 100:30) had the lowest surface tension of 33.2 mN/m, anionic active matter, 39.09 % active and CMC of 0.22 wt %.
4. Surfactant type SURF4 which was produced by sulfonation of extracted phenols of pyrolysis oil with C16 alpha olefin sulfonic acid (weight ratio of 100:30) had highest surface tension of 36.2 mN/m, lowest anionic active matter, 20.55 % active and CMC of 0.28 wt %.

5. Surfactant type SURF7 which was produced by direct sulfonation of pyrolysis oil with C14 alpha olefin sulfonic acid (weight ratio of 100:60) had surface tension of 33.0 mN/m, anionic active matter 29.90 % active and CMC of 0.22 wt %.
6. Polymer type PO5 which was produced from honeydew juice had highest dried weight of 8.3550 g/L while polymer type PO7 which was produced from starfruit juice had the lowest of dried weight of 3.5120 g/L.
7. Polymer type P1 which was produced from sago starch had highest dried weight of 9.9690 g/L while polymer type P4 had the lowest of dried weight of 5.5190 g/L.
8. FTIR and NMR characterization were given similarity characteristic of xanthan gum produced which was compared than commercial of xanthan gum.
9. The result of the viscosities measurement indicates that xanthan gum which was produced from local starches and fruits likely more viscous than commercial of xanthan gum.
10. Additives type SURF7PO4 yielded the highest recovery of 21.10 % of OOIP due to the lowering of the surface tension of the residual oil in the pore space followed by additives type SURF7P3 yielded the recovery of 20.21 % OOIP due to the surface tension reductions was not sufficient enough overcome the oil layer surrounding the sand particles.
11. Surfactant produced from pyrolysis oil resulted in additional oil recovery from 8 to 14 % of OOIP. Additional oil recovery in the displacement test using surfactant produced from pyrolysis oil of oil palm shell showed that it is a good candidate for EOR.

## 5.2 Recommendations

Several recommendations are made for future works:

1. More testing on the properties of additives should be done, such as adsorption and interfacial tension. Experiments should be designed and performed in the laboratory to determine the amount of additives adsorbed in reservoir rock and the interfacial tension between the oil and surfactant.
2. Phase behavior of the additives and the optimal salinity should be investigated.
3. Slug size and concentration of additives should be considered as important factors in the surfactant polymer flooding process. Experiments should be designed and performed to study the effect of different injection strategies on the oil recovery performance.

## REFERENCES

- Aisha A.A.Soliman et.al. (1997). “ Thermal Behaviour of Starch and Oxidized Starch” *Thermochimica Acta*, 296, 149 – 153.
- Ani, F.N. and Zailani, R. (1996). Characteristics of Pyrolysis Oil and Char from Oil Palm Shells. In: Bridgewater, A.V. and Boocook, D.G.B. (Ed). *Developments in Thermo-chemical Biomass Conversion Volume 1*. London: Blackie Academic and Professional. 425-432.
- Aubin, H. and Roy, C (1980). Study on the Corrosiveness of Wood Pyrolysis Oils. *Fuel Science and Technology International*. Vol 8: 77 – 86.
- Austad, T and Milter, J. (2000). Surfactant Flooding in Enhanced Oil Recovery. *Surfactants: Fundamentals and Applications in the Petroleum Industry*. UK: Cambridge University Press. 203 – 250
- Babadagli, T., Al-Bemani, A., Boukadi, F. and Al-Maamari, R (2002). A Laboratory Feasibility Study of Dilute Surfactant Injection for the Yibal Field, Oman. SPE 78352. *Proceedings of the SPE EUROPEC*. Oct. 29-31. Aberdeen, UK.
- Balzer, D. (1991). Alkylpolyglycosides, their Physio-chemical Properties and their Uses. *Tenside Surf. Det.* ,38. 419 – 427
- Berger, P.D. and Lee, C.H. (2002). New Anionic Surfactants Based on Olefin Sulfonic Acids. *Journal of Surfactants and Detergents*. Vol.5.No.1, January.



- Berger, P.D. and Lee, C.H. (2002). Ultra-low Concentration Surfactants for Sandstone and Limestone Floods. *SPE 75186 presented at the SPE/DOE Improved Oil Recovery Symposium*. 13-17 April. Tulsa, Oklahoma.
- Berger, P.D., Berger, C.H. and Herron, S.J. (2000). Chemistry of Olefin Acids. 1. Alkylation of Aromatic Sulfonic Acids. *Proceedings of the 5<sup>th</sup> World Surfactants Congress*. May 29 – 2 Jun. Florence, Italy.
- Berger, P.D., Berger, C.H. and Hsu, I.K. (2000), *Anionic Surfactants Based on Alkene Sulfonic Acid*. (United States Patent 6,043,391)
- Bridgwater, A.V and Bridge, S.A. (1991). A Review of Biomass Pyrolysis and Pyrolysis Technologies. *Biomass Pyrolysis Liquids, Upgrading and Utilization*. London: Elsevier Applied Science.
- Bridgwater, A.V. and Peacocke, G.V.C., (1999). Fast Pyrolysis Processes for Biomass. *Sustainable and Renewable Energy Reviews*. Vol 4. 1 – 73.
- Bridgwater, A.V., Meier, D. and Radlein, D. (1999). *An Overview of Fast Pyrolysis of Biomass*. Organic Geochemistry 30. London: Elsevier Applied Science. 1479 – 1493
- C.T. Andrade. *et.al* (1999). “Solution Properties Of The Galactomannans Extracted From The Seeds Of Caesalpinia Pulcherrima And Cassia Javanica : Comparison With Locust Bean Gum”. International J.l of Bio.l Macromolecules 26, 181–185
- C.Y. Lii, *et.al*. (2002). “Xanthan gum-gelation complexes” European Polymer Journal. 38. 1377- 1381.
- Carlos Amen- Chen, Pakdel, H. and Roy, C. (1997). Separation of Phenols from Eucalyptus Wood Tar. *Biomass and Bioenergy*. Vol 13, Number 1: 25-37.

Chum, H.L. and Black, S.K. (1990). *Process for Fractionating Fast-Pyrolysis Oils, and Products Derived Therefrom*. (United States Patent 4,942,269)

Diebold, J.P. and Bridgwater, A.V. (1997). Overview of Fast Pyrolysis of the Production of Liquid Fuels. In: Bridgwater, A.V. and Boocock, D.G.B.(Ed.). *Developments in Thermo- chemical Biomass Conversion Volume 1*. London: Blackie Academic and Professional. 5 – 23.

F.kamal et.al (2003). “Mutagenesis of *Xanthomonas campestris* and selection of Strains with Enhanced Xanthan Production”. Iran. Biomed. Journal. 7 (3) 91-98.

Feighner, G.C. (1976). *Anionic Surfactants, Vol.1*. In: Linfield, W.M., Ed. New York: Marcel Dekker. 253 – 314.

Gallivan, R.M. and Matschei, P.K. (1980). *Fractionation of Oil Obtained by Pyrolysis of Lignocellulosic Materials to Recover a Phenolic Fraction for Use in Making Phenol Formaldehyde Resin*. (US Patent 4,209,647).

Gilliland, H.E. and Conley, F.R. (1976). Pilot Flood Mobilizes Residual Oil. *Oil and Gas Journal (Jan)* 19. 43 – 48.

Gogarty, W.B and Tosch, W.C. (1968). Miscible-type Waterflooding: Oil Recovery with Micellar Solutions. *JPT (Dec)*. 1407 –1412.

Gogarty, W.B. (1976). Status of surfactant or micellar methods. *Journal of Petroleum Technology*. Volume 28: 93–102

Goh Meng Seng (2002). Projek Sarjana Muda Kejuruteraan Petroleum UTM.

Greminger, D. C., Burns, G. P., Lynn, S., Hanson, D. N. and King, C. J.,(1982). Solvent Extraction of Phenols from Water. *Industrial & Engineering Chemistry Process Design and Development*, 21. 51 -54.

Healy, R.N. and Reed, R.L. (1977). Immiscible Microemulsion Flooding. *SPEJ (April)*. 129 –139.

Hernandez, Clara; Chacon, L.J., Anselmi, L., Baldonado, A., Qi, J., Pitts, M.J. (2001). ASP System Design for an Offshore Application in the La Salina Field, Lake Maracaibo. *SPE 69544 presented at the SPE Latin American and Caribbean Petroleum Engineering Conference*. 25 –28 March. Buenos Aires, Argentina.

Hirasaki, G.J. (1981). Application of the Theory of Multicomponent, Multiphase Displacement to Three - Component, Two – Phase Surfactant Flooding. *SPEJ (April)*. 191 – 204.

Holm, L.W. (1982). Design, Performance , and Evaluation of the Uniflood Micellar-Polymer Process – Bell Creek Field. Paper SPE 11196. *Proceedings of the 57<sup>th</sup> Annual Fall Technical Conference of SPE*. .New Orleans, LA.

Iglauer, S., Wu., Y., Shuler, P.J., Blanco, M., Tang, Y., and Goddard III, W.A. (2004). Alkyl Polyglycoside Surfactants for Improved Oil Recovery. *SPE 89472 presented at 2004 SPE/DOE Fourteenth Symposium on Improved Oil Recovery*. 17 – 21 April. Tulsa, Oklahoma, U.S.A.

Islam, M.N., Zailani, R., and Ani, F.N. (1999). Pyrolytic Oil from Fluidized bed Pyrolysis of Oil Palm Shell and Its Characterization. *Renewable Energy*. Vol.17. 73 – 84.

J.A. Casas, V.E. Santos and F. Garcia-Ochoa (2000). “Xanthan gum production under several operational conditions: molecular structure and rheological properties”. *Enzyme and Microbial Tech*. 26. 282 – 291.

- J.W. Lubach *et.al.* (2004). "Solid State NMR Studies of Pharmaceutical Solids In Polymer Matrices". *Anal. Bioanal.Chem*, 378, 1504 – 1510.
- Jakobsen, S.R. and Hovland, F. (1994). Surfactant Flooding: Technical and Economical Conditions to Succeed. *SPE 27824 presented at the SPE/DOE Ninth Symposium on Improved Oil Recovery*. 17-20 April. Tulsa, Oklahoma, U.S.A.
- Jamil, M.K., Ani, F.N. (2000). Oil Palm Shell as a Source of Phenol. *Journal of Oil Palm Research*. Vol.12 No.1. 86-84.
- Kai Spila , Eeva Kuoppala, Leena Fagernae and Anja Oasmaa (1998), Characterization of Biomass-Based Flash Pyrolysis Oil. *Biomass and Bioenergy*. Vol. 14, No. 2. 103 – 113.
- Kalpakci, B., Arf, T.G., Barker. J.W., Krupa, A.S., Morgan. J.C. and Neira, R.D. (1990). The Low Tension Polymer Flood Approach to Cost Effective Chemical EOR. SPE/DOE paper 20220. *7<sup>th</sup> Symposium on Enhanced Oil Recovery*. 22 – 25 April.Tulsa, Oklahoma.
- Kishore Nadkarni, R.A. (2000). *Guide to ASTM Test Methods for the Analysis of Petroleum Products and Lubricants*. ASTM International, West Conshohocken, PA.
- L.S.Guinesi, et.al. (2006). "Kinetics of Thermal Degradation Applied to Starches from Different Botanical Origins by Non-isothermal Procedures". *Thermochimica Acta*.
- L.Su, W.K. Ji, W.Z. Lan and X.Q. Dong. (2003) "Chemical modification of xanthan gum to increase dissolution rate" *Carbohydrate Polymers*, 53, 497-499.
- L.Yu and G.Christie. (2001). "Measurement of Starch Thermal Transitions Using Differential Scanning Calorimetry". *Carbohydrate Polymers*. 46. 179-184

- Lake, L.W. (1989). Enhanced Oil Recovery. New Jersey: Prentice Hall, Inc.
- Lake, L.W. and Pope, G.W. (1979). Status of Micellar – Polymer Field Tests. *Petroleum Engineer International*. 38 – 60.
- Larry, N.B. (2000). Toxicity and Persistence of Surfactants Used in the Petroleum Industry. *Surfactants: Fundamentals and Applications in the Petroleum Industry*. Cambridge University Press. 541 – 565.
- Laura, L.W., Jeffrey, H.H. (2000). Surfactant Adsorption in Porous Medium, *Surfactants: Fundamentals and Applications in the Petroleum Industry*. UK: Cambridge University Press. 121 – 158.
- M.J. Lopez and A.R.-Cormenzana. (1996). “Xanthan Production from Olive-Mill Wastewaters”. Elsevier, 263-270.
- M.Papagianni et.al. (2001).”Xanthan production by Xanthomonas Campestris in Batch Cultures”. *Process Biochemistry*. 37, 73-80.
- M.Papagianni et.al. (2001).”Xanthan production by Xanthomonas Campestris in Batch Cultures”. *Process Biochemistry*. 37, 73-80.
- Maerker, J.M. and Gale, W.W. (1992). Surfactant Flood Process Design for Loudon, *SPE Reservoir Eng. (Feb)*. 36 – 44.
- Michels, A.M., Djojosoeparto, R.S., Haas, H., Mattern, R.B, Can der Weg., P.B and Schulte, W.M. (1996). Enhanced Water Flooding Design Using Dilute Surfactant Concentrations for North Sea Condition. *SPE /DOE 35372 presented at the 10<sup>th</sup> SPE/DOE symposium in Improved Oil Recovery*. 21 -24 April. Tulsa, Oklahoma.

Nelson, R.C. and Pope, G.A. (1978). Phase Relationships in Chemical Flooding. *SPEJ* 18, No.5. 325 – 338.

O.S. Azeez. (2005). “Production of Gum from Cashew Tree Latex”. Leonardo Electronic J. of Practices and Tech, 7, 17-22.

Oasmaa, A and Peacocke, C. (2001). *A Guide to Physical property Characterisation of Biomass Derived Fast Pyrolysis Liquids*. Espoo,Finland: VTT Publication 450.

P. Adhikary and R.P. Singh. (2004). “Synthesis, Characterization and Flocculation Characteristics of Hydrolyzed and Unhydrolyzed Polyacrylamide Grafted Xanthan Gum”. *J. of Applied Polymer Sci.* 94, 1411-1419.

P. Aggarwal and D. Dollimore. (1997). “The Combustion of Starch, Cellulose And Cationically Modified Products Of These Compounds Investigated Using Thermal Analysis” *Thermochimica Acta*. 291. 65 -72.

Pope, G.A. and Nelson, R.C. (1978). A Chemical Flooding Compositional Simulator. *SPEJ Oct, vol 18*. 339 – 354.

Rasheed, K., Carvey, R., Berger, P.D. and O’Brien, E. (1991). *Alkoxylated Alkyl Substituted Phenol Sulfonates Compounds and Compositions, the Preparation thereof and Their Use in Various Applications*. (United States Patent 5,049,311)

Reppert, T.R., Bragg, J.R., Wilkinson, J.R., Snow, T.M., Maer Jr, N.K. and Gale, W.W. (1990). Second Ripley Surfactant Flood Pilot Test. *SPE/DOE 20219 presented at SPE/DOE Symposium on Enhanced Oil Recovery*. Tulsa, Oklahoma.

Rubinson, K.A. (1987). *Chemical Analysis*. Toronto: Little, Brown and Company.

- S.D.Yoo and S.W. Harcum (1999). "Xanthan Gum Production From Waste Sugar Beet Pulp" *Bioresource Tech.* 70, 105-109.
- S.Rosalam & R. England. (2005). "Review Of Xanthan Gum Production from Unmodified Starches By *Xanthomonas Campestris* Sp". *Enzyme & Microbial Tech.* In press.
- Sipila, K, Kuoppala, E, Fagernas, L, Oasmaa, A. (1998). Characterization of Biomass-based Flash Pyrolysis Oils. *Biomass and Bioenergy*. Volume 14, Number 2: 103-113.
- Soltes, E.J (1988). *Pyrolysis Oils from Biomass, Producing, Analyzing and Upgrading*. American Chemical Society Symposium Series 376. 1- 7.
- Soltes, E.J and Elder, T.J (1983). *Pyrolysis in Organic Chemicals from Biomass*. (Goldstein, I.S.ed.). Boca Raton, FL: CRC Press.
- State of the Environment in Malaysia*. Consumers' Association of Penang.
- Stosur, G.J. (2003). EOR: Past, Present and What the Next 25 Years May Bring. SPE paper 84864. *SPE International Improved Oil Recovery Conference*. 20 – 21 Oct. K.L, Malaysia.
- Suryo Purwono and Bardi Murachman (2002). Development of Surfactants and Co-surfactants for EOR from Pyrolysis of Oil Palm Husks Lignin. *Proceedings of the 6th Asia Pacific international Symposium on Combustion and energy Utilization*. 20-22 May. Kuala Lumpur.
- T.S.Gibson et. al. (1997). "A Procedure to Measure Amylose in Cereal Starches and Flours with Concanavalin A". *J. of Cereal Sci.* 25. 111-119.
- Tabary, R., Bazin, B. (2007). Advances in Chemical Flooding. *IFP - OAPEC Joint Seminar "Improved Oil Recovery (IOR) Techniques and Their Role in Boosting The Recovery Factor*. 26-28 June 2007. Rueil-Malmaison, France.

- Taber, J.J., Martin, F.D. and Seright, R.S. (1997). EOR Screening Criteria Revisited—Part 2: Applications and Impact of Oil Prices. *SPE* Aug. 199-205
- Thomas, L.K., Dixon, T.N., Evans, C.E. and Vienot, M.E. (1987). Ekofisk Waterflood Simulation. *JPT Feb.* 221-232.
- Tiong Swee Tin (2003). Projek Sarjana Muda Kejuruteraan Petroleum UTM
- Toft, A.J. and Bridgwater, A.V. (1996). Biomass Gasification and Pyrolysis. *Conference Papers for Applications of Bioenergy Technologies*. NZ Forest Research Institute, Rotorua, New Zealand. 78-90:
- Toth, L.(1980). Separation and Analysis of Phenol Fractions from Smokehouse. *Fleischwirtsch.*, 60. 728-736.
- Vargo, J.J. (1978). Site Selection, Reservoir Definition and Estimation of Tertiary target Oil for the Bell Creek Unit “A” Micellar Polymer Project. SPE 7072. *Proceedings of the 5<sup>th</sup> Symposium on Improved Methods for Oil Recovery of the SPE of AIME*. 16 -19 April. Tulsa, OK.
- Wellington, S.L. and Richardson, E. A. (1995). Low Surfactant Concentration Enhanced Water Flooding. SPE 30748. *70th Annual Technical Conference & Exhibition of the SPE*. Oct. 22-25. Dallas, T.
- Whiteley, R.C. and Ware, J.W. (1977). Low Tension Water Flood Pilot at the Salem Unit, Marion Country, Illinois – Part I: Field Implementation and Results. *JPT Aug.* 925 –932.
- Widmyer, R.H., G.D. Frazier, L.K. Strange, and Talash, A.W (1979). Low Tension Water Flood at Salem Unit: Post Pilot Evaluation. *JPT Sep.* 1185 –1190.



- Wilson, J.F. (1960). Miscible Displacement – Flow Behavior and Phase Relationships for a Partially Depleted Reservoir. *Trans, AIME* 219.
- Won, K.W. and Prausnitz, J.M. (1975). Distribution of Phenolic Solutes between water and Polar Organic Solvents. *Journal of Chemistry Thermodynamic*, 7. 661 – 670.
- Wong Chuan Chin (2002). *Thermochemical Recycling of Oil Palm Shell to Phenolic Resin*. Universiti Teknologi Malaysia: Master Thesis.
- Wong, C.C., Ani, F.N. and Nor, H.M. (2003). Quantification of Extracted Pyrolysis Oil from Oil Palm Shells. *Proceedings of International Conference on Chemical and Bioprocess Engineering*. 27-29 August. 39-43.
- Y.Brummer , W.Cui and Q.Wang. (2003). “Extraction, Purification and Physicochemical Characterization of Fenugreek Gum”, *Food hydrocolloids*, 17, 229-236.
- Yassin, A.A.M. (1988). Enhanced Oil Recovery in Malaysia. SPE 17693. Proceedings of the 7<sup>th</sup> Offshore South East Asia Conference. 2 – 5 February. Singapore.
- Yatim, B.B (1996). *Energy: Options for Malaysia’s Industrial Development*, in *State of the Environment in Malaysia*. Consumers’ Association of Penang.
- Zaitoun, A. and Berger, P. (2003). New Surfactant for Chemical Flood in High Salinity Reservoir. SPE 80237. *SPE International Symposium on Oilfield Chemistry*. 5 – 7 February. Houston, Texas.

\

### **LIST OF PUBLICATIONS**

Goh Meng Seng, Mariyamni Awang, Lim Xin Yi, Farid Nasir Ani (2006).  
“Production of Pyrolytic oil for Enhanced Oil Recovery. *1<sup>st</sup> International  
Conference on Natural Resources Engineering and Technology (INRET-2006)*,  
24-25 July, Putrajaya Malaysia

## TABLE OF CONTENTS

CHAPTER	TITLE	PAGE
	TITLE	i
	ACKNOWLEDGMENTS	ii
	ABSTRACT	iii
	ABSTRAK	iv
	TABLE OF CONTENTS	v
	LIST OF TABLE	xi
	LIST OF FIGURES	xiv
	LIST OF SYMBOLS	xx
	LIST OF ABBREVIATIONS	xxi
<b>1</b>	<b>INTRODUCTION</b>	<b>1</b>
1.1	Overview	1
1.1.1	Introduction on enhanced oil recovery (EOR)	1
1.1.2	Introduction on surfactant	2
1.1.3	Introduction on xanthan gum	4
1.2	Statement of Problems	6
1.3	Objectives	7
1.4	Scopes	7

<b>2</b>	<b>LITERATURE REVIEW</b>	<b>9</b>
2.1	Surfactant Polymer Flooding	9
2.1.1	Field Tests	14
2.2	EOR Chemicals	16
2.2.1	Surfactants	18
	2.2.1.1 Alcohol Ether Sulfates (AES)	20
	2.2.1.2 Alcohol Ethoxylates (Alkoxylates)	21
	2.2.1.3 Alkyl Aryl Sulfonates and Petroleum Sulfonates	21
	2.2.1.4 Alkyl Phenol Ethoxylates (APE)	22
	2.2.1.5 Dialkyl Sulfosuccinates	23
	2.2.1.6 Quaternary Ammonium Surfactant	23
	2.2.1.7 Fast Pyrolysis Principles	24
	2.2.1.8 Pyrolysis Oil	27
2.2.2	Extraction of Phenol from Pyrolysis Oil	31
2.2.3	Basic Chemistry of Sulfonation and Sulfatation	39
2.2.4	Ethoxylated Alkyl-Phenols	40
2.2.5	Synthesis of New Alkylaryl Sulfonic Acids as Potential Surfactant for EOR Application	41
	2.2.5.1 Example of Preparation of Alkoxylated Alkylphenol Sulfonic Acid	44
2.3	Xanthan gum	45

<b>3</b>	<b>MATERIALS AND METHODOLOGY</b>	<b>51</b>
3.1	Preparation of surfactants	51
3.1.1	Procedures	51
3.1.2	Production of pyrolysis oil	52
3.1.3	Material	53
3.1.4	Experiments	53
3.1.5	Characterization of Pyrolysis Oil	56
3.1.6	Density	56
3.1.7	Kinematic Viscosity	56
3.1.8	Pour Point	58
3.1.9	Heating Value	60
3.2	Flash Point	60
3.2.1	Acidity	61
3.2.2	Infra – Red (IR) Characterization	61
3.2.3	Miscibility	62
3.2.4	GC – MS Analysis	62
3.3	Extraction of Phenols from Pyrolysis Oil	63
3.3.1	Sulfonation	65
3.3.2	Sulfonation of Alpha Olefin	65
3.3.3	Sulfonation and Alkylation of Extracted Pyrolysis Oil	66
3.3.4	Analysis of Surfactant	69
3.3.5	Acid Value	70
3.3.6	Hyamine Titration for Anionic Active Matter Using Methylene Blue Indicator	71
3.3.7	Surface Tension Measurements	72
3.4	Preparation of xanthan gum	73
3.4.1	Microorganisms	73

3.4.2	Slant Culture Inoculum	73
3.4.3	Culture Media	75
3.4.4	Local fruit juices shaker fermentations	76
3.4.4.1	Inoculum preparation	76
3.4.4.2	Experiment method	76
3.4.4.3	Local fruits	76
3.4.5	Analytical methods	78
3.4.5.1	Extraction and purification process of Xanthan Gum	78
3.4.5.2	Pyruvate and acetate content	79
3.4.5.3	Gelatinization of refined xanthan gum	80
3.4.5.4	Viscosity measurements	80
3.4.5.5	FTIR analysis	80
3.4.5.6	Glucose Concentration	81
3.4.5.7	Solid-state NMR Spectroscopy	81
3.4.5.8	Oil Displacement Experiment	81
<b>4</b>	<b>RESULTS AND DISCUSSION</b>	<b>84</b>
4.1	Production of surfactant	84
4.2.1	Physical and Chemical Characterization of Pyrolysis Oil	84
4.1.2	Physical Properties of Pyrolysis Oil	85
4.1.3	Solubility with Water and Other Solvents	87
4.1.4	FTIR Characterization	89
4.1.5	GC – MS Characterization	93
4.1.6	Extraction of Phenolic Compounds	97
4.1.7	Liquid-liquid Extraction of Phenols from Pyrolysis Oil	97
4.1.8	Identification and Quantification of Extracted Pyrolysis Oil	100

4.1.9	Sulfonation of Alpha Olefin	102
4.1.9.1	Sulfonation of 1-Tetradecene using	
1.2	Mole Ratio of $\text{SO}_3$	102
4.1.9.2	Sulfonation of 1-Hexadecene using	
1.2	Mole Ratio of $\text{SO}_3$	104
4.1.9.3	Alkylation and Sulfonation of the Extracted Oil Using Alpha Olefin Sulfonic Acid	106
4.1.9.4	Alkylation and Sulfonation of the Pyrolysis Oil using Alpha Olefin Sulfonic Acid	108
4.1.9.4	FTIR Characterization of Produced Surfactants	109
4.2	Production of Xanthan Gum from Local Fruits	110
4.2.1	Dry weight of xanthan gum produced	110
4.2.2	FTIR Characterization of Produced Xanthan Gum	111
4.2.2.1	Unrefined Xanthan Gum Produced	111
4.2.2.2	Refined Xanthan Gum Produced	112
4.2.2.3	Viscosity Measurements	114
4.2.2.4	Gelatinization of Refined Xanthan Gum	122
4.2.2.5	Glucose Concentration of Fruits juice	124
4.2.2.6	Pyruvate and Acetate Content	124
4.2.2.7	Solid State $^{13}\text{C}$ NMR	126
4.3	Dry weight of Xanthan Gum Produced from local starches via shaker fermentation	127
4.3.1	IR Spectroscopy	128
4.3.1.1	Unrefined Xanthan Gum Produced	128
4.3.1.2	Refined Xanthan Gum Produced	129
4.3.1.3	Viscosity Measurement	130
4.3.1.4	Pyruvate and acetate content	134

	4.3.1.5 Gelatinization of refined xanthan gum	136
	4.3.1.6 Measurement of Amylose And Amylopectin using TGA	138
	4.3.2 Surfactant Polymer Flooding	142
	4.3.2.1 Surfactant Produced and Polymer Commercial as Additive	142
	4.3.2.2 Surfactant And Polymer Produced From Local Starches As Additive	146
	4.3.2.3 Surfactant And Polymer Produced From Local Fruits As Additive	149
<b>5</b>	<b>CONCLUSIONS AND RECOMMENDATIONS</b>	<b>153</b>
	5.1 Conclusions	153
	5.2 Recommendations	155
	<b>REFERENCES</b>	<b>156</b>
	<b>LIST OF PUBLICATIONS</b>	<b>166</b>



## LIST OF TABLES

TABLE NO.	TITLE	PAGE
2.1	Physical properties of different pyrolysis oils	27
2.2	Identification and quantification of chemical compounds in pyrolysis oil from oil palm shell (Islam <i>et al.</i> , 1999)	30
3.1	Different extraction conditions set	65
3.2	Types of the surfactant used in the experiment	67
3.3	Estimation of sample size for acid value determination	70
3.4	Details of the oil displacement experiment	82
4.1	Physical properties of palm shell pyrolysis oil and its comparison	85
4.2	FTIR functional groups and the indicated compounds of the pyrolysis oil	92
4.3	Tentative GC – MS characterization of pyrolysis oil A from oil palm shell	94
4.4	Tentative GC – MS characterization of pyrolysis oil B from oil palm shell	95
4.5	Yields of pyrolysis oil based on starting oil In experiment run no.1	97
4.6	Yields of pyrolysis oil based on starting oil	

	in experiment run no.2	98
4.7	Yields of phenol/neutral fraction based on starting oil (without NaOH)	99
4.8	Identification of chemical compounds in extracted oil (without NaOH)	101
4.9	Acid value of C14 AOS acid	103
4.10	Acid value of C16 AOS acid	104
4.11	Experiment details for alkylation and sulfonation by AOS acid	106
4.12	Acid value of C14 sulfonated pyrolysis oil	107
4.13	Acid value of C16 sulfonated pyrolysis oil	107
4.14	Anionic active matter and CMC of surfactants produced	108
4.15	Surface tension of surfactants in concentration of 5 wt%	108
4.1.6	Experiment detail for alkylation and sulfonation by AOS acid	109
4.17	Anionic active matter and CMC of surfactants produced	109
4.18	Surface tension of surfactants in concentration of 5 wt %	109
4.19	FTIR Spectra Data ( $\text{cm}^{-1}$ ) of xanthan gum unpurified	112
4.20	FTIR Spectra Data ( $\text{cm}^{-1}$ ) of xanthan gum purified after dry at 50° C	113
4.16	Displacement recovery performance of different surfactants	109
4.17	Weight of refined xanthan gum after purification process	114
4.18	FTIR Spectra Data ( $\text{cm}^{-1}$ ) of xanthan gum unpurified	128
4.19	FTIR Spectra Data ( $\text{cm}^{-1}$ ) of xanthan gum	

	purified after dry at 50° C	130
4.20	Thermogravimetric analysis of starches	138
4.21	Thermal degradation of starches using TGA	139
4.22	Displacement recovery performance of different surfactants	145
4.23	Summary of sandpack flood tests	146
4.24	Summary of sandpack flood tests	149

## LIST OF FIGURES

FIGURE NO.	TITLE	PAGE
2.1	Schematic illustration of a surfactant polymer flooding	11
2.2	Schematic capillary desaturation curve for a nonwetting phase (Lake, 1989)	12
2.3	Schematic illustration of a LTPF	13
2.4	Representative surfactant molecular structures (Larry, 2000)	19
2.5	Typical yields of organic liquid, reaction water, gas and char from fast pyrolysis of wood, wt% on dry feed basis (Toft and Bridgwater, 1996)	25
2.6	Conceptual fluid bed fast pyrolysis process (Bridgwater and Peacocke, 1999)	27
2.7	Flow sheet of extraction of phenol from pyrolysis oil (Gavillan <i>et al.</i> , 1980)	33
2.8	Liquid-liquid extraction of phenols from primary oil (Carlos <i>et al.</i> , 1997)	38

2.9	Flow sheet of extraction of phenol from oil palm shell pyrolysis oil (Jamil <i>et al.</i> , 2000)	33
2.10	Comparison of conventional and new process alkylphenol sulfonic acid	42
2.11	Reaction of alpha olefin sulfonic acid with alkylaryl compounds	43
2.12	The repeating unit of xanthan gum	46
2.13	Building Units of Starch (a) Amylose and (b) Amylopectin	47
2.14	The repeating unit of xanthan gum	48
3.1	Flow chart of surfactant production process	52
3.2	Flow chart of pyrolysis production process	53
3.3	Pyrolysis process – general layout	55
3.4	Fludized bed pyrolysis unit	55
3.5	Koehler KV 3000	58
3.6	Pour point measurements	59
3.7	Koehler rapid tester model K16491	61
3.8	Extraction of phenol from pyrolysis oil	64
3.9	Sulfonation unit with falling film reactor	68
3.10	Sulfonation and alkylation of extracted pyrolysis oil	69
3.11	Tensiometer K6	72
3.12	Stock cultures of <i>xanthomonas campestris</i> in 7 mL sterile YM	74
3.13	Colonies of <i>xanthomonas campestris</i> on a streak plate	74
3.14	Stock cultures of <i>xanthomonas campestris</i>	

	microcentrifuge tubes	75
3.15	Flow chart of preparation of local fruits	77
3.16	Flow chart representatives of the extraction and purification process of xanthan gum produced using local carbon sources	79
3.17	Experimental apparatus for displacement experiment	83
4.1	The solubility of pyrolysis oil in methanol in 1:1 volume fraction	88
4.2	The dissolubility of pyrolysis oil in hexadecene in 1:1 volume fraction	88
4.3	Infra-red spectrum of pyrolysis A from oil palm shell	90
4.4	Infra-red spectrum of pyrolysis B from oil palm shell	90
4.5	Infra-red spectrum of pyrolysis C from oil palm shell	91
4.6	Infra-red spectrum of pyrolysis D from oil palm shell	91
4.7	Infra-red spectrum of extracted phenolic and neutral fractions	100
4.8	Infra-red spectrum of 1- Hexadecene	105
4.9	Infra-red spectrum of C16 AOS acid	105
4.10	Dry weights (g/L) of produced Xanthan gum	111
4.11	Comparison viscosity graph for xanthan gum commercial and unrefined in distilled water (DW)	116
4.12	Comparison shear stress graph for xanthan gum commercial	

	and unrefined xanthan gum in distilled water (DW)	116
4.13	Comparison viscosities of unrefined xanthan gum in 0.2 % w/v NaCl	117
4.14	Comparison viscosities of unrefined xanthan gum in 0.4 % w/v NaCl	117
4.15	Comparison shear stress graph for unrefined xanthan gum in 0.2 % w/v NaCl	118
4.16	Comparison shear stress graph for unrefined xanthan gum in 0.4 % w/v NaCl	118
4.17	Comparison viscosity graph for refined xanthan gum in distilled water (DW)	119
4.18	Comparison shear stress graph for refined xanthan gum in distilled water (DW)	119
4.19	Comparison viscosities of refine xanthan gum in 0.2 % w/v of NaCl	120
4.20	Comparison viscosities of refine xanthan gum in 0.4 % w/v of NaCl	120
4.21	Comparison shear stress graph for refine xanthan gum in 0.2 % w/v of NaCl	121
4.22	Comparison shear stress graph for refine xanthan gum in 0.4 % w/v of NaCl	121
4.23	The gelling of refined xanthan gum {1500 ppm, 10 : 1 ratio of XG to Cr (III)}	122
4.24	Gelling of refined xanthan gum after 2 days at 60° C	123
4.25	Gelling of refined xanthan gum after 6 days at 60° C	123
4.26	Glucose concentration of fruits juice as carbon sources	124
4.27	Acetate content of 72 h xanthan samples from shaker fermentor	125
4.28	Pyruvate content of 72 h xanthan samples from shake fermentor	126
4.29	Dry weights (g/L) of produced xanthan gum from starches	127
4.30	Comparison viscosity graph for xanthan gum refined in distilled water (DW)	131

4.31	Comparison shear stress graph for xanthan gum refined xanthan gum in distilled water (DW)	132
4.32	Comparison viscosities of refined xanthan gum in 0.2 % w/v NaCl	132
4.33	Comparison viscosities of refined xanthan gum in 0.4 % w/v NaCl	133
4.34	Comparison shear stress graph for refined xanthan gum in 0.2 % w/v NaCl	133
4.35	Comparison shear stress graph for refined xanthan gum in 0.4 % w/v NaCl	134
4.36	Acetate content of 72 h xanthan samples from shaker fermentor	135
4.37	Pyruvate content of 72 h xanthan samples	135
4.38	The gelling of refined xanthan gum {1500 ppm, 10 : 1 ratio of XG to Cr (III)}	136
4.39	Gelling of refined xanthan gum after 2 days at 60° C	137
4.40	Gelling of refined xanthan gum after 5 days at 60° C	137
4.41	Thermogravimetric curves for tapiocastarch measured at heating rate of 20° C min <sup>-1</sup> under nitrogen	140
4.42	Thermogravimetric curves for rice starch measured at heating rate of 20° C min <sup>-1</sup> under nitrogen	140
4.43	Thermogravimetric curves for Sago starch measured at heating rate of 20° C min <sup>-1</sup> under nitrogen	141
4.44	Thermogravimetric curves for Sweet potato starch measured at heating rate of 20° C min <sup>-1</sup> under nitrogen	141
4.45	Infra-red spectrum of SURF 1	142
4.46	The oil recoveries due to waterflooding and subsequent surfactant polymer flooding	143



4.47	The performance of waterflooding succeeded by surfactant polymer flooding	144
4.48	The performance of waterflooding succeeded by surfactant polymer flooding	148
4.49	The oil recoveries due to waterflooding and subsequent surfactant polymer flooding	148
4.50	The performance of waterflooding succeeded by surfactant polymer flooding	150
4.51	The oil recoveries due to waterflooding and subsequent surfactant polymer flooding	151
4.52	The sand pack saturated with oil dyed red (before flooding)	152
4.53	The sand pack after waterflooding succeeded by surfactant polymer injection	152

## LIST OF SYMBOLS

$N_c$	-	Capillary number
$N_{cri}$	-	Critical capillary number
$W_a$	-	Weight of pcynometer
$W_f$	-	Weight of pcynometer with sampel
$\mu_w$	-	Viscosity of displacing fluid
$\theta$	-	Contact angle
$v$	-	Effective flow rate
$\sigma$	-	Interfacial tension
$S_{orw}$	-	Residual oil saturation

## LIST OF ABBREVIATIONS

AES	-	Alcohol ether sulfates
AOS	-	Alpha olefin sulfonate
APE	-	Alkyl phenol ethoxylates
APG	-	Alkyl polyglycosides
ASP	-	Alkaline surfactant polymer
AV	-	Acid value
BO	-	Butylene oxide
CMC	-	Critical micelle concentration
DDBS	-	Dodecylbenzene sulfonate
EO	-	Ethylene oxide
EON	-	Ethylene oxide number
EOR	-	Enhanced oil recovery
FTIR	-	Fourier transform infra-red
GC- MS	-	Gas chromatography – mass spectrometry
I.D.	-	Inner diameter
IFT	-	Interfacial tension
IR	-	Infra-red
LTPF	-	Low tension polymer flood
M	-	Molarity
N	-	Normality
NPE	-	Nonylphenol ethoxylate
OOIP	-	Original oil in place
OPE	-	Octylphenol ethoxylate
O/W	-	Oil/water
PO	-	Propylene oxide
POME	-	Palm oil mill effluent
ppm	-	Part per million
PV	-	Pore volume
ROIP	-	Residual oil in place
rpm	-	Revolutions per minute
UTM	-	Universiti Teknologi Malaysia
wt	-	Weight